Along-Strike Variations in Detrital Zircon Provenance of the Tava Sandstone Injectites, Colorado Front Range: insights into terrestrial paleoenvironments of Rodinia

A Senior Thesis presented to
The Faculty of the Department of Geology

Bachelor of Arts

Sally Mae Shatford
The Colorado College
May 2015

TABLE OF CONTENTS

LIST OF FIGURES

LIST OF TABLES

ACKNOWLEDGEMENTS

Much appreciation goes to my academic and thesis advisor and mentor C. Siddoway. Many thanks go to the Colorado College Geology Department, specifically the Patricia Buster Grand Research Fund and Steve Weaver for his technical support. U-Pb analyses were carried out using the Laserchron Facilities at the University of Arizona, Tucson. SEM imaging and thin section preparation were performed using Colorado College facilities. Great appreciation to S. Elkind for his field assistance. Lastly, my gratitude to the Weber Women and the Weber Men.

ABSTRACT

An assemblage of massive remobilized sandstone bodies and subsidiary sedimentary dikes, hosted by Pikes Peak Granite and older Proterozoic rocks, exists in the Colorado Front Range (CFR). Detrital zircon (DZ) zircon provenance analysis reveals the Tava sandstone is Neoproterozoic (800-680 Ma). Tava contains multiple DZ ages including a broad 'Grenville' age plateau (Gehrels and Pecha, 2014) and sharp, narrow age peaks at ~1400 Ma and ~1700 Ma (Figure 2) correlating to known Neoproterozoic age samples. There are no other non-metamorphosed sedimentary rocks of Proterozoic age known in Colorado, excluding the Uintah Mountains.

Field-based research, U-Pb DZ geochronology and scanning electron microscope (SEM) imaging of quartz grains were the research methods used. Field-based research entailed observation of Tava sandstone sedimentology and variation in sandstone characteristics at sites along the Ute Pass Fault. U-Pb DZ geochronology produced minimum ages of deposition for Tava sandstone sediment. SEM imaging determined if some quartz and zircon grains were a result of aeolian transport.

U-Pb DZ geochronology produced DZ spectra for the eleven sample sites. Within these sites that are ~11 km apart, the DZ spectra varied in its major peaks. Differences in DZ age abundances between Tava sample sites are reflected in varying P-values that are used to assess statistical probability of correlation among Tava samples (Siddoway and Gehrels, 2014). These variations in sedimentary and

DZ provenances indicate the presence of topographic relief at the time of Tava sandstone formation. Evidence of extensive river systems in the Neoproterozoic provides a mechanism for zircon transport and a paleoenvironment to transport zircons to Colorado from the opposite side of Laurentia (Figure 4, Yonkee et al., 2014; Dehler et al., 2010; Rainbird et al., 2012). The Tava sandstone is a test for existing hypotheses about the region's paleogeography.

Comparing the weighted means of the detrital zircon populations in each Tava sample to the age of igneous sources and detrital zircon populations of Proterozoic igneous rocks of Colorado, reveals potential local igneous sources for the zircons. Cross cutting relationships indicate a generation younger than the Tava parent bodies. The ~1.4 Ga and ~1.7 Ga aged peaks from bedrock exposure suggests potential erosion of uplifted bedrock caused by tectonism. These differences in DZ spectra provide evidence for the presence of an intracontinental rift across Colorado.

I. INTRODUCTION

A perplexing assemblage of massive remobilized sandstone bodies and subsidiary sedimentary dikes, hosted by Pikes Peak Granite and older Proterozoic rocks, exists in the Colorado Front Range (CFR). Informally named Tava sandstone, the sandstone bodies and injectites occur along the Ute Pass Fault (UPF) (Figure 1). Geologists have speculated about the age and mechanism of emplacement for the dikes for more than a century. While the Pikes Peak Granite host rock (1.08 Ga; Howard, 2013) provides the maximum age of emplacement, there has been no direct means to determine the age. Recently, a resolution was achieved through comparison with U-Pb detrital zircon (DZ) geochronology reference data sets of the western USA (Siddoway and Gehrels, 2014). DZ analysis cannot offer the exact date of formation, but provides a minimum age of emplacement.

Zircons ($ZrSiO_4$) are accessory minerals in a variety of different rock types, igneous, metamorphic and sedimentary rock in the forms of crystals or detrital grains. U-Pb geochronology yields the time since the last crystallization or metamorphic growth of zircon, which was most likely a result of an igneous or metamorphic event.

Zircons are formed during plutonic events. DZs are zircons that have undergone erosion and transport from the plutonic source and incorporated with detritus. The age of sedimentary units is found by dating the individual DZs in that unit. DZ spectra are created by dating ~100 grains using U-Pb geochronology. The ages found using this method create unique spectra for each sample, grouped in a

histogram of age abundances. The age of deposition for the unit can be constrained based on the relative abundances.

DZs from the Tava sandstone were transported from a source location of metamorphic or igneous activity to where they are situated within the mature quartz sandstone today in the CFR. For the CFR's Tava sandstone, DZ zircon provenance analysis reveals that Tava is Neoproterozoic in age, 800-680 Ma. Tava contains a distinctive distribution of DZ ages, including a broad 'Grenville' age plateau (Gehrels and Pecha, 2014) and sharp, narrow age peaks at ~1400 Ma and ~1700 Ma (Figure 2) that correlate to reference spectra for formation in the Southwest that are of known Neoproterozoic age. This is a surprising discovery, as no non-metamorphosed sedimentary rocks of Proterozoic age have previously been identified in Colorado (Uinta Mountains, excluded).

The sample sites for U-Pb DZ geochronology were selected based on their exposure. Most Tava samples are available at the surface along the UPF and subsidiary splay although there are two more northern locations. The sample sites that sit along the UPF were ~ 10 km apart. The DZ data also reveal variations among Tava sandstone in respect to age spectra and DZ provenance over small distances between Tava sample sites (~10 km). Evidently, varying amounts of zircon from local versus distant sources were incorporated from one site to another along the UPF. The variation in DZ provenance, together with the compositional maturity of Tava sandstone (Scott, 1963) is a paradox that is explored in this thesis research. A possible explanation is that topographic relief existed at the time of Tava sandstone

formation, with effects on sediment distribution that caused variations in DZ age concentrations, grainsize of sandstone, and makeup of granule and pebble clasts.

The methods used to explore this paradox involve field-based research, U-Pb DZ geochronology and scanning electron microscope (SEM) imaging of quartz and zircon grains. Field-based research entailed observation and description of Tava sandstone sedimentology and variation in sandstone characteristics at sites along the UPF. With the age of the Tava sandstone known in general terms, the Tava's paleoenvironment of formation can be inferred in the proper context of the interior of the Rodinia supercontinent that existed in the Neoproterozoic time (Yonkee et al., 2014). The sedimentological characterizations broaden the knowledge of the Tava sandstone system and provide information about sandstone remobilization events and dike emplacement processes. U-Pb DZ geochronology of selected sites along the UPF provide age data that can be tied to potential sources and used to examine variations, in abundance, in order to test the hypothesis of dynamic topography. SEM imaging of quartz and zircon grains in the Tava sandstone was employed to test the mechanism of transport; imaging showed evidence of aeolian contribution to the transport of zircon and quartz grains.

Ultimately, the results have bearing on existing hypotheses about extensive river systems that may have transported zircons across Laurentia (within Rodinia) from the Grenville Mountains, providing a mechanism for transporting of zircons to Colorado from the opposite side of Laurentia (Figure 4, Yonkee et al., 2014; Dehler et al., 2010; Rainbird et al., 2012), leading to development of the Grenville Sand Sheet (Figure 3A and 3B, Yonkee et al., 2014; Rainbird et al., 1992 and 2012), and

providing evidence for topographic relief. In the CFR, the Tava sandstone represents a new source of information about the region's paleogeography, in a region where no supracrustal rocks had been known to exist for the interval ~1.0 Ga to 540 Ma.

Possible implications of the DZ research are that the results show that there was extensive exposure of crystalline rocks long before the deposition of Cambrian sediments, possibly before 680 Ma, with consequences for the time of formation of the Great Unconformity (Siddoway and Gehrels, 2014). The Tava sandstone is the only proxy that can provide information during a 500-million-year span for which no source had previously been available.

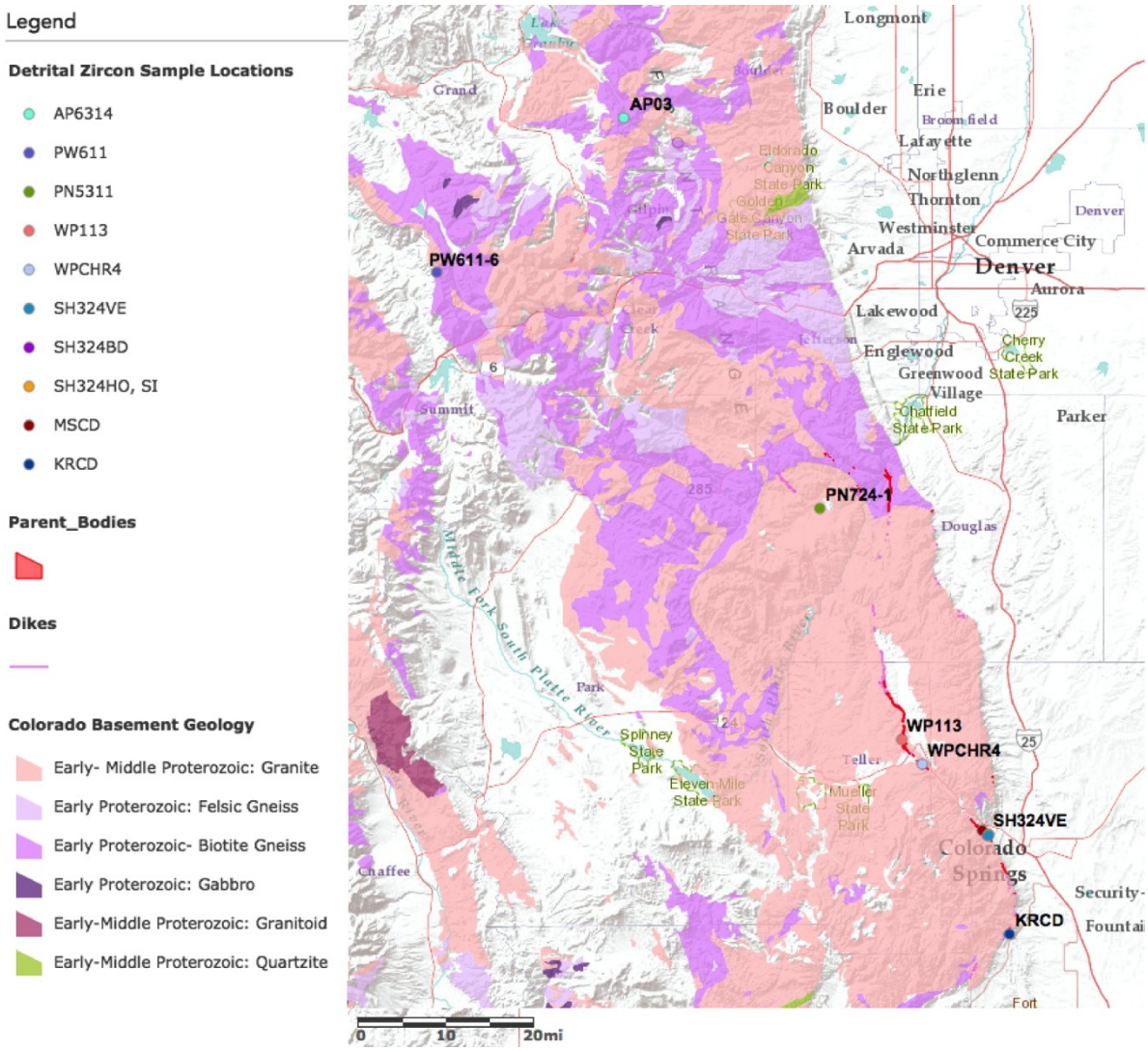

Figure 1: Simple geological map of the Ute Pass Fault. Red pattern show the study locations for Tava sandstone field research. DZ sample locations from previous research are shown with yellow dots (however, sample HARD-13 is not from Tava). Pine, CO site not included in this figure. Figure taken from Siddoway and Gehrels, 2014.

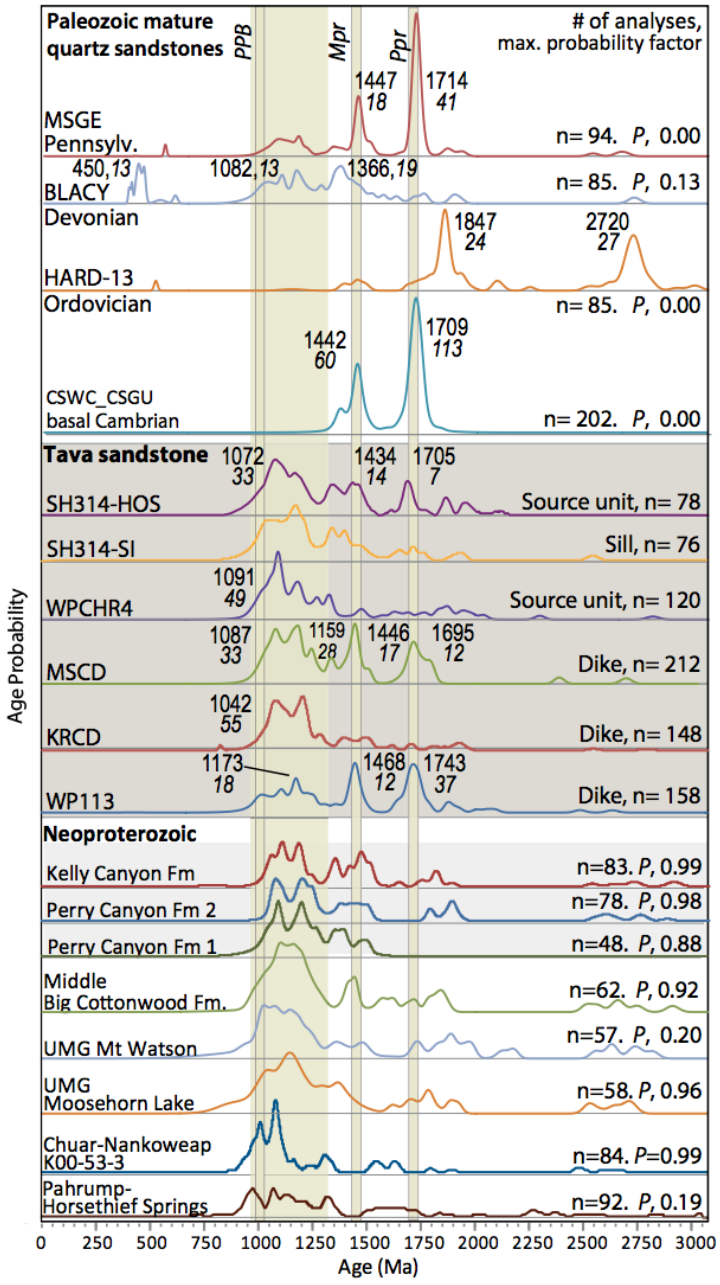

Figure 2: Above: age probability density plot comparing known Paleozoic samples in CFR to Tava sandstone samples. Figure indicates no correlation between Tava and regional Paleozoic sandstones. Below: detrital zircon provenance of Tava compared to Proterozoic sandstones in the Western United States. Figure shows high correlation from Tava to western United States Proterozoic units. Figure taken from Siddoway and Gehrels, 2014.

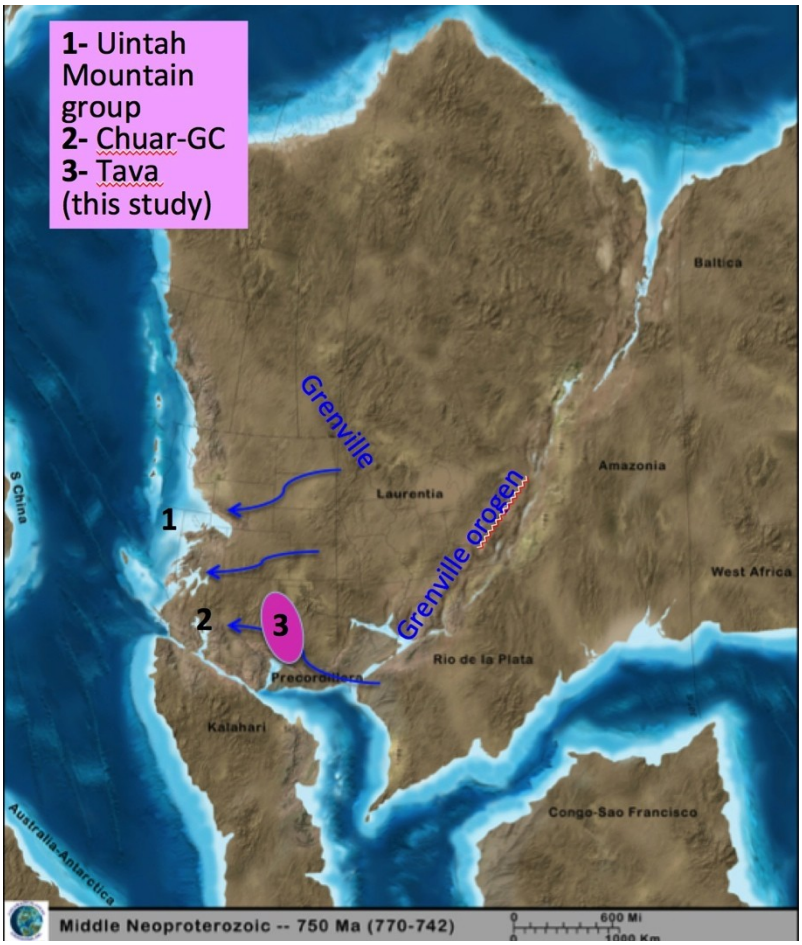

Figure 3: Paleographic reconstruction by Ron Blakey show presence of a rift basin and topography at the Grenville Orogeny. This ruggedness and topography allows for an extensive river system due to the differences in elevation. This is supported by established evidence that Grenville grains are present in other Neoproterozoic sandstones in the Western US, indicated by 1 and 2 in figure. These correlative units are vestiges of a regionally extensive Grenville sand sheet. C. Siddoway's GSA 2013 Presentation.

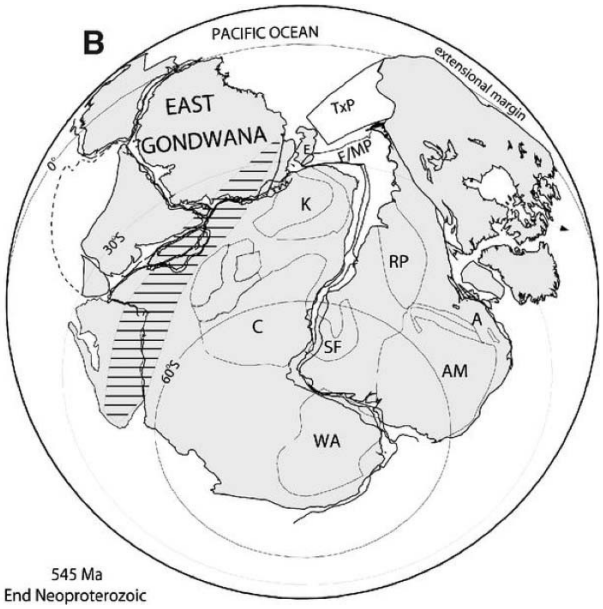

Figure 4A: Paleographic reconstructions for the Precambrian-Cambrian transition. The tectonics responsible for building of the supercontinent Rodinia is also responsible for the Grenville Orogeny. This figure shows the extent of the supercontinent and the magnitude of the Grenville Orogeny (Daziel, 2014).

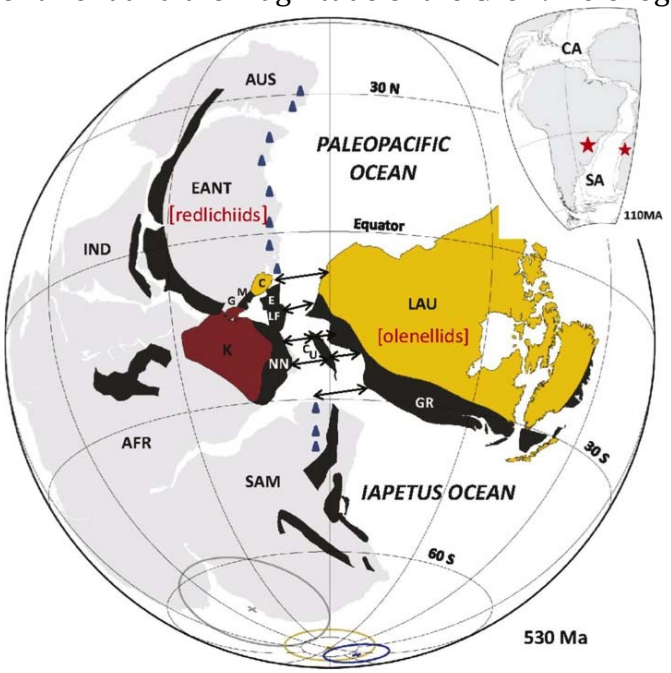

Figure 4B: Cambrian paleogeography proposed here on geological grounds for ca. 530 Ma as an Iapetus-Pacific deep oceanic connection developed. Black shows remnants of the Grenville Orogeny as it spans the rifted continents. The extent of the Grenville Orogeny was vast, leaving many parts across the supercontinent. Daziel, 2014.

II. GEOLOGIC BACKGROUND

The Tava sandstone occurs in several locations in the CFR (Figure 1), mostly along the UPF with a few exposures along the Rampart Range fault. The UPF is believed to have formed during breakup of Rodinia (Siddoway et al, 2013), participated in the tectonic movement of the Ancestral Rocky Mountains, and been reactivated during the Laramide Orogeny in the Cretaceous (Temple et al., 2007). The CFR experienced uplift during the Laramide Orogeny, producing reverse faults, mountain building, and intermountain basins (Sonnenberg and Bolyard, 1997). The Ute Pass Fault runs in a north-south to north-northwest direction, containing a few subsidiary faults that splay to the northwest.

The Tava sandstone occurs within the hanging wall along the UPF (Figure 1 and 4) over a distance of 75 km (Harms, 1965) as well as at other sites in the CFR (Vinitage, 1954; Scott, 1963). A majority of locations for this study were along the UPF. Pine, CO (PN5311) is the northernmost study location, where there is a dike positioned on a splay of the UPF (Figure 1). The Tava sandstone is composed of two elements hosted by sandstone, granite or gneiss. The first is a sandstone parent body, and the second is an injectite (general term covering dikes and sills).

The parent or source bodies have large dimensions that exceed volumes that could reasonably be emplaced as sandstone intrusions (Siddoway et al., 2013), with lengths ≥ 2km long, widths ≥250m, and heights ≥ 125m (e.g. Temple et al., 2007). Dikes and sills are centimeters to meters wide and can have long lateral continuity. One system of meter-scale dikes can be traced for ≥ 3 km (Siddoway et al., 2013).

DZ geochronology has become a powerful tool for investigation of paleoenvironments, due to recognition that there are diagnostic "detrital zircon reference spectra" that are strongly indicative of sources or time periods. In the western USA and worldwide, there is a 1300-1600 Ma broad age peak that is characteristic of 'Grenville' spectra (Mueller et al., 2007; Dehler et al., 2010; Gehrels et al., 2011; Howard, 2013). This Grenville spectra of grains is also present in the Tava sandstone and could only be sourced from the Grenville Orogen on the opposite side of Laurentia (Figure 3). The Grenville orogeny took place between 1300-1000 Ma (Davidson, 1998), a time span also present in the broad age peak of Tava. Additionally, there are narrowly defined and pronounced peaks at 1400 and 1700 Ma (Figure 2), suggestive of local distribution (Doe et al., 2012). A possible source of ~1400 Ma grains is the Berthoud plutonic suite, and for the ~1700 Ma zircons is the Routt plutonic site in the Proterozoic Yavapai-Matatazal provinces (Sims et al., 2003).

DESCRIPTIVE ASPECTS OF THE TAVA SANDSTONE:

Tava sandstone parent bodies and dikes consist of conglomeratic, matrix-supported, moderately to well-rounded, mature, quartz sandstone. The sandstone generally lacks grading and sorting, and contains granules to pebbles suspended in a fine-grained sand matrix (0.13-0.5 mm), but ordinarily lacks clays and mudstone clasts. This texture falls under the classification of "structureless" sandstone (Duller et al. 2010). The absence of primary sedimentary structures such as bedding, cross bedding, grading and sorting has only been noted recently (Siddoway et al., 2013).

The lack of sedimentary structures is attributed to sand remobilization and injection (Siddoway et al., 2013), which many times is a product of liquefaction and remobilization under conditions of high fluid pressure (Duller et al., 2010; Hurst et al., 2011). A few things can trigger injectites: fluid overpressure due to sedimentary loading, catastrophic fluid migration, and seismicity (Hurst et al., 2011). The Tava injectite cross cutting relationships possibly are best explained by seismicity-induced liquefaction (Siddoway and Gehrels, 2014), which results in a change in the overlying pore fluid pressure, pushing sand into weaknesses and fractures (Hurst and Glennie, 2008). Injection of dikes or sills occurs when a mechanism injects sand into preexisting fractures in combination with aqueous fluids (Rodrigues et al., 2009; Vigorito and Hurst et al., 2011). Remobilization of sandstone destroys evidence of previous sedimentary structures, causing uncommon geometries (Strachan, 2002).

Tava's characteristics are consistent with emplacement by liquefaction and remobilization under conditions of high fluid pressure (e.g., Gruska and Zielinski, 1966). Anisotropy of magnetic susceptibility of dike samples, used to determine the direction of movement of material during dike emplacement, showed that injection was lateral rather than vertical (Freedman, 2014). Hence, the interpretation of a process of gravitational infilling of tectonic fractures (Harms, 1965) could not have been the mechanism for sandstone intrusion.

The timing of injection has eluded investigators until recently. Previous work hypothesized the age of the Tava sandstone to be Cambrian (Vinitage, 1954; Scott, 1963), Pennsylvanian(Kost, 1984), Cretaceous (Harms, 1965), or Holocene (Austin

and Morris, 1986). At the time of early field investigation of the injectites, there was no way of determining their age. Since the 1980's U-Pb DZ geochronology has provided a new means for dating sedimentary rocks. Comparison of age distributions from differing samples can be used to determine if they are correlative or not. Additionally, U-Pb DZ age distributions provide information about whether the zircons have a proximal or distal source. Two sets may have peaks bracketing the same date but may not share the same peak intensity, attributable to zircon abundance. The steeper and more narrow the peak, the more homogenous the zircon source, and therefore, the less distance the detrital zircon grain has travelled; conversely, a more sloping, broader peak indicates a distal source (Doe et al., 2012).

III. METHODS:

SEDIMENTARY DESCRIPTIONS:

For sedimentary characterization, I studied three parent bodies, two of which are cut by injectites and one large dike. The sites are the "Sugarlump" at the Sutherland Creek drainage in Manitou Springs (Figure 5), "the Duplex" near Painted Rocks, situated on the boundary of the Woodland Park graben (Figure 6; Figure 1) and Pine, where there is a basement-hosted dike. The site at Pine, CO is situated upon a splay of the UPF (Figure 1). Sample sites are positioned ~35 km apart.

Due to faulting, the position of the top and bottom of the sandstone bodies is unknown, and the bodies lack bedding that customarily provides a datum for paleohorizontal. Therefore, conventional stratigraphic column description could not be done. My approach was to perform detailed descriptions of three to six one-

meter square areas at each site, describing a wide, continuous exposure across a parent body from one edge to the other of. Within a 10 x 10 cm^2 grid that subdivides the 1-m^2 area (Figure 7), I recorded matrix grain size, clast size range, clast makeup, rounding, degree of sorting, color, type of cement, and other observational characteristics. When an exposure was covered with vegetation or affected by extreme weathering, fresh surfaces were obtained by using a rock hammer. Depending on available exposure, some areas are less than 1-m^2 and split into fewer in-grids. I used the larger grids to create summary descriptions that illustrate variation (or not) in sedimentary structure within and among the three different sites. To accompany each description, a photograph of each grid frame was taken (Appendix A).

Crosscutting injectites exist at two ("Sugarlump" and "Duplex") of the three parent sites. For these sites, dikes or sills are described in a similar fashion as the parent bodies. For at least one of each generation of injectites, I performed detailed description of two square areas (area delimited by width of intrusion) that are spaced apart by a reasonable distance.

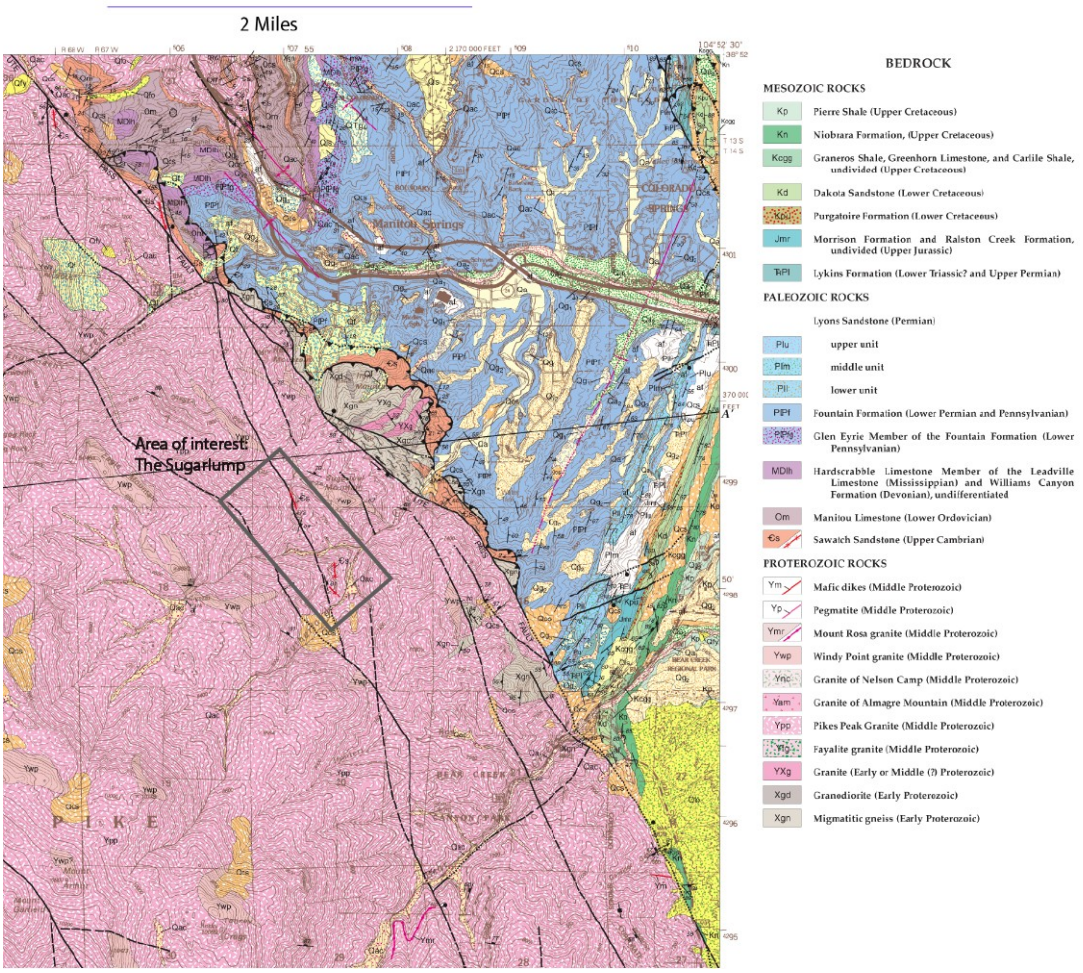

Figure 5: Area of interest demarcated upon a geological map of Manitou Springs, the "Sugarlump" and Sutherland Creek area specifically. On published maps, Tava is mislabeled as Cambrian Sawatch Formation. Figure shows proximity to PPG and the UPF. Taken from Morgan et al., 2003 and Keller et al., 2005.

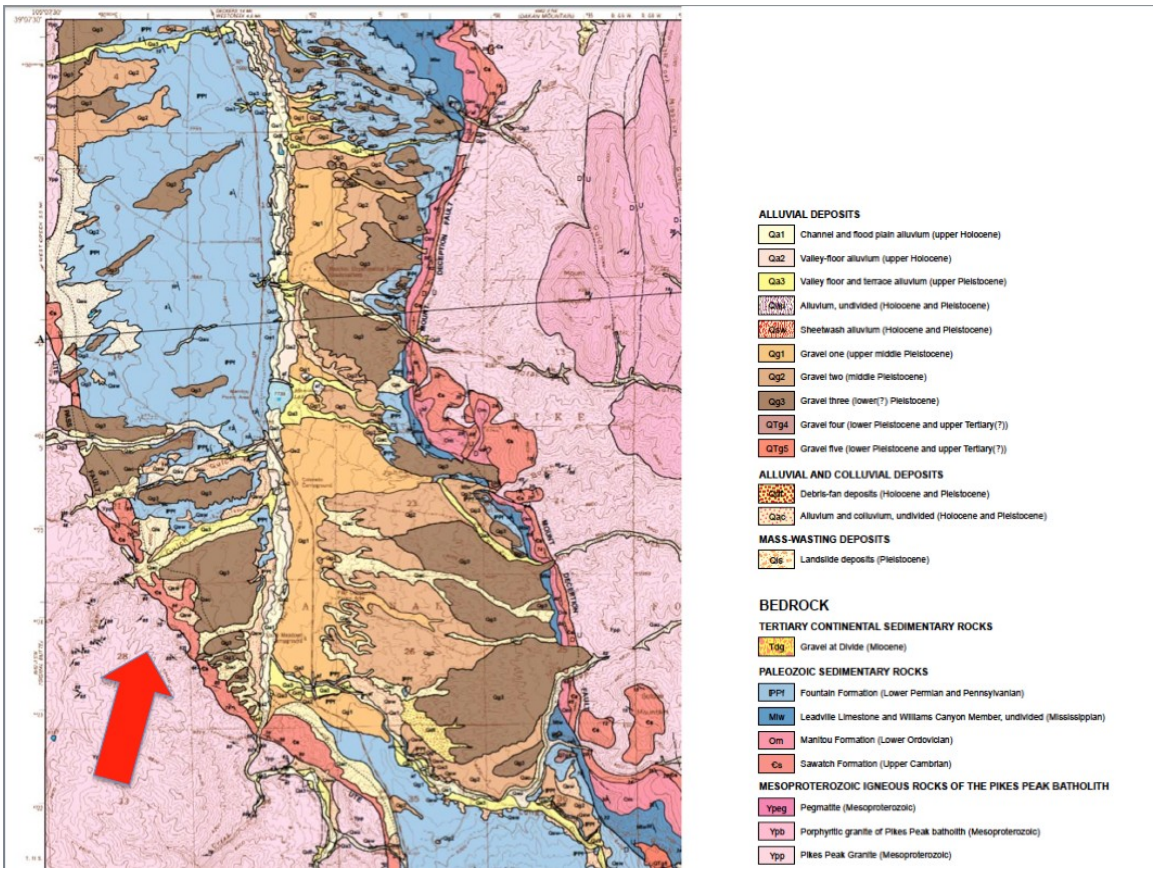

Figure 6: Geological map of the region surrounding the "Duplex" study site. The "Duplex" is indicated with a red arrow. Basemap is a portion of the geological quadrangle map of Mount Deception in Teller County. Figure emphasizes proximity to the UPF and PPG. Taken from Temple et al., 2007.

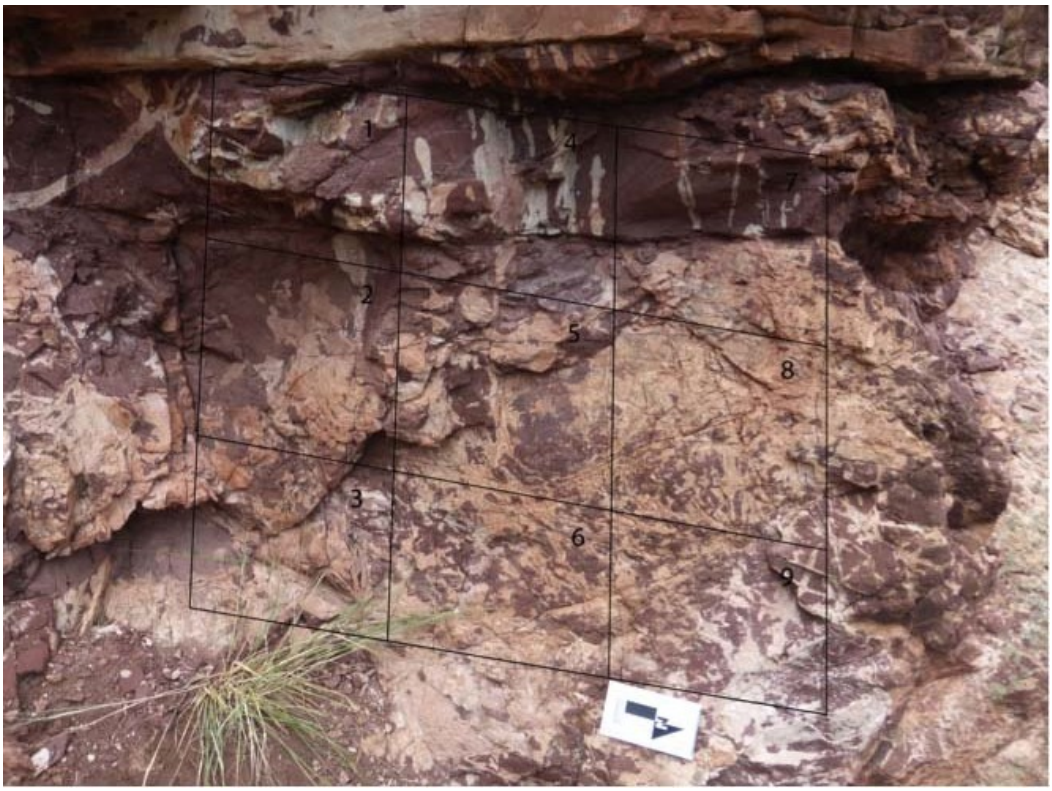

Figure 7: Example of a square meter description with grids numbered in order of that described. This grid is on a sandstone parent body at The "Sugarlump" in Manitou Springs, CO. Photo taken by S. Shatford.

THIN SECTION PREPARATION:

Hand samples were collected at each locality, and a representative sample was cut for a thin section and sedimentary petrography. Thin sections of the host (HO), dikes (BD, VE, and DI) and sills (SI, when applicable) were made in order to determine mineral composition and texture. Using Colorado College facilities, I cut the samples into thin-section dimensions using the large, medium and small saw and sent them to be prepared by a commercial facility. Thin sections were impregnated with epoxy when necessary for fragile rock billets. Full-section photomicrographs were acquired using the tabletop digital scanner (Figure 8).

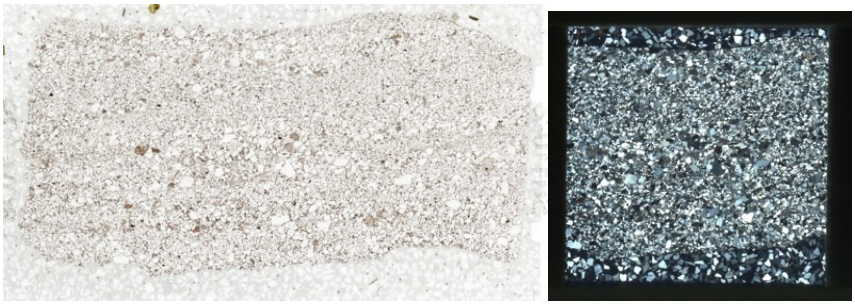

Figure 8: Thin sections of SH324HO samples. Images show ~97% quartz. The sandstone matrix suspends the larger grains. Some intrusions of larger grain sizes, but no distinctive primary structures.

SCANNING ELECTRON MICROSCOPE IMAGING (SEM):

The maturity and rounding of the Tava quartz sand is surprising in light of the DZ detting within a crystalline host. In order to examine the degree of rounding and surface characteristics of quartz and zircon grains and the possibility of aeolian transport processes, I performed SEM imaging. To disaggregate samples, fragments were put into the Bico jaw crusher followed by the Bico disk mill in order to separate the sample into its individual grains. After the sample had been crushed, each sample was cleaned in a 50 mL beaker with 12 M HCl to dissolve cement, and left overnight on a hot plate set on low heat. The samples were then decanted and returned to the hot plate to dry overnight. Once the samples were completely dry, they were poured into a plastic dish with methanol. Detrital zircon from previous U-Pb geochronology sessions, and dried, cleaned quartz clasts to be imaged were separated under a microscope and individually picked with tweezers and placed into new dishes. Grains were chosen based on size, degree of rounding and composition (quartz and zircon).

Quartz sample names for imaging are: SH 324 HO, SH 324 BD, SH 324 VE (Sugarlump); DX HO, DX DI (Duplex); and PN HO (Pine) and two detrital zircon samples PN HO DZ and SH HO DZ. Each of the samples was mounted on a circular, double sided sticky tab. Each tab was placed with tweezers on its own aluminum plug. The aluminum plug was placed into a gold coating sputterer and kept at 1000 volts and exposed to gold sputter for approximately 70 seconds per rotation. Each sample was rotated a third clockwise two times in order to coat every surface of the grains in the samples. After each rotation, the coating procedure was repeated.

Exposure time remained constant throughout the samples in order to maintain consistent thickness of the gold coating.

When coating was complete, each grain had a gold coat of uniform thickness. When exposed to an electron beam, this allowed electrons to coat the surface, grounding the specimens without creating an electrostatic charge. The aluminum plugs were placed in a tray with a four-plug capacity and into the scanning electron microscope. Using high magnification possible in the beamed instrument, grains were examined for pitting, frosting and roundedness (Figure 9A and 9B) that could be produced by aeolian transport mechanisms.

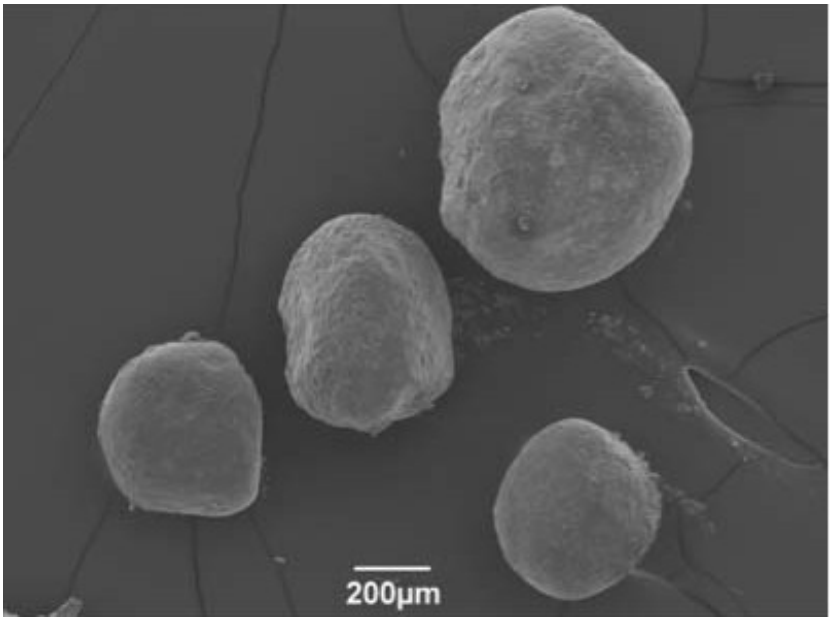

Figure 9A: Frosted and pitted quartz grains imaged using the SEM on the Colorado College campus. Images of a group of quartz grains from the parent body in Pine, CO, sample PNHO.

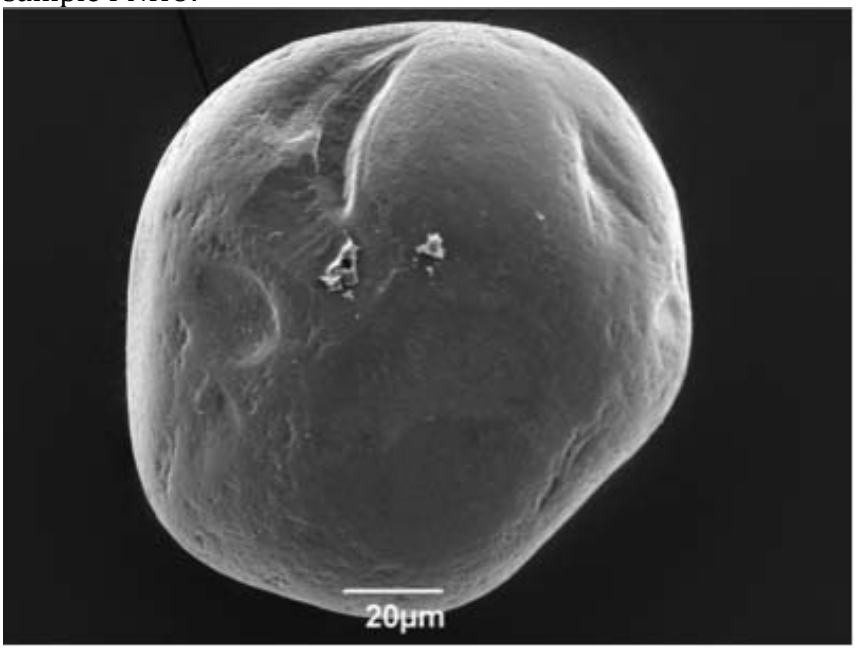

Figure 9B: This image is a detrital zircon taken from a parent body in Pine, CO, sample PN HO DZ. Both quartz and zircon grains exhibit high degree of rounding. Although the surface is smooth, both quartz and zircon grains exhibit pitting and frosting characteristics indicative of aeolian transport.

U-PB DETRITAL ZIRCON GEOCHRONOLOGY:

i. Sample Collection

For each site, I chose two to three locations for DZ sampling. Two to four kg of samples were collected in order to ensure representative DZ samples from parent bodies, dikes and sills. DZ sample sites for this study were spaced at intervals of ~17 km along the UPF. Larger pieces were broken with a rock or sledge hammer into pieces approximately 0.5-1.5 inches in long dimension. Breaking was done upon the outcrop in order to avoid contamination by other materials. Fragments were placed in plastic sample bags to minimize contamination of grains with other materials (Pepper et al., 2012) and shipped to Tucson, AZ for processing according to rigorous methods for crushing and mineral separation (Simpson et al., 2012) by Zirchron LLC.

ii. Mineral Separation

Mineral separation was carried out according to procedures specified in the Rock Crushing & Water Table and Mineral Separation Instruction Manual from University of Arizona, Tucson (Pullen et al., 2011; Simpson et al., 2012; Johnston et al., 2009). Sample preparation involved separation of Tava groundmass from granules and clasts followed by DZ mineral separation from the groundmass. Fragmented samples were first put in the jaw crusher to create gravel-sized clasts and then caught in a clean, plastic bucket lined with a garbage bag. Second, the crushed pieces were placed in a roller mill, pulverized to (~0.063-2mm), sand pieces are put into a clean trash bag. The third step involved water separation of

grains based on density using a Wilfley table, angled at 25°. Dense grains were then placed in ~400 micrometer sieve and back over the Wilfley table. Next, the materials from the Wilfley table were further separated using a hand magnet to separate magnetic material, followed by a more sensitive magnetic separation using a Frantz LB1 (barrier field) magnetic separator. Next, heavy liquid separation using Methylene Iodide and the "MI 'popsicle' technique" separated zircon from other dense minerals. Last, heavy liquid separation was performed again to separate apatite from zircon using a Separatory Funnel. The methodical procedure of mineral separation ensures that there is no bias with the zircon samples obtained at the end (Gehrels et al., 2006). Following grain separation, magnetics and heavy liquids are used

iii. Laser Ablation Technique

Once the zircons were separated, a portion of ~200 grains was mounted onto an epoxy disks using the methods outlined in Preparing & Cleaning Mounts (Pullen and Pepper, 2009), at the University of Arizona in Tucson. Analyses were performed in the Laserchron Lab using LA-ICP mass spectrometry. The LaserChron Lab uses a Nu Plasma multicollector ICPMS and two Photon Machines Analyte G2, and a Hitachi 3400N SEM, according to methods for laser ablation described in Gehrels, (2000; 2010) and Gehrels et al., (2006; 2008). The epoxy disks mounted with zircon separates and standards we placed in a chamber containing He atmosphere. The laser (Analyte G2) ablates the selected grain (laser beam diameter ranges from 20-35 μm, sample depending) and He gas takes the accelerated

material and travels with it along a curved trajectory, causing separation of heavier from lighter isotopes. With the use of plasma mass spectrometry, the NuPlasma multicollector ICPMS counts the number $^{204, 206, 207, 208}$Pb, ^{232}Th and ^{238}U using nine Faraday collectors and Channeltron ion counters (Figure 10). The isotopic ratios produce a radiometric age for the spot on the grain. Oscillatory zoning on certain zircon grains can produce different ages for the same grain, but this can be detected using cross polarization and backscatter images to distinguish between different zones, inclusions and cracks.

Approximately 100 spots were analyzed per sample mount. The ages are calculated based on the ratio of unknown quantitites to known quantities in the Sri Lanka standard (SR) (Black et al., 2003), measured every five analyses during analysis as well as three in the beginning and three at the end of each sample. The standard is used to correct for the fractionation of U/Pb that tends to drift during analysis. Discordant and high 206/207 values, indicative of presence of common Pb are thrown out since discordant values that lie beyond ± two-sigma are considered to be outliers (Gehrels, 2000; 2010; Gehrels et al., 2006; 2008; Cecil et al., 2011).

Developments in U-Pb geochronology have allowed geologists to date individual zircon grains. The laser ablation method was used in this study to analyze individual grains that had little zoning, cracks or inclusions. This method is important in dating detrital zircon populations, which can come from more than one source. The instrument counts the isotopes, and using ratios, produces a radiometric age of the grain.

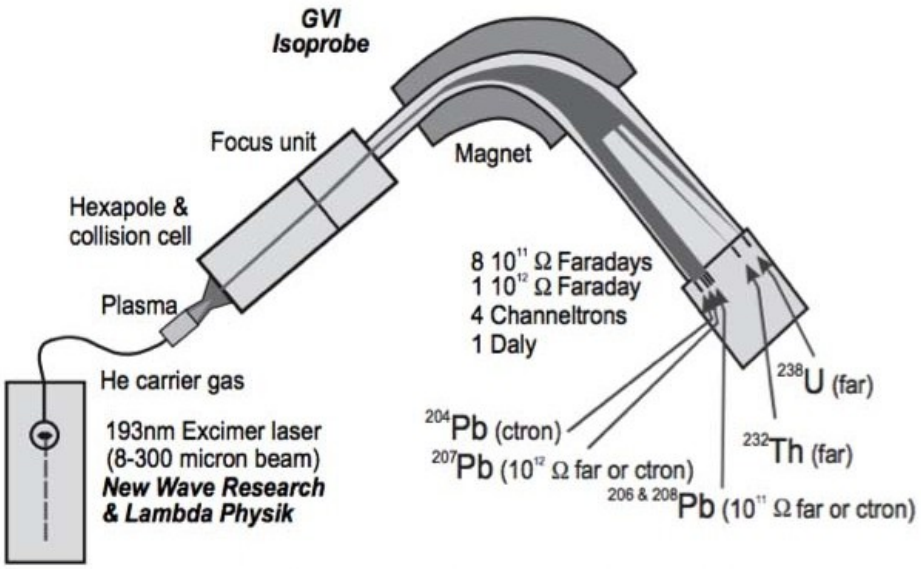

Figure 10: Diagram of ICPMS instrument used for laser ablation dating for U-Pb geochronology at the Laserchron Lab at University of Arizona. Gehrels et al., 2009.

IV. SEDIMENTARY DESCRIPTIONS, BASED ON OBERVATION AT THREE STUDY SITES

THE "SUGARLUMP": MANITOU SPRINGS, CO

The "Sugarlump" is a parent body located within a structural block that was transferred to the foot wall of the Ute Pass Fault (Siddoway et al., 2013), a hill so named because it is situated near a higher feature named the Sugarloaf.. The SE end of the Tava exposure corresponds to a hill bordering the Sutherland Creek drainage (Figure 5). The study location is accessed via a trailhead for the Paul Intemann Trail, located approximately 1.5 miles up Crystal Park Road from Highway 24. The Ute Pass Fault Zone is characterized by a zone of steep, left reverse oblique faults that place basement granite and gneiss above inclined Paleozoic sedimentary units. The city center of Manitou Springs is situated on the footwall of the UPF, resting upon exposures of Pennsylvanian Fountain Formation. Sedimentary successions from Upper Cambrian Sawatch through Quarternary fluvial deposits are present, with only the Silurian missing (Keller et al., 2005). The "Sugarlump" is the southernmost site for sedimentological description of Tava sandstone and injectites.

The "Sugarlump" offers all three types of Tava sandstone bodies: parent sandstone, cross cutting dikes, and sills (Figure 11). DZ samples were taken from the parent body (SH324HO), the sill (SH324SI), the basement hosted dikes (SH324BD) and the large laterally continuous vertical dike (SH324VE). The parent body is overlain by basement rock and rests in fault contact upon the arkose Fountain Formation. Both the parent body and basement rock host dikes and sills, but the Fountain Formation does not. There are three types of injectites observed at this

site. The first is a vertical dike that cuts through the parent sandstone body and is laterally continuous for >30 m. The dike ranges in width from 0.5 to 1.5 m. The second is a basement-hosted purple-red dike that is crosscut by a second white dike, approximately 15 cm wide, a relationship that provides evidence of a second generation of dikes and/or multiple injection events. Lastly, there are sills within the upper part of the parent body, aligned parallel to the contact between the parent body and the overlying basement rock. The sills are 0.3 to 1.5 m wide.

The parent body at this location was described at five grid locations (Figure 9) of 1x1 m^2 (Figure 7). The parent body exhibits a uniform bimodal sand matrix, consisting of fine and medium grained sand (0.13 to 0.5 mm) comprised primarily of quartz. The finer grains are well-rounded with evidence of frosting visible with a hand lens. The matrix supports granules and pebbles, ranging in size from 2 to 8 mm, composed of quartz (95%) and other minerals (5%): mica, feldspar and polycrystalline clasts of granite. The shape of the larger grains varies from sub-rounded to well-rounded. There is no evidence of grading or imbrication. The parent body exhibits color variations in the form of red and white mottling. Grids above and below the sill (Grids 3 and 4, respectively) exhibit more variation of red and white mottling while the other (1,2,5) were mostly red. Other than different mottling patterns, there was no significant difference in composition between grids of parent bodies.

The sill and large vertical dike at this location contain coarser grains than the parent bodies. Their matrix consists of fine and medium, well-rounded quartz clasts. They have the same mineral makeup as the parent bodies: quartz (95%), detrital

mica flakes, lithic granite fragments and feldspar. The granule and pebble clasts range from 2 to 10 mm in size and are composed primarily of well-rounded quartz with some sub-rounded granitic lithic fragments. The vertical dike contains flakes of green clay (XRD). The presence of clay distinguishes the dike from other injectites at the "Sugarlump."

The "Sugarlump" exhibits evidence of three sediment remobilization events and crosscutting relationships. One pair of crosscutting dikes within granite is much smaller than the previously described sill and dike that are hosted by the Tava sandstone. They are approximately 30 cm wide. Consistent with the sill and dike, they contain a fine and medium-grained sand quartz matrix. The pebble-sized clasts in the dikes are coarse and very poorly sorted in comparison to the sill and vertical dike. Granules and pebbles ranging from 1 to 12 mm, composed of quartz and lithic granite fragments, are concentrated in patches instead of randomly distributed throughout the outcrop (Figure 12). Larger grains are composed of quartz, feldspar and lithic granitic fragments. There is no evidence of sorting or grading.

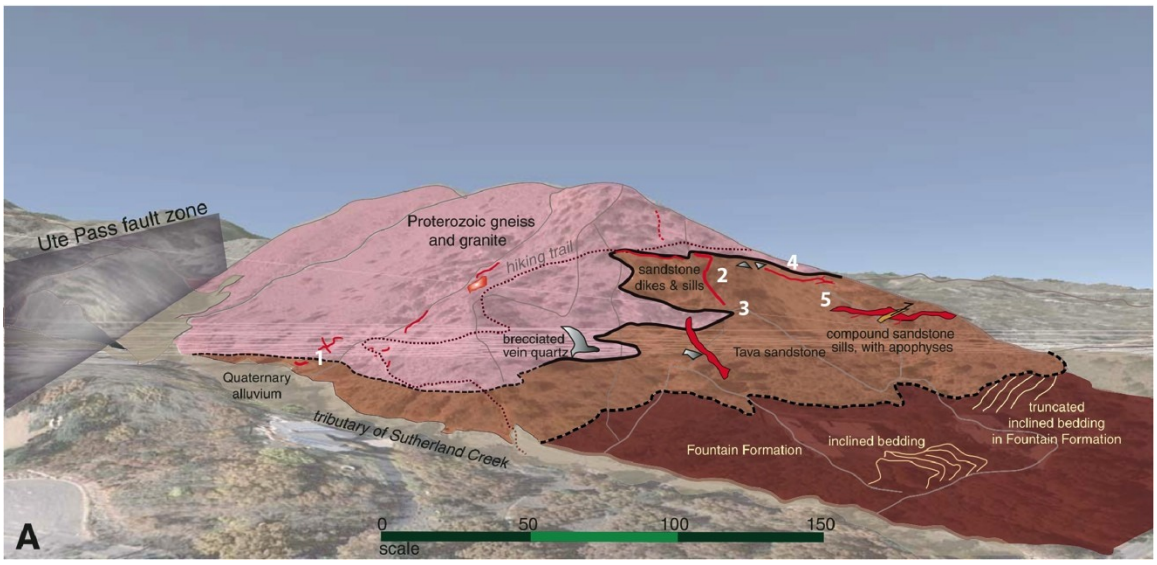

Figure 11: Perspective view and cross section of the "Sugarlump" locality in Manitou Springs showing a parent body (in brown) overlain by an irregular body of gneiss and granite (in pink). In this hill bordering the Ute Pass fault zone (on left of diagram), key relationships are preserved in the hanging wall of an abandoned fault segment (fault is of Ancestral Rockies or Laramide age). Sandstone dikes and sills (in red) exist in both the Tava sandstone parent body and basement rock, and pass from the Tava parent into the crystalline rock, above. In addition there are cross cutting relationships between dikes , indicating at least two injection events. Sedimentology sites are numbered according to the order in which they were analyzed. View is to the NE. Fountain Formation with ~25° dips to SE forms the footwall of the fault. Figure from Siddoway et al, 2013.

Figure 12: Image shows cross cutting relationships between dikes within Pikes Peak Granite. Consistently at several locations, white Tava sandstone dikes cut red oxidated or mottled hosts (Howard, 2013). Two generations of dikes indicate multiple emplacement events.

THE "DUPLEX": WOODLAND PARK, CO

The second study locality called the "Duplex," in reference to the structural context (Temple et al., 2007) is located north of Woodland Park, CO. Two to three parallel strands of the UPF exist in the Mount Deception quadrangle. The fault strands bind the Duplex structure on the west wide of the Woodland Park Graben (Figure 6, Temple et al., 2007). The UPF strikes approximately north south and is responsible for brittle deformation and reverse faulting. The basement rock (granite and granite pegmatites) is faulted up with respect to Paleozoic rocks within the graben including Cambrian Sawatch Sandstone through Pennsylvanian Fountain Formation. Unlithified Pliocene to Quaternary alluvial sands and gravels comprise some parts of the basement rock.

At the "Duplex," the Tava parent body ranges in thickness from 2 to 12 m. One ridge has 100 m of laterally continuous parent sandstone (Temple et al., 2007). Dikes range from 2 cm to 4 m thick.

The parent bodies at the "Duplex" consist of a fine and medium sandstone matrix which suspends larger clasts. No grading or sorting is present in any grids. The larger clasts that are supported by the matrix range in width from 2 to 7 mm and have a well-rounded shape. The granules and pebbles correspond to lithic fragments of granite and quartz, while the finer grains primarily are made of quartz, with some feldspar. In comparison to the "Sugarlump," the parent body at the "Duplex" contains smaller overall clasts and fewer lithic fragments of granite than the exposures at the "Sugarlump."

The large dike at the “Duplex” exhibits grading features that might correspond to bedding oriented N28W, 22 (Figure 13). The study area measured 46 x 46 cm^2. The thicker “bed” is made up of competent, quartz sandstone with a few small pebbles and granules. The thinner “bed” is made up of friable sand, possibly corresponding to fault gouge. Quartz sand grains exhibit frosting, detected using a hand lens in the field. The granules and pebbles range in diameter from 2 to 5 mm, much smaller on average than granules in the parent bodies at this site. Other dikes at the “Duplex” do not exhibit any indication of primary structures. Additionally, there were no crosscutting relationships observed between dikes.

Figure 13: Layered feature at the Duplex that could be a result of fault movement or primary depositional structures. Differences in grain sizes makes the tabular structures more pronounced. The larger version of outcrop is on the left while the right image depicts the planar features more closely.

PINE, CO:

The third and most northern site is located north of Pine, CO and south of Hwy. 285 (Figure 14). This site is situated on a splay of the UPF (Figure 1), approximately nine km NW of the main trace of the UPF. DZ samples from a Tava parent body PN5311 were taken for U-Pb analysis. The matrix is consistent with that of other sites: fine and medium sand suspending granules and pebbles. All clasts are well-rounded to sub-rounded. Granules and pebbles range in size from 2 to 4 mm at the grid observed at this site. Grains are composed of quartz, feldspar and detrital mica. No clay flakes were observed at this outcrop.

A primary sedimentary structure observed at this location is made of laminations, ~1 cm thick (Figure 15) with uniform grain size and composition; "redox" colorations follow the plane of bedding, accentuated by maroon and white stripes.

A second road cut studied on the northern UPF is much larger and contains a parent body and basement-hosted dikes (Figure 16). There were two distinct "types" of Tava parent sandstone. The first is very similar to the parent body at the "Sugarlump" and at the "Duplex," and the second is a maroon quartz sandstone with green intrusions and large lithic fragments of granite. The first has fine and medium grained quartz sand suspending larger grains. The minerals present are quartz (>95%), feldspar and sparse detrital mica (<5%). There were no lithic fragments of granite, despite its proximity to the basement granite (Figure 14).

The second type of parent body was only observed in Pine. Similarly to the first "type," it has a fine and medium quartz grain matrix that supported other

larger grains. The larger grains in this parent body are primarily large (2 to 40mm) lithic fragments of granite (Figure 16). These large fragments were very angular and look very similar to Pikes Peak granite due to the pink pigmentation. Another difference from other parent bodies at this site is that this exposure contains large green patches of material, which is chemically altered groundmass that also contains lithic fragments of granite (Figure 16). XRF analysis revealed that the green material is chlorite.

Overall, a consistent aspect of the parent bodies at the three different sites is the fine and medium quartz sandstone matrix. The larger grains vary in size and abundance of the different minerals. The abundance of lithic fragments of granite also changes from site to site. Pine, CO contains the largest lithic granite fragments, the "Sugarlump" contains a consistent, equal distribution, and the "Duplex" contains the lowest distribution and smallest clasts.

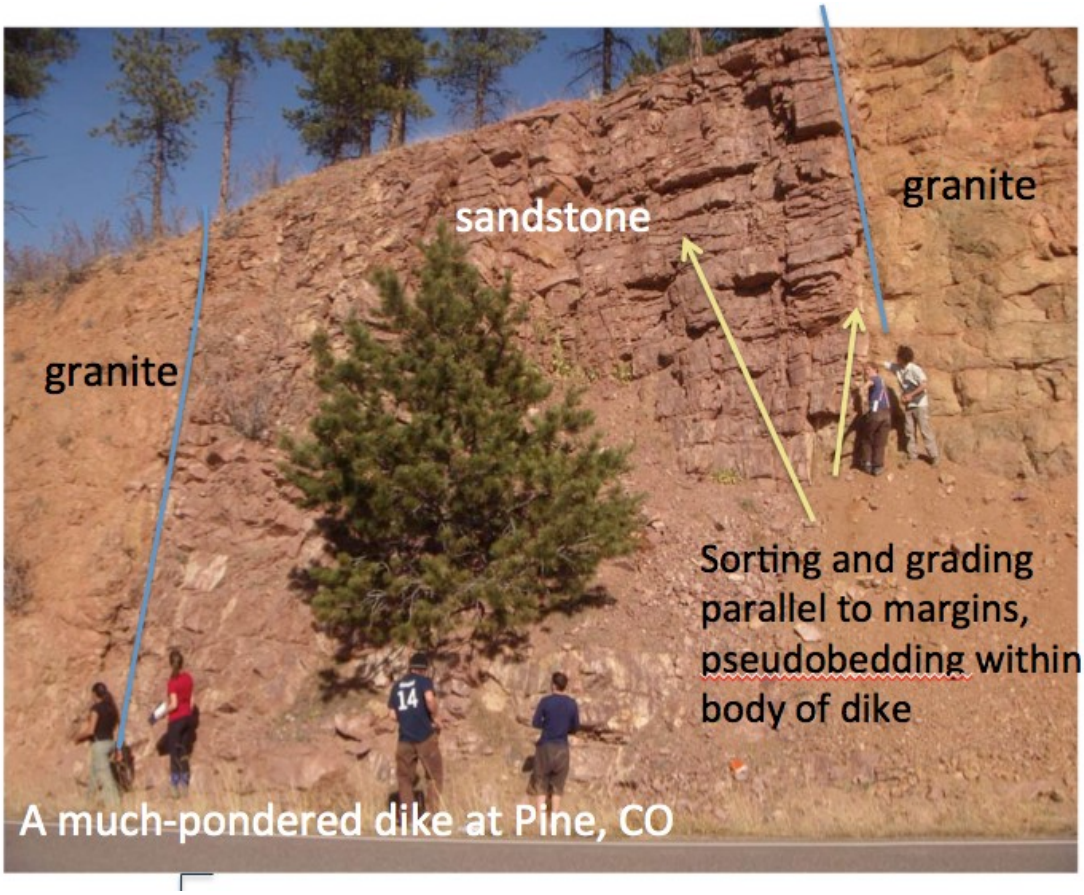

Figure 14: Photo of second site upon a NW splay of UPF at Pine, CO off of Hwy 126 south of Beaver Creek, CO. Tava sandstone parent body emplaced between Pikes Peak Granite. This is the type of parent body that is most similar to those at the "Sugarlump" and at the "Duplex". Figure taken by C. Siddoway.

Figure 15: Fine-scale layering that may represent primary parallel lamination, contorted during liquefaction or mildly folded due to deformation on UPF. Photo taken by S. Shatford.

Figure 16: This photo shows the second type of parent body observed at Pine, CO. Green, irregular mass of material that is mixed within parent sandstone body. The green color corresponds to chemically altered material that has a swirled, irregular contact with the Tava quartz sandstone. Analysis using the XRF shows the green material to be chlorite.

V. RESULTS

ZIRCON DESCRIPTIONS:

Zircons from the Tava formation are transparent and colorless to very light pink. They are sub rounded to well-rounded with varying sizes per sample (Figure 18). The coarsest grain sizes range from 75-135 μm in long dimension in samples SH324BD, PW611 and SH324SI. The smallest visible grains are present in MSCD and KRCD, ranging from 10-25 μm.

i. Parent Bodies:

AP6314 (Figure 17 A)

Zircons from this sample are on average 75 μm, ranging from 10 to 200 μm. This sample exhibits variability in the degree of rounding for the zircons. Most zircon grains are broken fragments from larger grains, resulting in small, angular fragments with one rounded edge, distributed equally across the mount. Discounting the fractured edges, fragments are sub-angular to rounded. Some grains display oscillatory zoning and others contain inclusions that can be seen using backscatter electron (BSE) images. Complete concentric zoning is rarely visible in a single grain, consistent with the abrasion and removal of material that occurs during sedimentary transport. There are few prismatic grains in this sample.

PN5311 (Figure 17 B)

Zircons from this sample are mostly 100 μm on their longest axis; larger grains reach up to 250 μm. The difference in length between the smallest to largest grain is ~175 μm. This sample contains fragments of zircons that are sub-angular;

the rest of the grains are ellipsoidal ranging from sub-rounded to well-rounded. Fractures and inclusions are present in zircons within this sample. Most grains are subhedral and/or have longer lengths than widths. Oscillatory zoning is observed in BSE.

PW611 (Figure 17 C)

Zircons from this sample are on average 125 μm, ranging from 25 to 350 μm. The largest grain is very large and well-rounded. This sample contains angular fragments and elongate grains that make the grain shapes appear rectangular. Fractures and inclusions are present, indicating transported and aged grains. There are fewer small grains in this sample than AP6314 and PN5311. Sporadic large, well-rounded grains placed among smaller, sub angular, rectangular grains best characterize this sample. Oscillatory zoning is present.

SH324HO (Figure 17 D)

Zircons from this sample are on average 75 μm, ranging from 25 to 200 μm. The largest grain is elongate and well-rounded. This sample contains small fragments, but mostly oblong well-rounded grains. Fractures and inclusions are present. Some grains have evidence of partial oscillatory zones. Oblong, well-rounded and small angular fragments best characterizes this sample.

WCHR4 (Figure 17 E)

Zircons from this sample are on average 100 μm and are much larger in general than the DZs obtained in other parent bodies, ranging from 50-250 μm. The size of the grains is more uniform than other samples. The grains are well-rounded with a few prismatic grains and angular fragments. There is oscillatory zoning and inclusions in most grains. Zoning is cut off by fractures but some grains show growth zone on the perimeter.

ii. Dikes

KRCD (Figure 17 F)

Zircons from this sample are on average 75 μm, ranging from 15 to 250 μm lengthwise. The sizes of the DZ grains are much smaller than the parent bodies, and shapes are very angular to well-rounded. The small fragments tend to be more angular, but there are also small, very well-rounded grains. Larger grains are rounded in general and some exhibit elongate, prismatic grain shapes while others are very circular and smooth. There appears to be much more fracturing of the DZs, and presence of inclusions, in this sample. Oscillatory zoning in these zircons is truncated upon broken or rounded margins due to sedimentary transport.

MSCD (Figure 17 G)

Zircons from this sample are mainly angular, fractured and fragmented. Most grains are ~50 μm, ranging from 15 – 150 μm. There are fewer large (>100 μm), rounded grains in this sample. Oscillatory zoning is present in most grains. Overall, the grains in this sample are less rounded and more fractured than other dikes.

Oscillatory zoning can be seen on the grains that don't have fractures; zones are incomplete and have been cut off against the margins of DZs.

SH324BD (Figure 17 H)

Zircons from this sample are ~100 μm, ranging from 20 to 400 μm lengthwise. This sample is best characterized by large, rounded, and subhedral grains placed among small, very well-rounded spherical grains. There are few very angular clasts.

SH324 VE (Figure 17 I)

Zircons from this sample are ~75 μm, ranging from 20 to 200 μm lengthwise. This sample is best characterized by sub rounded to well-rounded grains with a small range in size. This sample lacks large DZs that the other dikes had. Oscillatory zoning is present.

WP113 (Figure 17 J)

Zircons from this sample are ~ 150 μm, ranging from 25 to 300 μm in long dimension. This sample is best characterized by large, sub rounded to well-rounded grains. Smallest grains are uniformly ~ 75 μm in dimension. There are few angular fragments as most of the grains are unfractured. Few prismatic grains are present in this sample. Oscillatory zoning is truncated at grain margins but is present in most grains.

iii. Sill:

SH324SI (Figure 17 K)

Zircons from this sample are ~175 μm, ranging from 25-350 μm lengthwise. This sample is best characterized by fractured and rounded grains, with prismatic, sub-rounded grains. Oscillatory zoning and sector zoning is evident in some grains in this image.

Figure 17 A-K: Labeled backscatter electron (BSE) images of zircon grain mounts taken using the SEM at the Laserchron Center at the University of Arizona, Tucson. Sri Lanka standards appear at the bottom of each mount and can be differentiated by their size, as they are much larger than the Tava DZs. Grains that appear as bright white are not zircons. Some zircon grain maps have been labeled with ages an uncertainty (AP6314, PN5311, PW611, SH324HO, SH324BD, SH324VE, and SH324IS). Yellow circles indicate the number and age of spots that are concordant. Red circles indicate number and age of spots that are discordant. Unlabeled BSE images (WPCHR4, KRCD, MSCD, and WP113) are provided when labeled grain maps were not available.

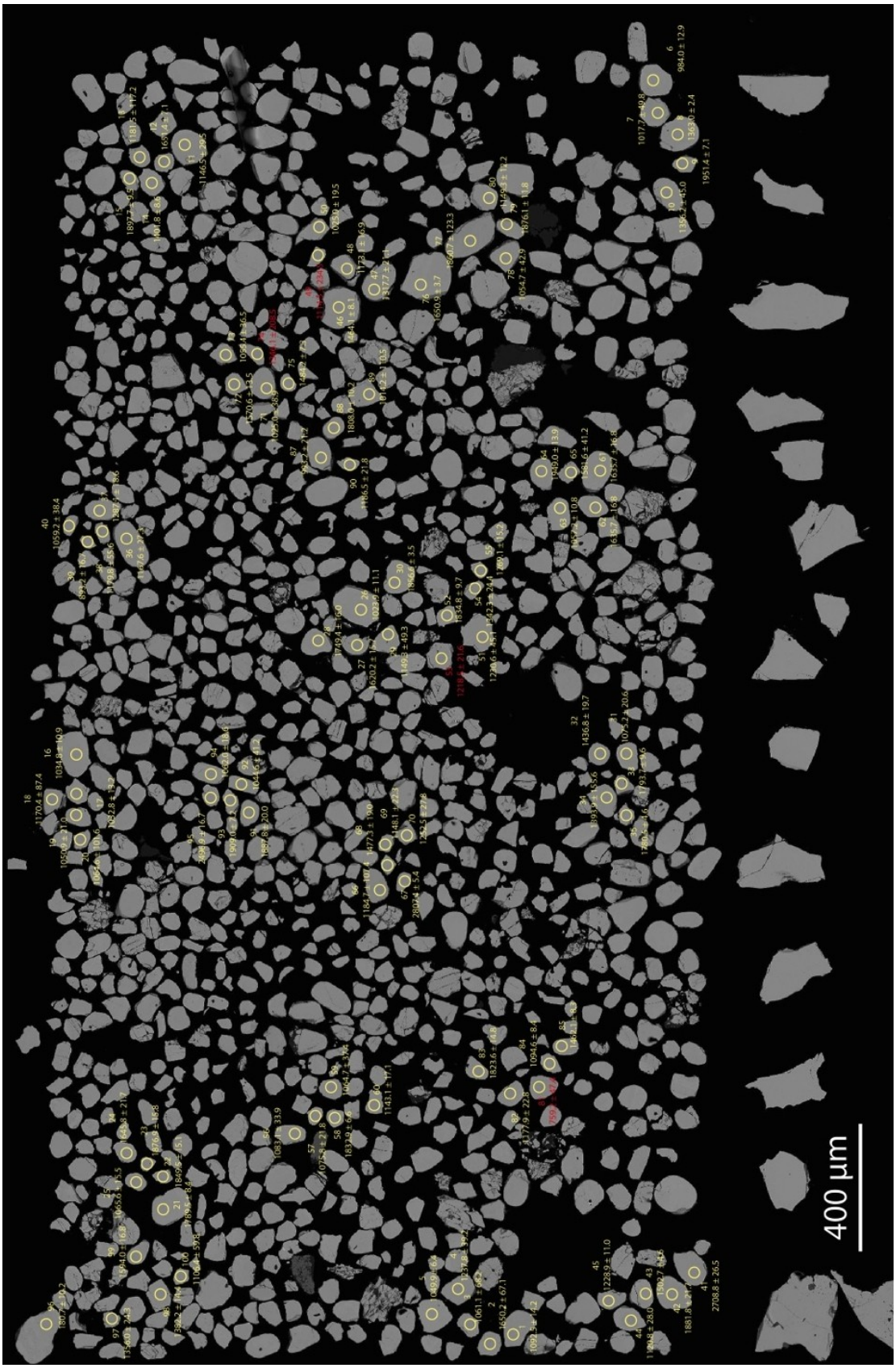

Figure 17A: BSE images of zircon grain mount for sample AP6314.

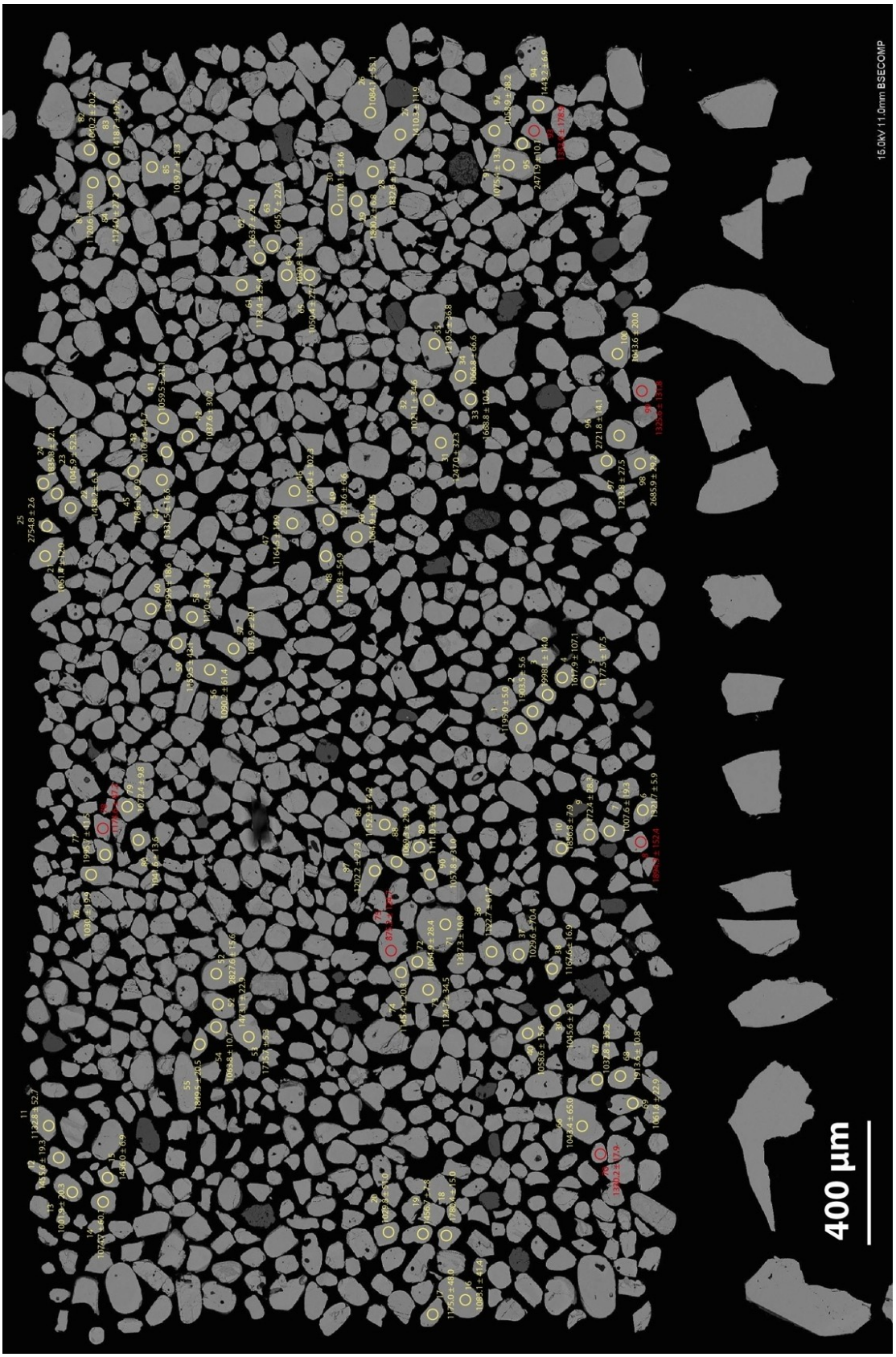

Figure 17B: Labeled BSE images of zircon grain mount for sample PN5311

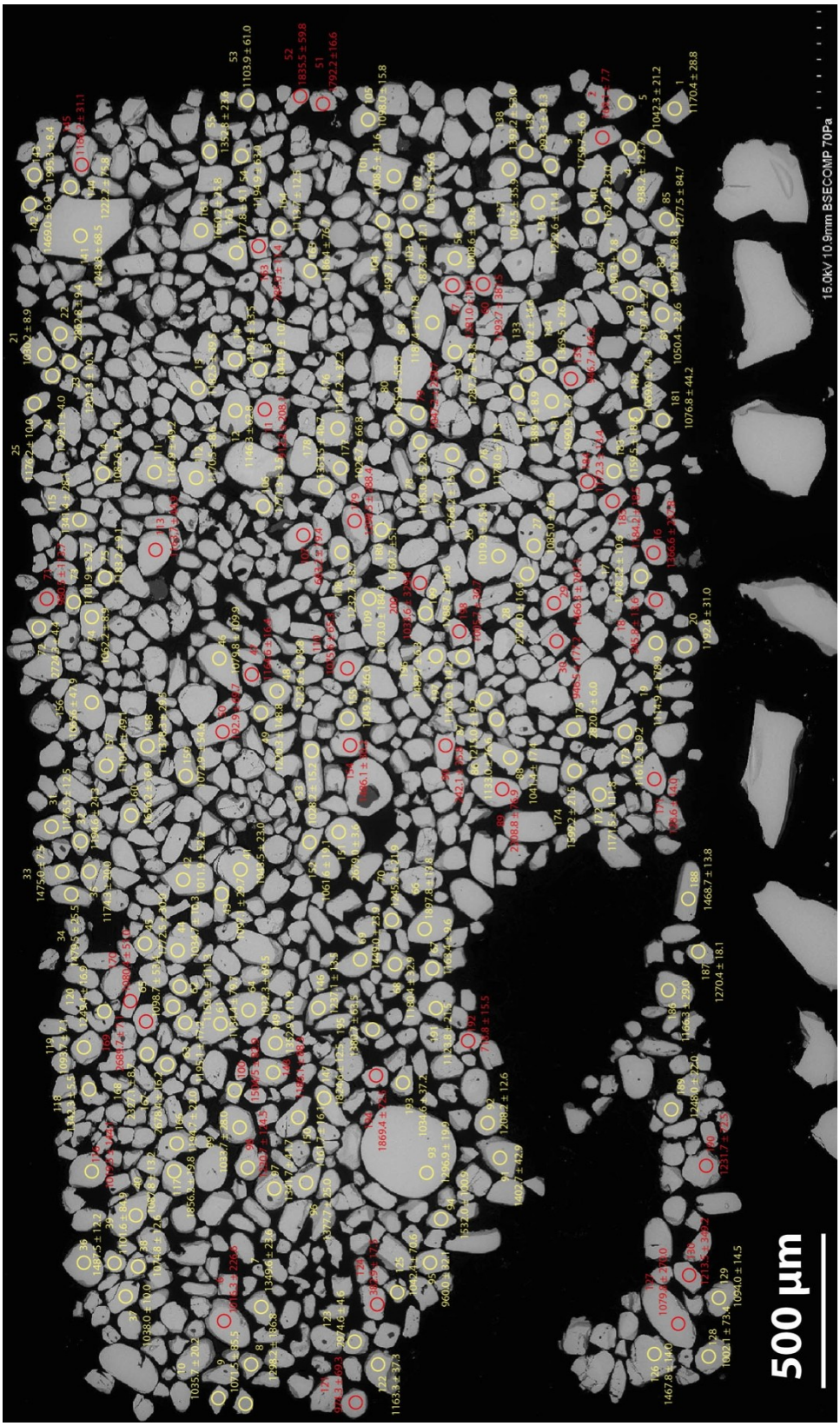

Figure 17C: Labeled BSE images of zircon grain mount for sample PW611

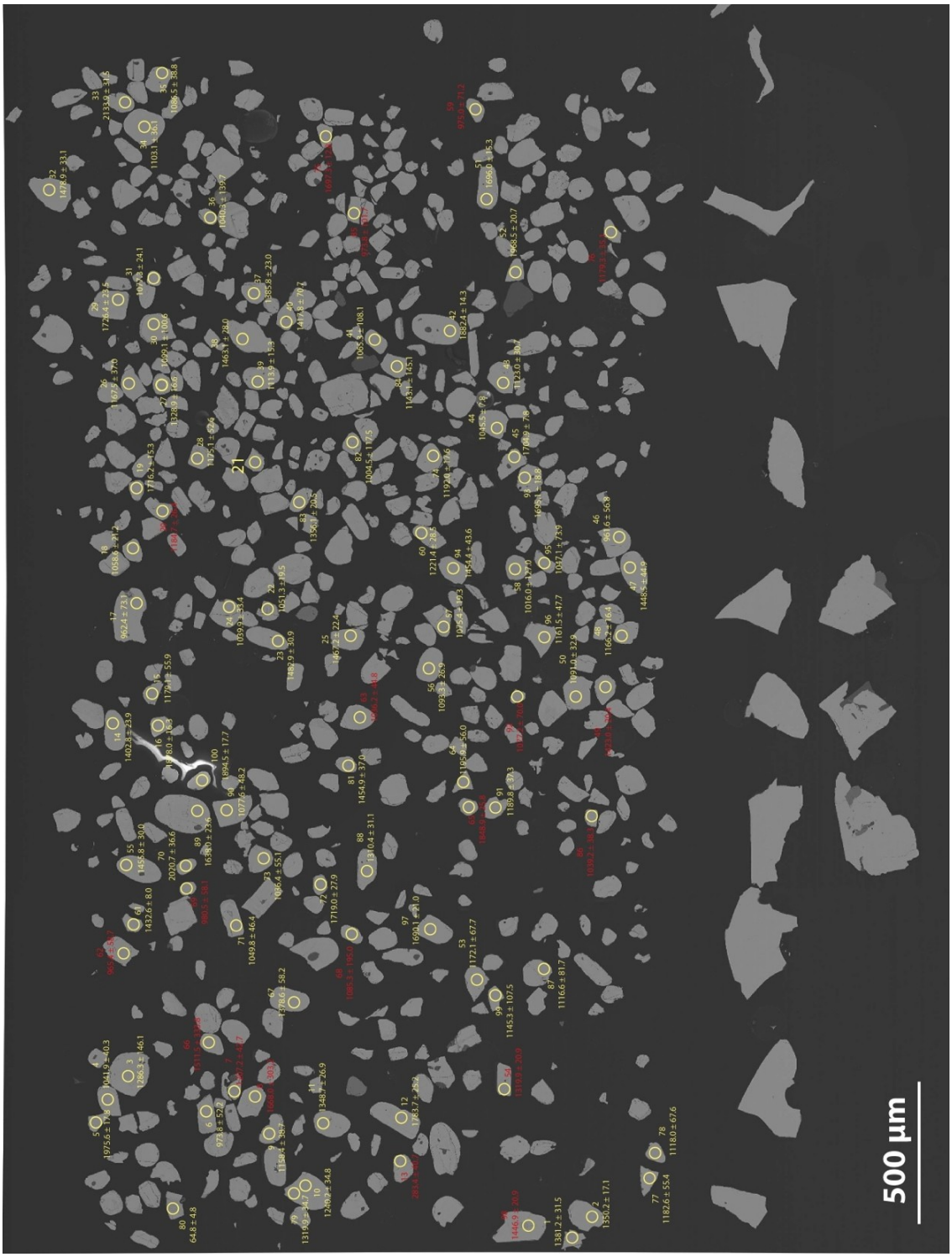

Figure 17D: Labeled BSE images of zircon grain mount for sample SH324HO

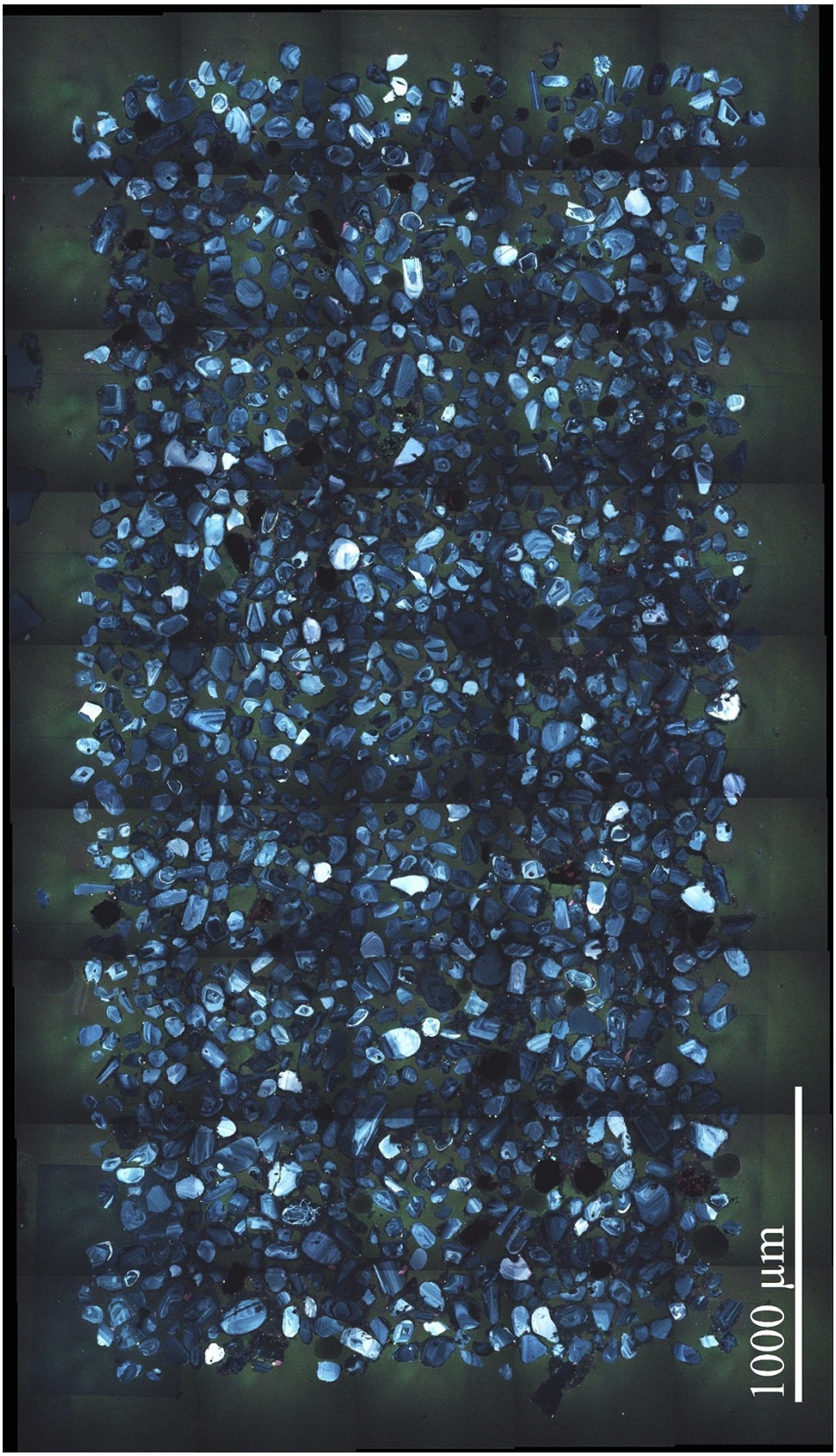

Figure 17E: Unlabeled high-resolution BSE images of zircon grain mount for sample WPCHR4. The blue color is a result of the higher resultion images.

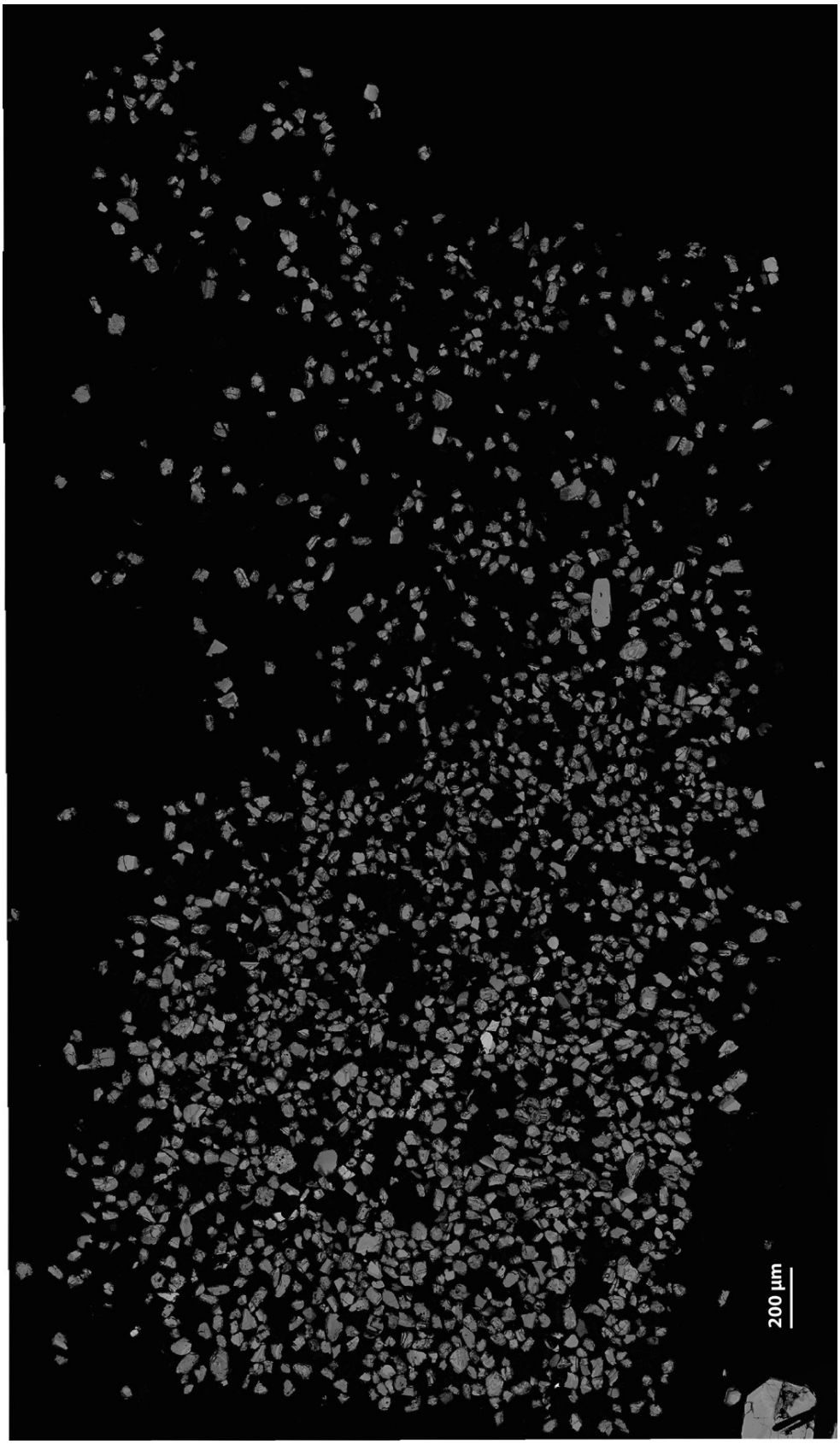

Figure 17F: Unlabeled BSE images of zircon grain mount for sample KRCD

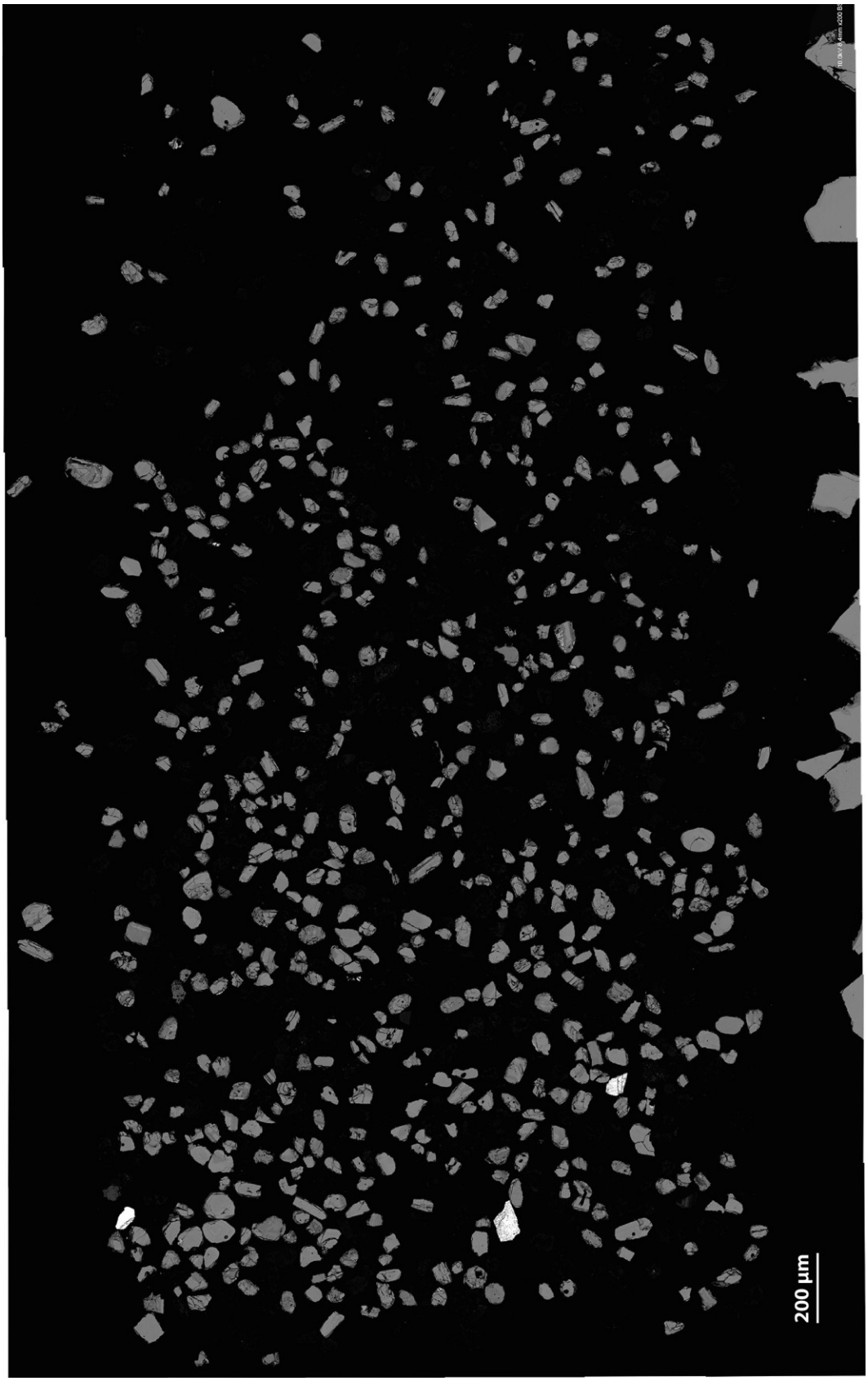

Figure 17G: Unlabeled BSE images of zircon grain mount for sample MSCD

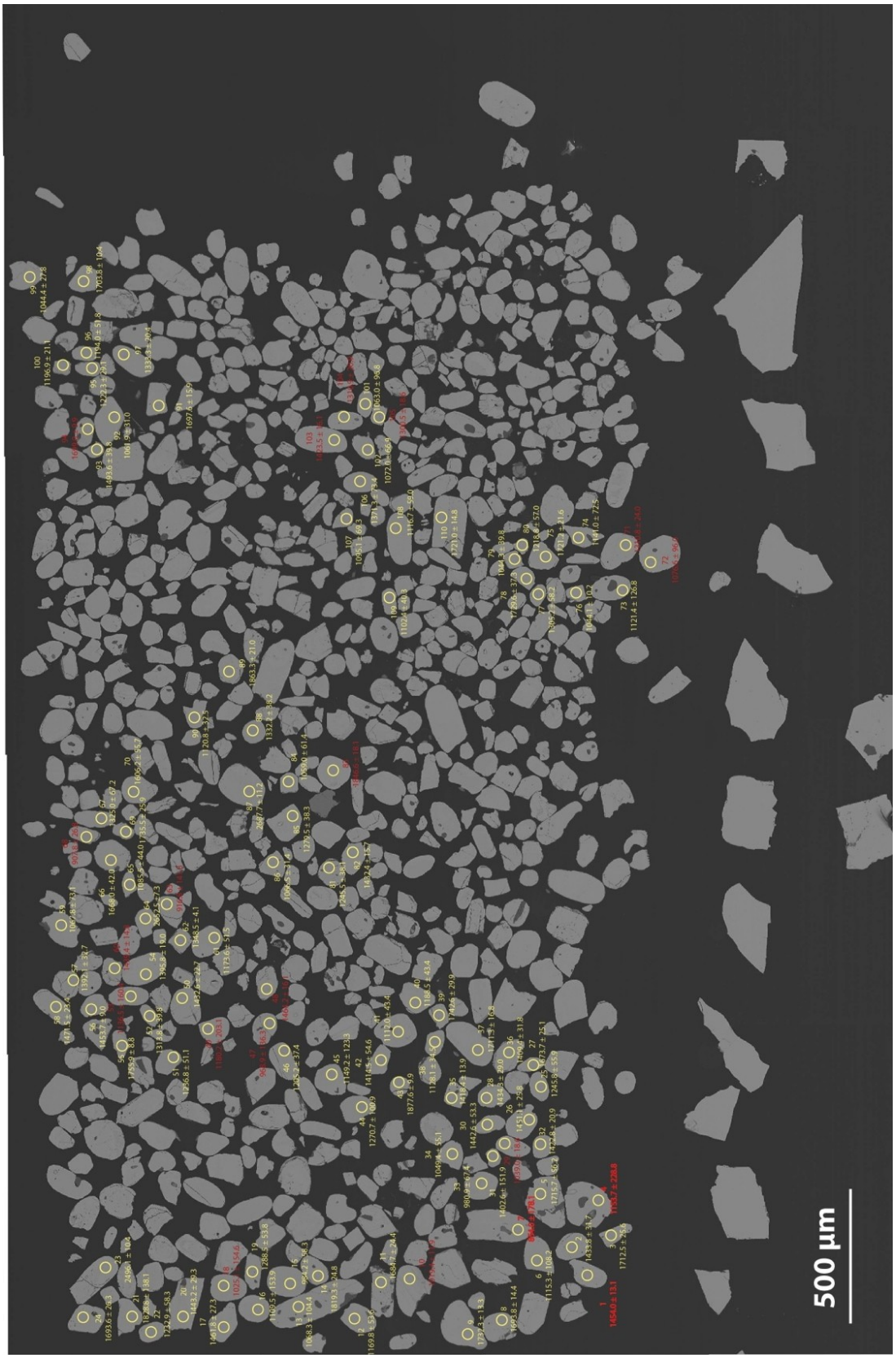

Figure 17H: Labeled BSE images of zircon grain mount for sample SH324BD

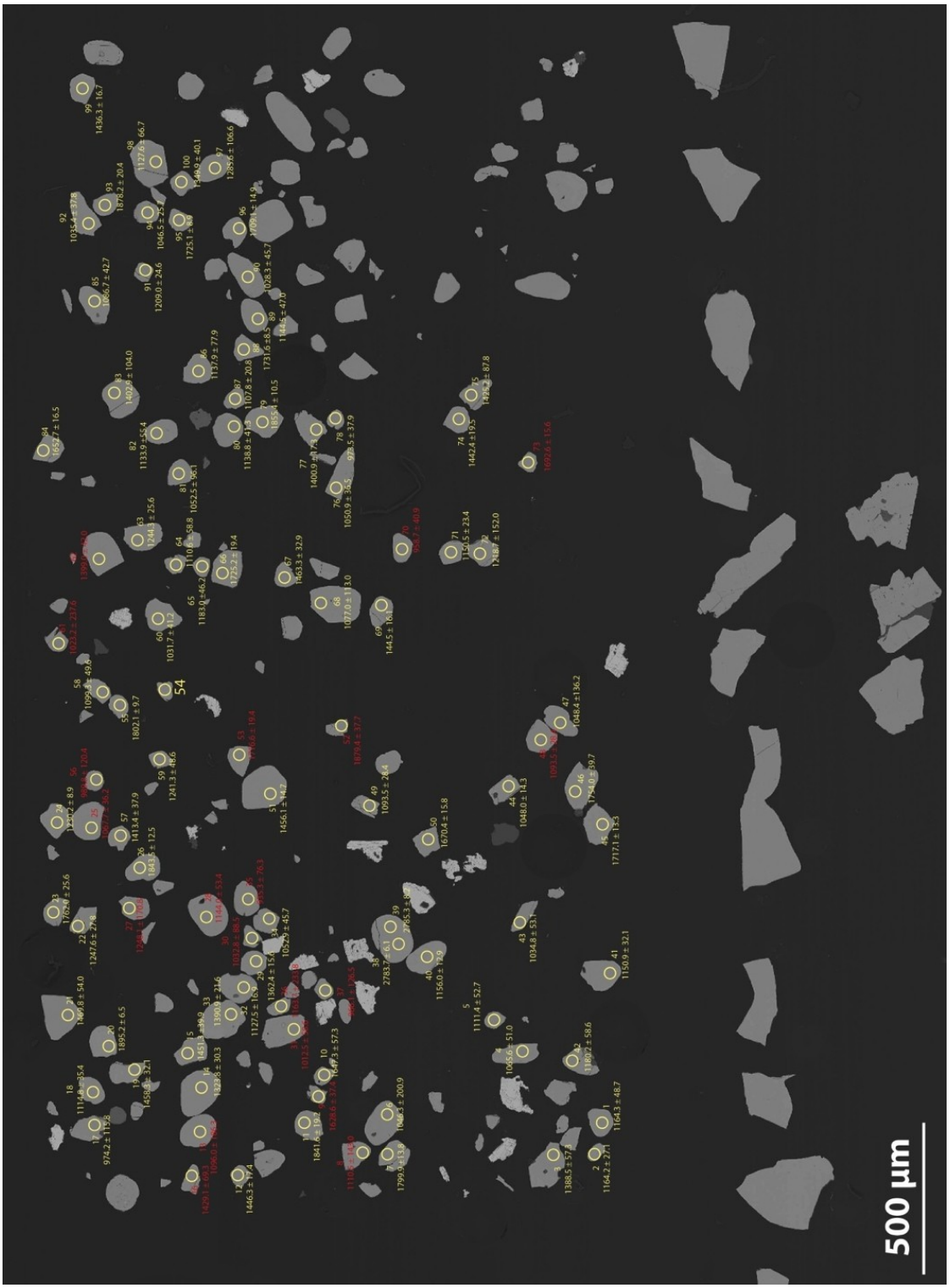

Figure 17I: Labeled BSE images of zircon grain mount for sample SH324VE

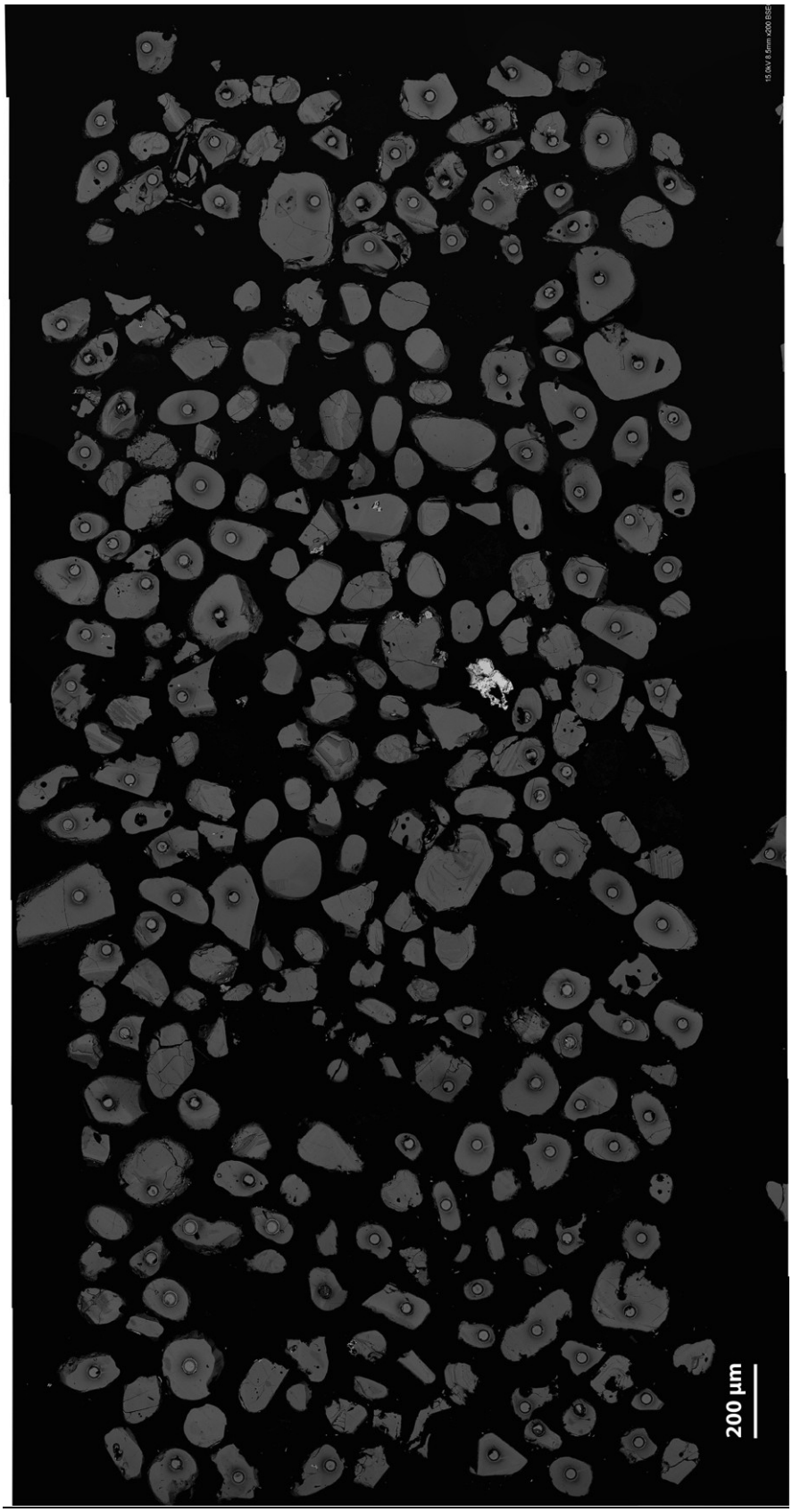

Figure 17J: Unlabeled BSE images of zircon grain mount for sample WP113

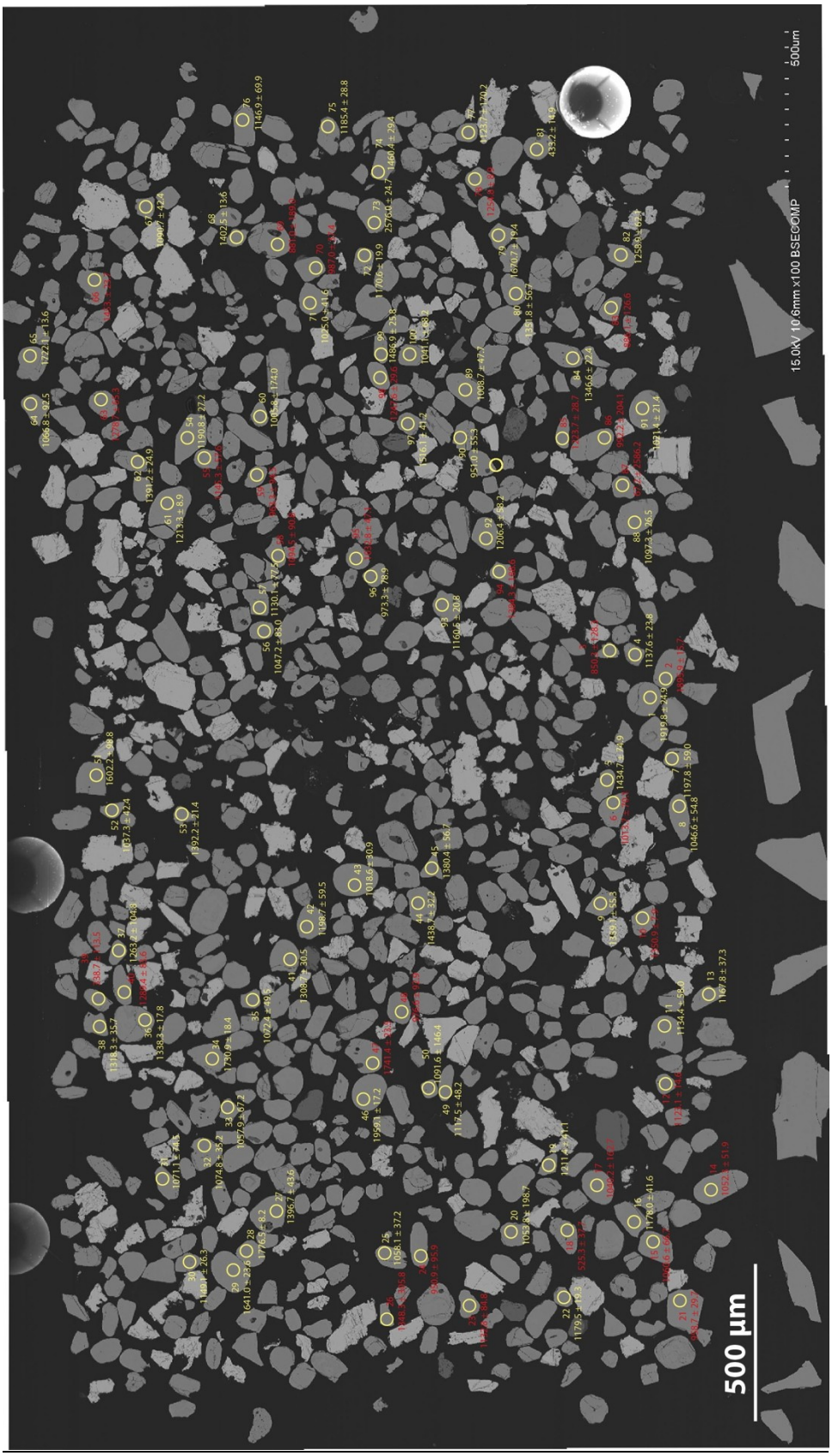

Figure 17K: Labeled BSE images of zircon grain mount for sample SH324SI

U-PB GEOCHRONOLOGY AND NORMALIZED PROBABILITY PLOTS

All analyses were performed at the Laserchron Center at the University of Arizona, Tucson. Laser beam size was 35 μm, except in the few instances when small grain size required the use of a smaller beam of 25 μm. Ages for DZs were calculated using U-Pb geochronology. Ages were eliminated based on concordance between U, Pb, and Th. Ages outside of ± two-sigma were rejected based on discordant isotope ratios shown in the concordia diagram and in Appendix B. Peaks were labeled and abundances were determined using the Age Pick excel macro (Gehrels, 2009) (Figure 18A-K). Peaks on the DZ age spectra are not mentioned if the number of grains is less than 12 but are labeled in their respective figures. A table of age peaks and the number of grains corresponding to that peak is shown in Table 1.

i. Parent Bodies

AP6314, n=94 (Figure 18A)

This sample comes from a fault-bounded Tava sandstone parent body in Arapahoe Pass, CO near the Fourth of July Mine. Laserchron analyses were performed in June 2014. Notable features in this age spectra are a small peak at ~900 Ma; this represents the minimum age groups for this sample; a sharp peak from 1050-1091 Ma that superimposes a shorter, narrower peak at 1228 Ma; and peaks between 1228-1400 Ma. The older peaks contain ≤ 12 grains. Few significant ages > 1228 Ma were obtained. The main feature of this sample is a broad peak from 1050-1228 Ma.

PN5311, n=93 (Figure 18B)

This sample was collected in Pine, CO from a Tava sandstone parent body hosted by PPG. This is the northernmost sample studied from the standpoint of both DZ analysis and sedimentology. U-Pb geochronology analyses were performed in June 2014. This sample has a tall peak at 1056 Ma that forms an element of a broad peak that spans 900-1250 Ma. Remaining peaks are shorter with wide or narrow bases, depending on spread of grain ages. All peaks older than 1239 Ma contain an insignificant amount of grains. The main feature of this sample is a broad peak from 1056-1194 Ma.

PW611, n=156 (Figure 18C)

This sample was collected from the Ptarmigan wilderness north of Dillon, CO; the site is within the Williams Fork Range. U-Pb analyses were performed in June 2014. There are distinct peaks at 1038 Ma and 1177 Ma that make part of a broad peak from 900-1259 Ma. The 1386 and 1473 peaks are older and contain less grains but contribute to the broad base. There are little significant peaks older than 1473 Ma. The prominent features of this sample are a broad peak from 1038-1234 Ma and a shorter, defined peak at 1473 Ma.

SH324HO, n=79(Figure 18D)

This sample comes from a Tava sandstone parent body from “the Sugarlump” in Manitou Springs, CO. U-Pb analyses were performed in March 2014. There is a

broad peak from 950-1300 Ma. There are two older peaks at 1349 Ma and 1434 Ma that contain 13 and 14 grains respectively. These peaks are narrow and sharp. The main features for this sample are the broad peak from 950-1300 Ma and the sharper peaks at approximately 1400 Ma.

WPCHR4, n=121 (Figure 18E)

This sample comes from a Tava sandstone parent body Chrystola, CO. Analyses were performed in May 2013 and January 2014. The youngest peak is dated 1091 Ma and is steep and tall. There is a broad peak that from 900-1350 Ma that includes the 1178, 1271, and 1325 Ma peaks. This is the main feature of this sample as there are no peaks older than 1325 Ma.

ii. Dikes:

KRCD, n=95 (Figure 18F)

This sample comes from a 1.5 m wide Tava sandstone dike hosted by Boulder Creek granodiorite at Keeton Ranch, CO. U-Pb analyses were performed in January 2011 and January 2014. The majority of grains are between 900-1210 Ma, and the ages define a broad peak. There is a broad peak between 1042 and 1175 Ma. Short peaks defined by few grains occur at 1248 and 1359 Ma. The broad peak is the prominent feature in this sample as there are no significant peaks older than 1359 Ma.

MSCD, n=114 (Figure 18G)

This sample comes from a 1.5 m wide Tava sandstone dike from Manitou Springs, CO. U-Pb analyses were performed in January 2011 and in January 2014. The youngest substantial peak occurs at 1086. A broad peak occurs from 900-1248 Ma that includes the 1086, 1159, 1221, and 1248 Ma peaks. There is an intense, sharp peak at 1446 Ma and 1696 Ma. In summary, this sample exhibits three dominant features: A broad, 900-1248 Ma peak, a 1446 Ma peak and a 1696 Ma peak.

SH324BD, n=89 (Figure 18H)

This sample comes from a ~10-20 cm thick Tava sandstone dike hosted by basement gneiss from "the Sugarlump" in Manitou Springs, CO. U-Pb analyses were performed in March 2014. A broad peak occurs from 900-1426 Ma, which includes the 1047, 1079, 1202, 1325, and 1426 Ma aged peaks. Older peaks occur at 1448 and 1705 Ma peaks and are very steep and sharp. There are three prominent features in this sample: a broad 900-1426 Ma peak and two sharply defined peaks at 1448 and 1705 Ma.

SH324 VE, n=79 (Figure 18I)

This sample comes from a Tava sandstone dike that is vertically continuous for ~30 m and 1-1.5 m wide. The dike intrudes the Tava sandstone and gneiss at "the Sugarlump" in Manitou Springs, CO. U-Pb analyses were performed March 2014. Similar to MSCD and SH324BD, this sample contains three major well-defined

peaks. There is a broad peak at 900-1250 Ma that includes peaks at 1053, 1145, and 1229 Ma. Two well-defined peaks occur at 1445 and 1727 Ma. The three notable peaks in this sample are the broad peak from 900-1250 Ma and the two sharp peaks at 1445 and 1727 Ma.

WP113, n= 159 (Figure 18J)

This sample comes from a Tava sandstone dike 0.8 m wide hosted by PPG in Woodland Park, CO. There is a broad peak from 900-1440 Ma that includes peaks at 1040, 1087, 1173, 1316, and 1330 Ma. There are two well-defined peaks at 1445 and ~1700 Ma. The ~1700 Ma contains three ages: 1654, 1731, and 1757 Ma. The major features in this sample are the broad peak from 900-1440 Ma and the three well-defined peaks at 1445 Ma, ~1700 Ma and 1757 Ma.

iii. Sill:

SH324SI, n=67 (Figure 18K)

This sample comes from a Tava sandstone sill 0.75 m wide hosted by a Tava parent body at "the Sugarlump" in Manitou Springs, CO. The youngest age for this sample occurs at 1039. A broad peak occurs from 900-1350 Ma that contains peaks at 1039, 1168, 1208, and 1341 Ma. There are no significant peaks after 1341 Ma. This sample contains one major feature, the broad peak from 900-1350 Ma.

iv. Normalized DZ Spectra

All 11 samples were graphed on a normalized probability plot (Figure 19) to better compare shapes and intensity of peaks. Based on the major features of each DZ spectrum, the samples can be placed into two different groups. One group (orange) is made up of the Tava samples that have one major feature of the broad peak from ~900-1300 Ma. The second group (blue) is comprised of Tava samples that have three major features: the broad peak (~900-1300 Ma) and two well-defined peaks at ~1400 and ~1700 Ma.

Figure 18 A-K: Individual DZ spectra with corresponding concordia plots for 11 Tava samples that underwent U-Pb geochronology using ICP-MS at LaserChron Center.

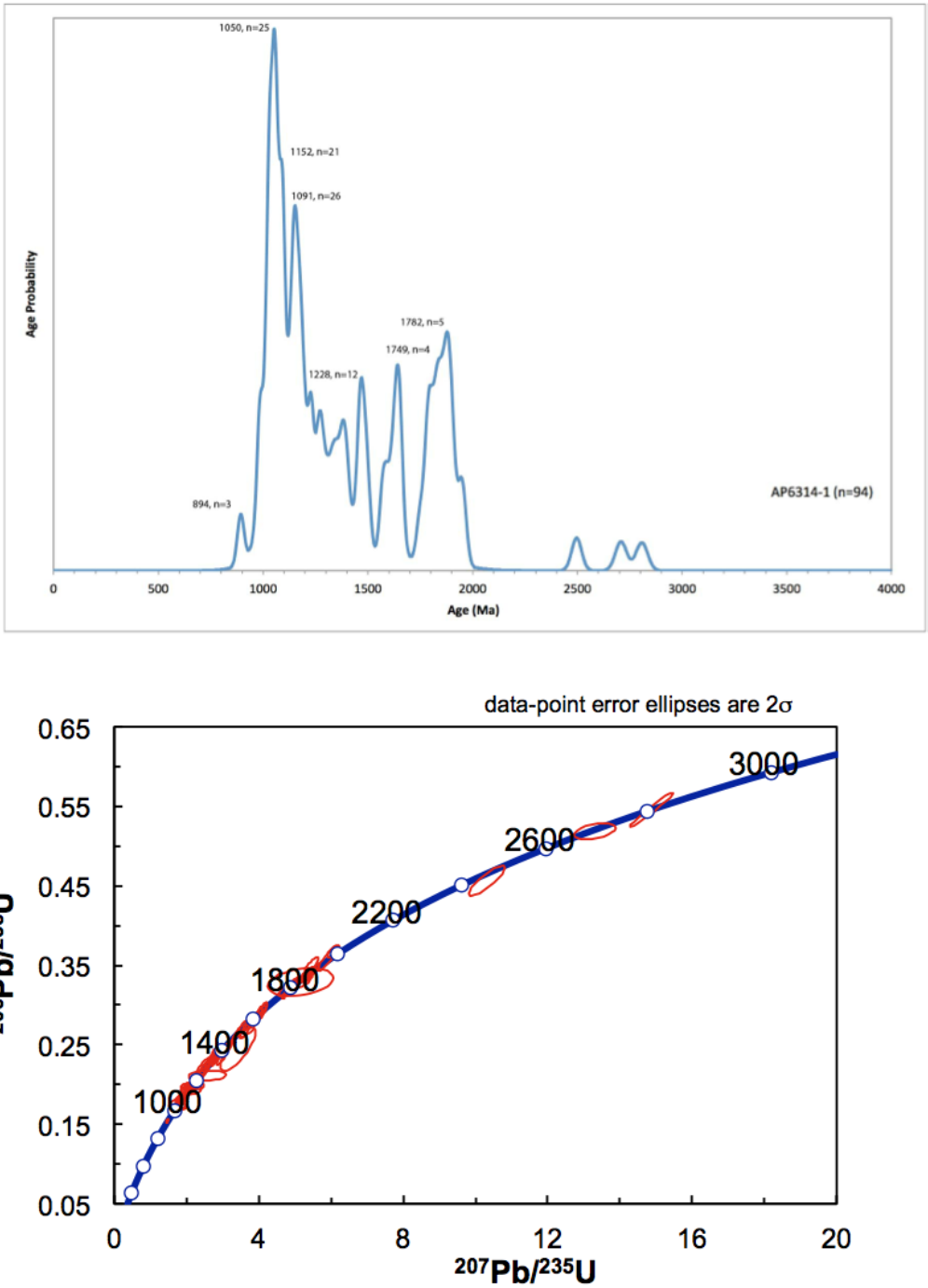

Figure 18A: The concordia plot (below) and the DZ spectra (above) form a unique age distribution for sample AP6314.

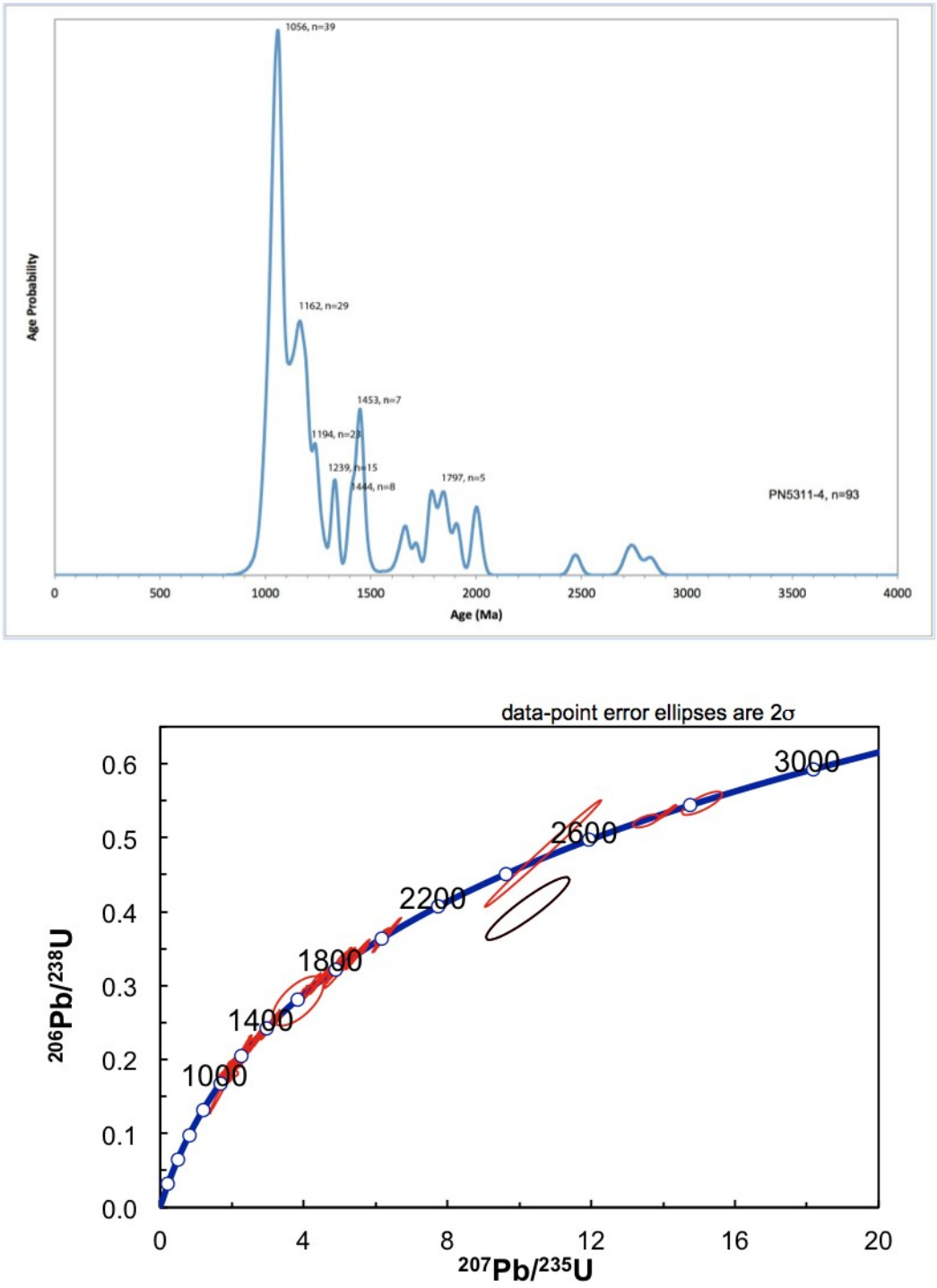

Figure 18B: The concordia plot (below) and the DZ spectra (above) form a unique age distribution for sample PN5311

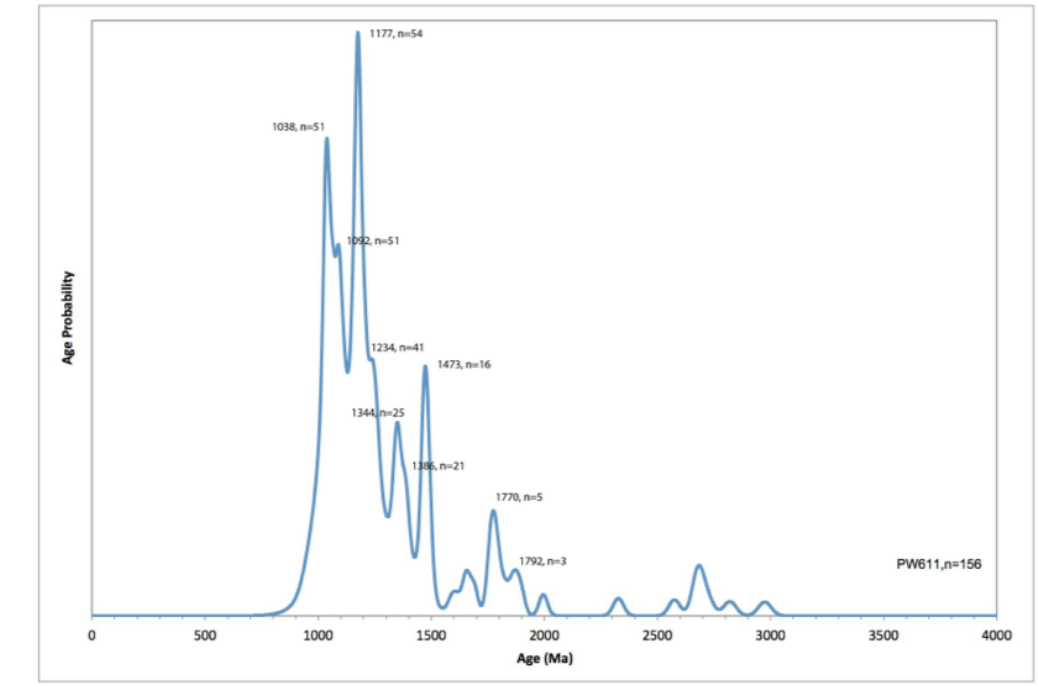

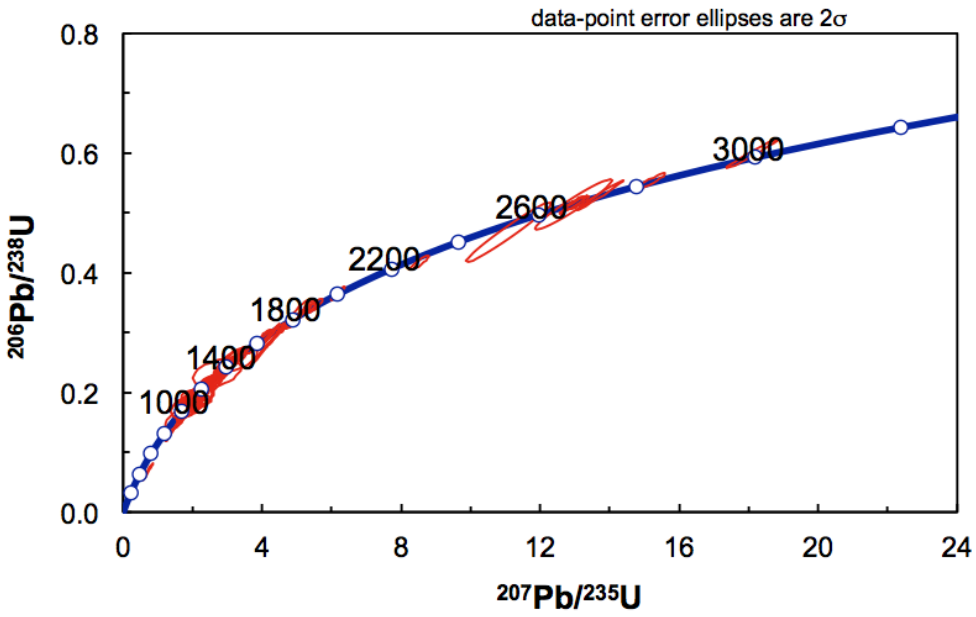

Figure 18C: The concordia plot (below) and the DZ spectra (above) form a unique age distribution for sample PW611

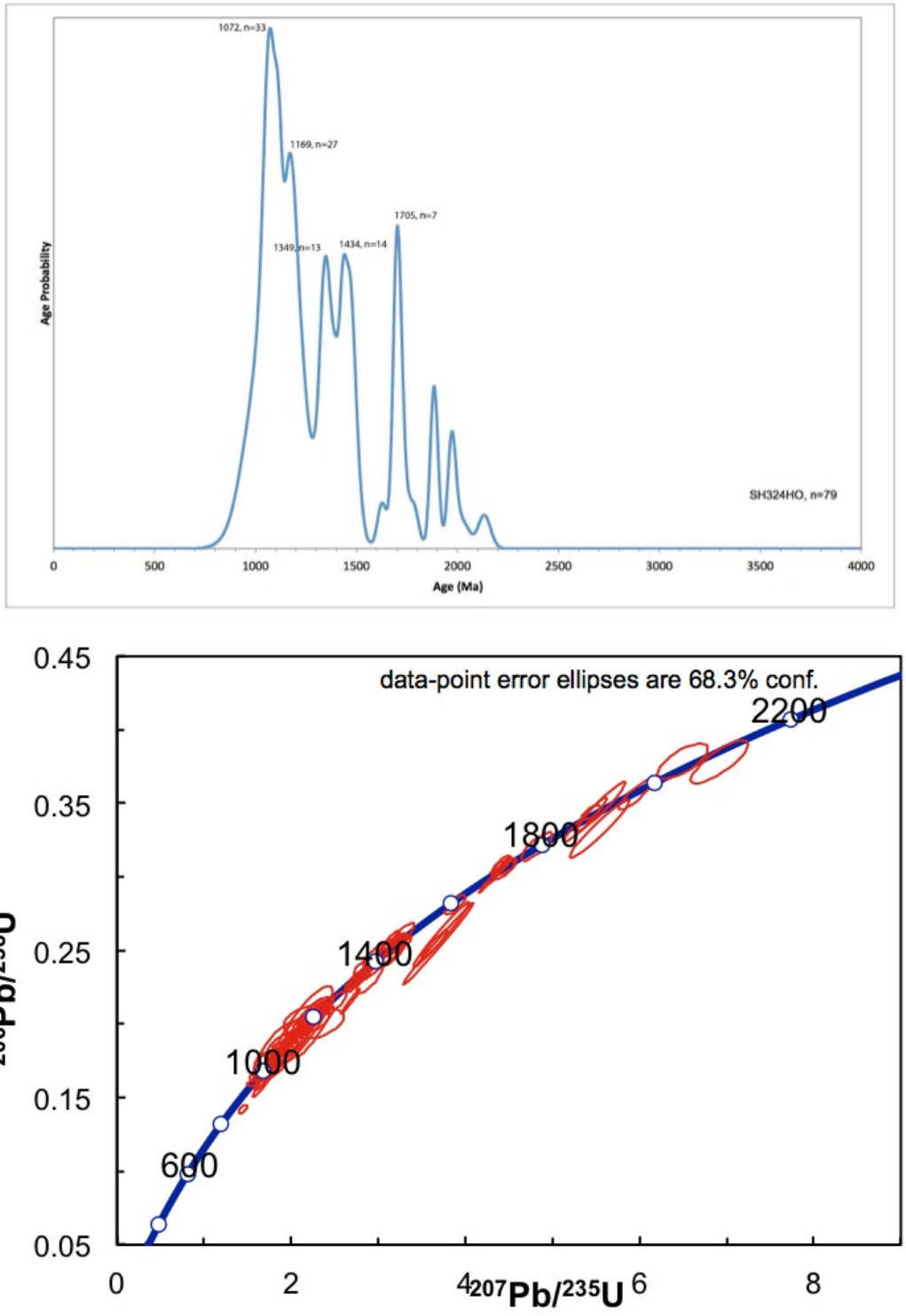

Figure 18D: The concordia plot (below) and the DZ spectra (above) form a unique age distribution for sample SH324HO

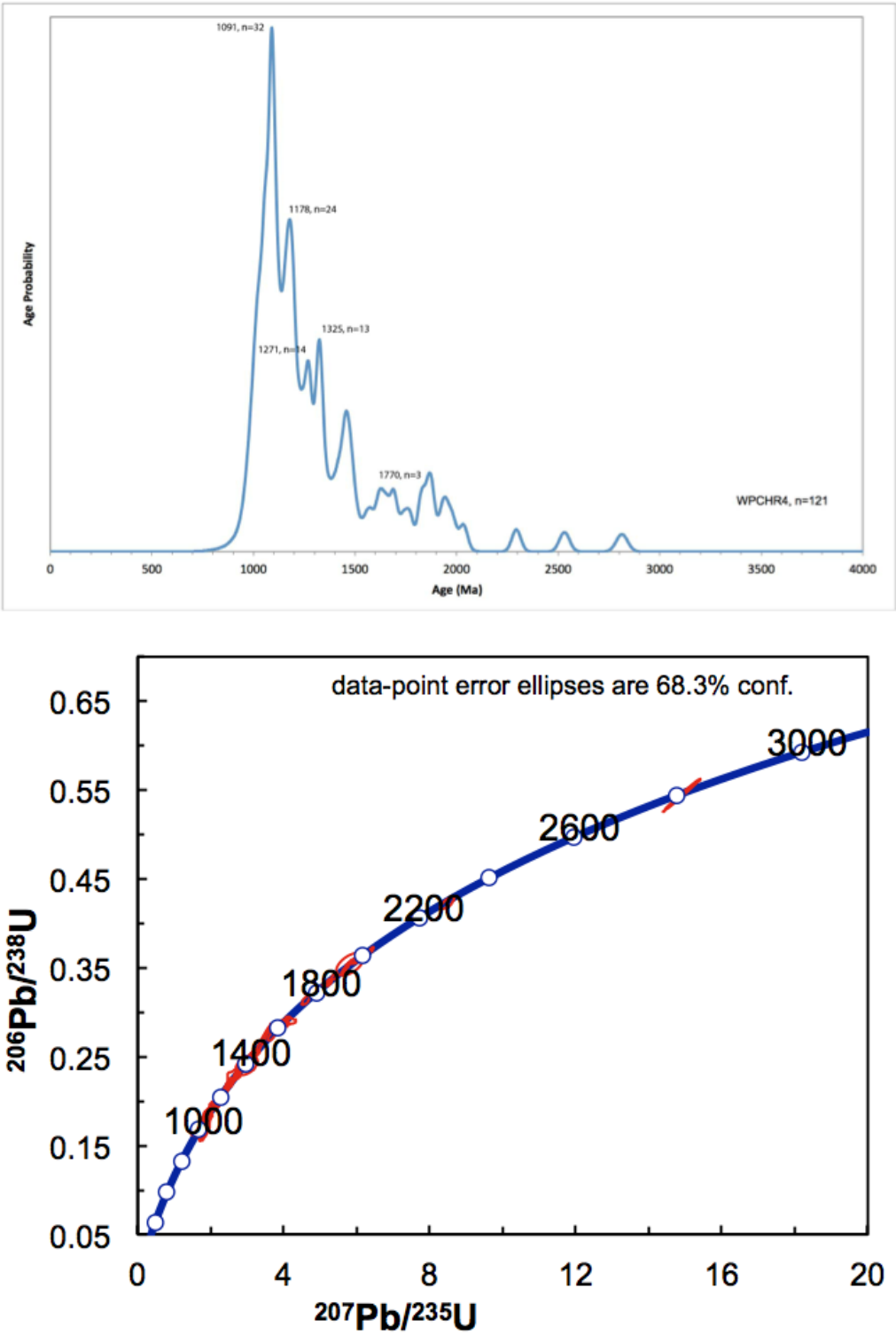

Figure 18E: The concordia plot (below) and the DZ spectra (above) form a unique age distribution for sample WPCHR4

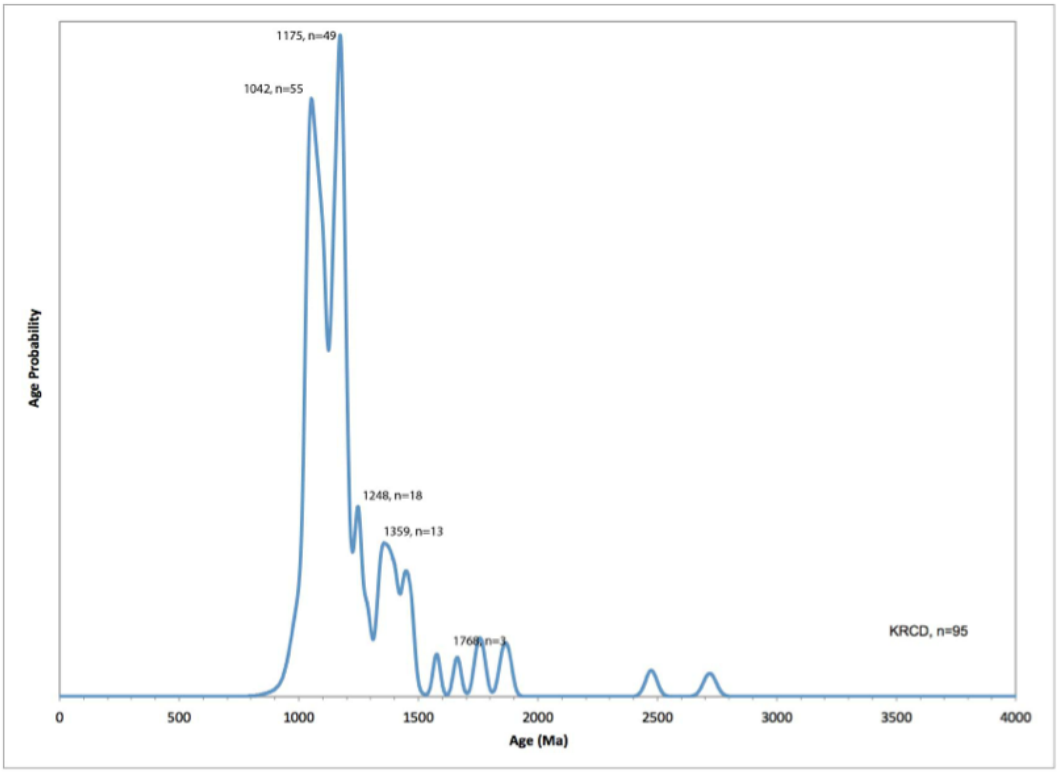

Figure 18F: The DZ spectra (above) form a unique age distribution for sample KRCD. Concordia plot is not available for sample KRCD.

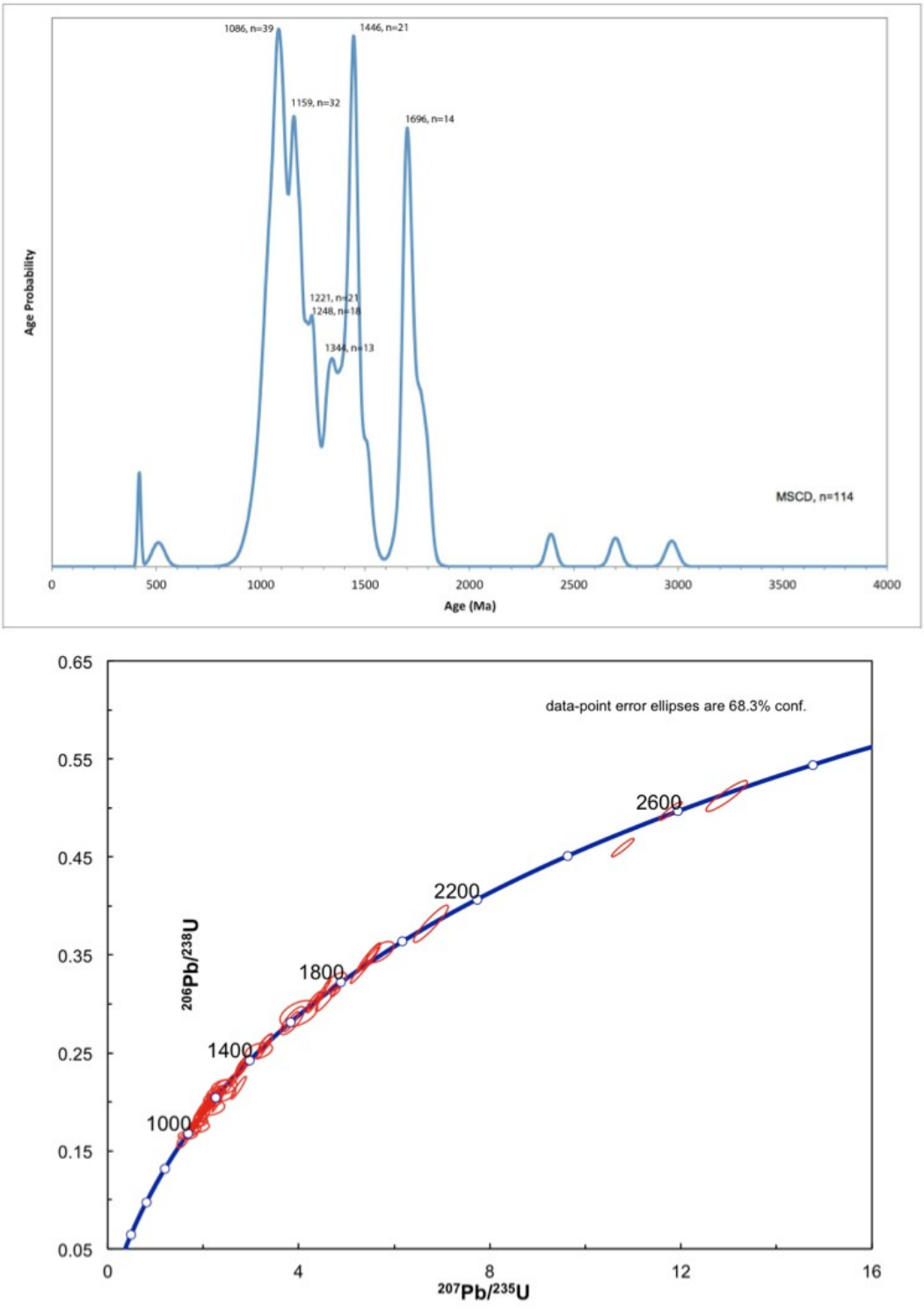

Figure 18G: The concordia plot (below) and the DZ spectra (above) form a unique age distribution for sample MSCD

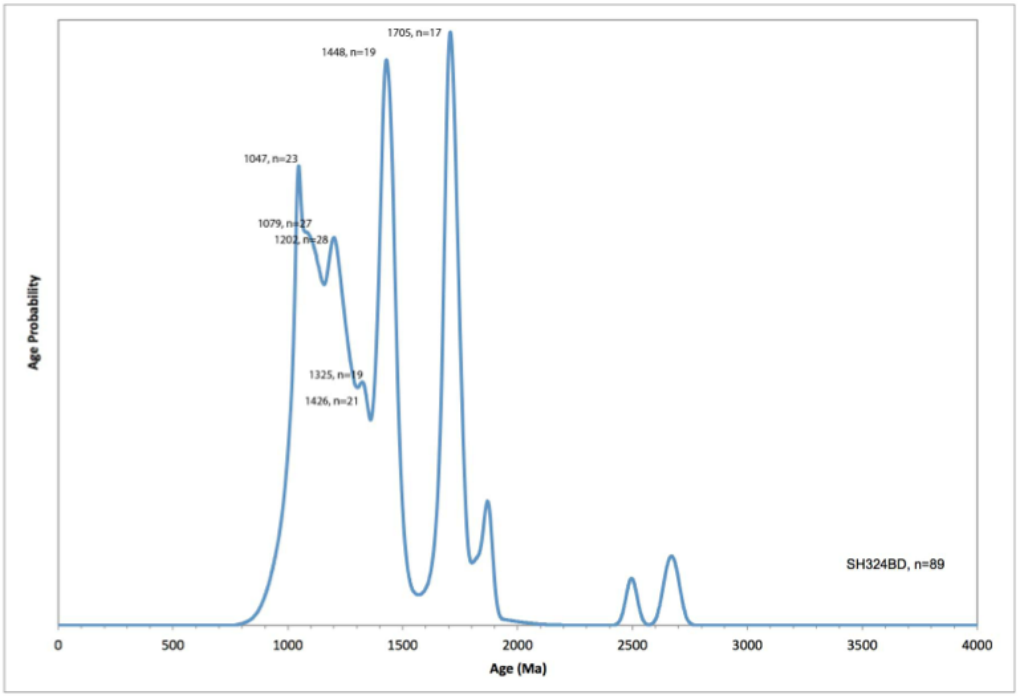

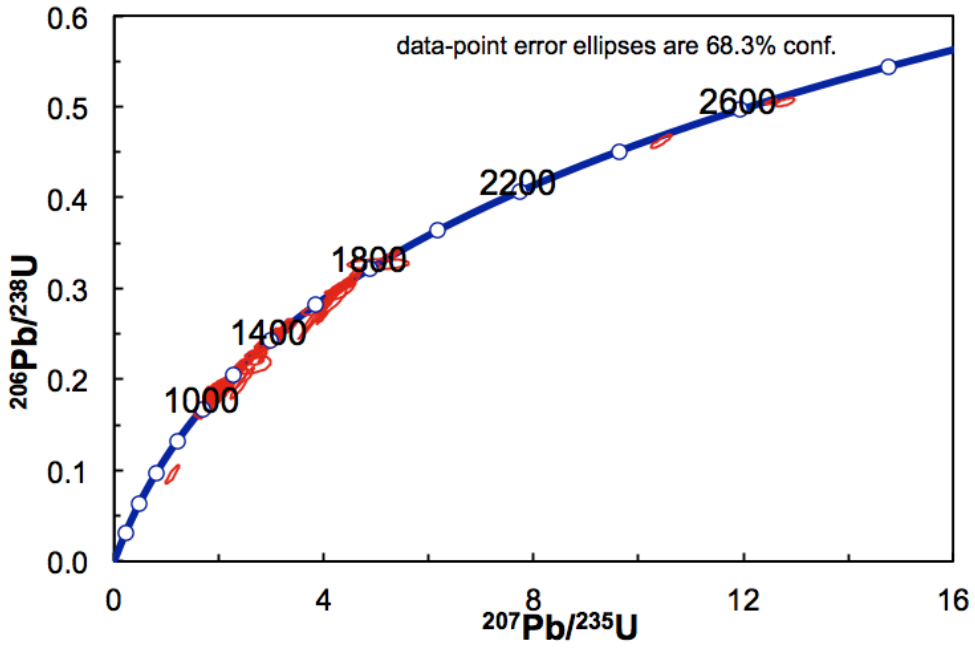

Figure 18H: The concordia plot (below) and the DZ spectra (above) form a unique age distribution for sample SH324BD

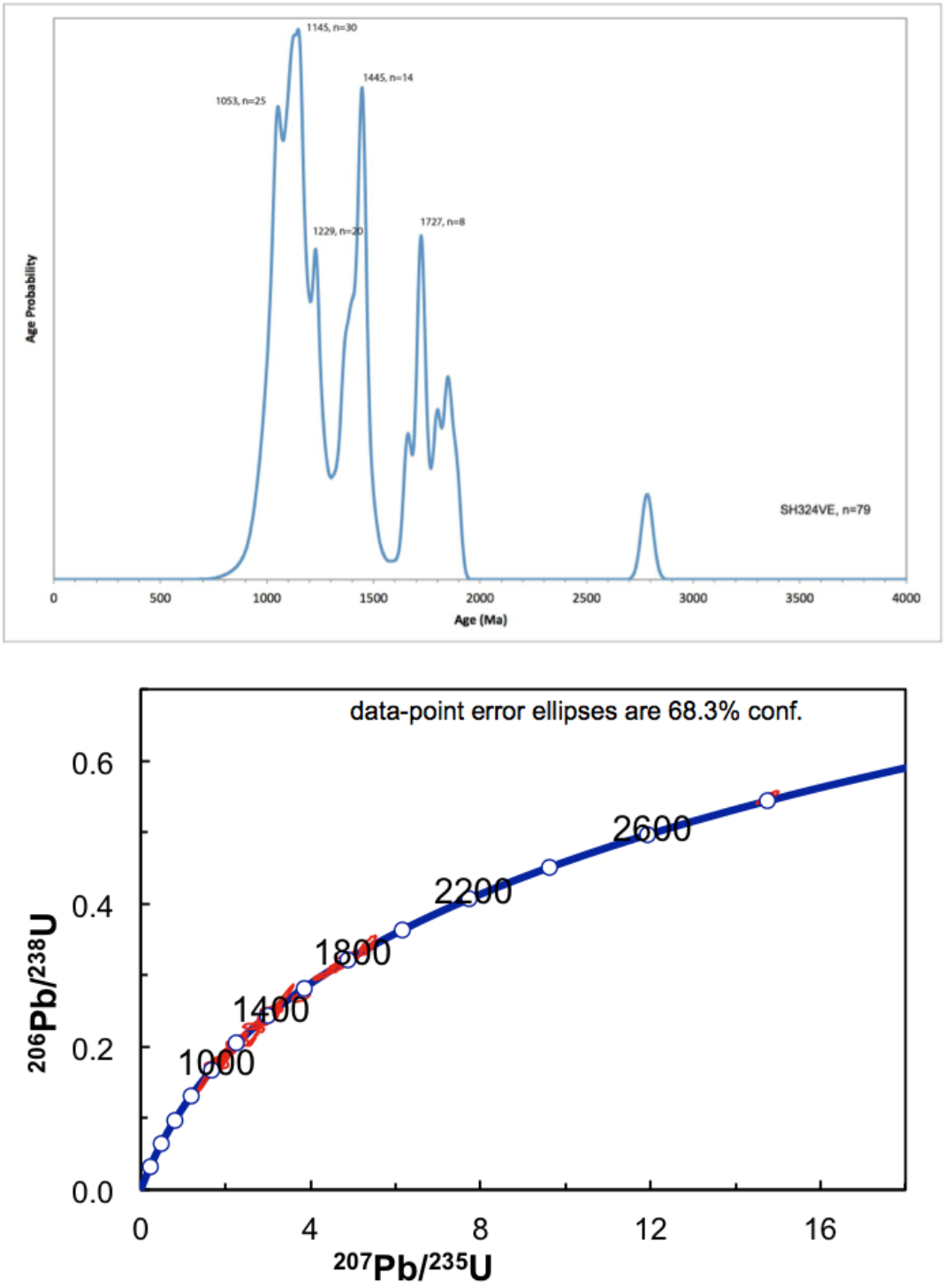

Figure 18I: The concordia plot (below) and the DZ spectra (above) form a unique age distribution for sample SH324VE

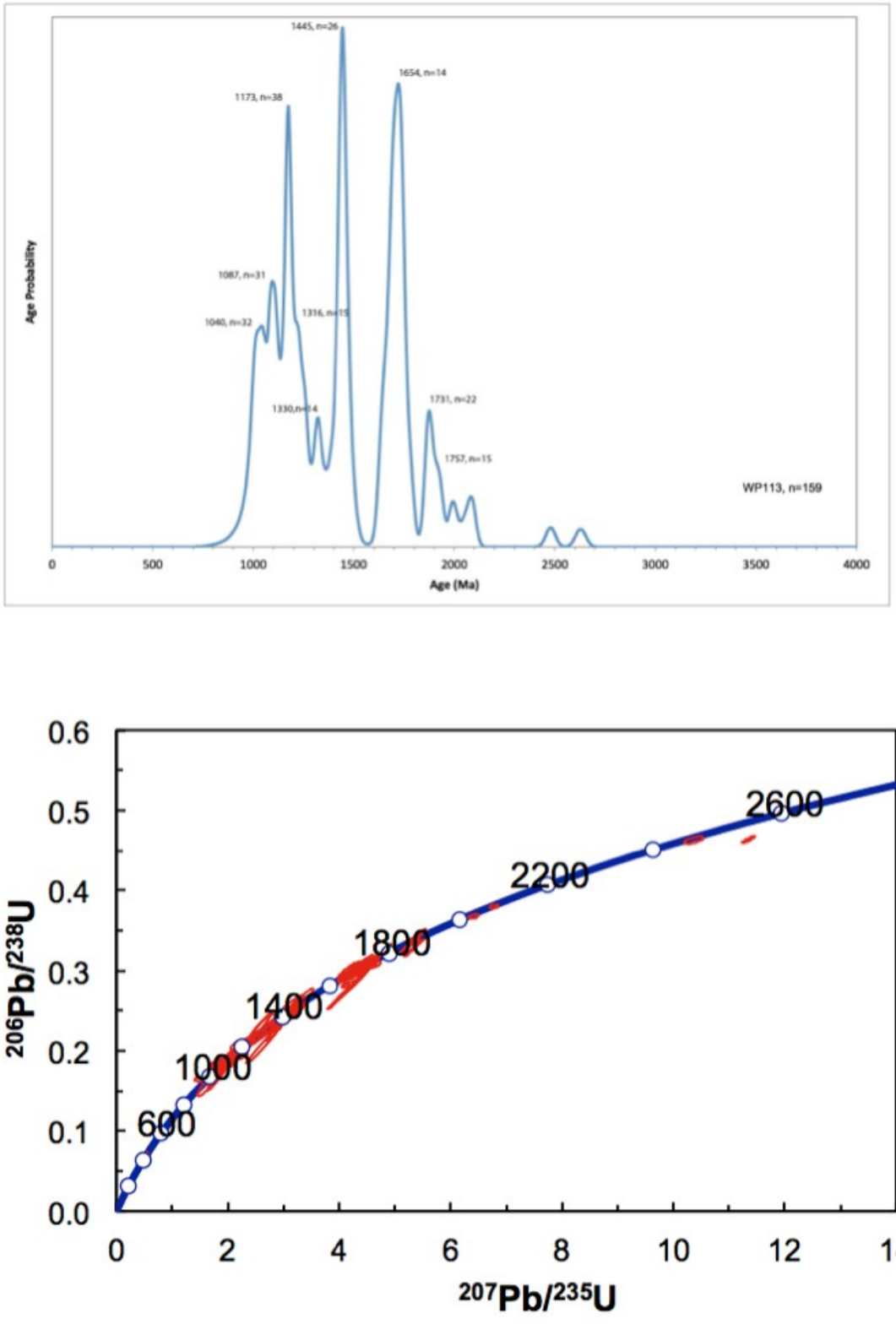

Figure 18J: The concordia plot (below) and the DZ spectra (above) form a unique age distribution for sample WP113

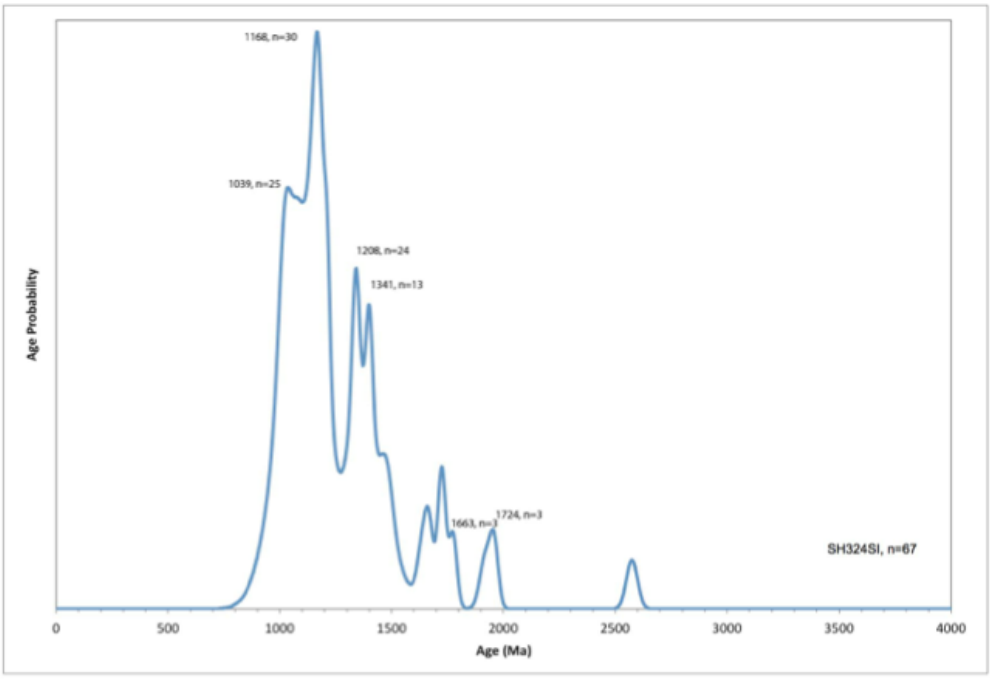

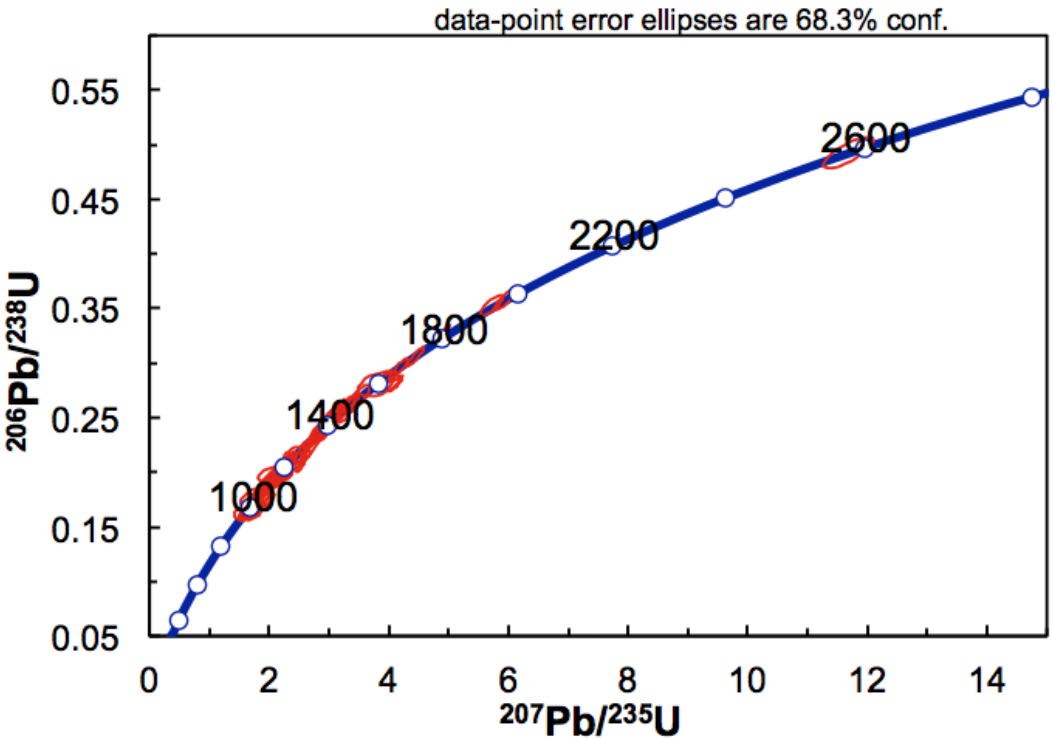

Figure 18K: The concordia plot (below) and the DZ spectra (above) form a unique age distribution for sample SH324SI

Table 1: The peak ages of the DZ spectra from Figure 18 A-K are located in this table. Peak ages are ordered from youngest to oldest. Peaks with < 12 grains were considered insufficient to be considered a significant peak and were not included in this table, but are in Appendix C. Peaks were calculated using G. Gehrels Age Pick excel macro.

Sample	Peak Age	# Grains
AP6314	1050	25
	1091	26
	1152	21
	1228	12
PN5311	1056	39
	1162	29
	1194	23
	1239	15
PW611	1038	51
	1092	51
	1177	54
	1234	41
	1344	25
	1386	21
	1473	16
SH324HO	1039	25
	1168	30
	1208	24
	1341	13
WPCHR4	1091	32
	1178	24
	1271	14
	1325	13
KRCD	1042	55
	1175	49
	1248	18
	1359	13
	1468	12
MSCD	1086	39
	1159	32
	1221	21
	1248	18
	1344	13
	1446	21
	1696	14
SH324BD	1047	23
	1079	27
	1202	28
	1325	19
	1426	21
	1448	19
	1705	17
SH324VE	1053	25
	1145	30
	1229	20
	1445	14
WP113	1091	32
	1178	24
	1271	14
	1325	13
SH324SI	1039	25
	1168	30
	1208	24
	1341	13

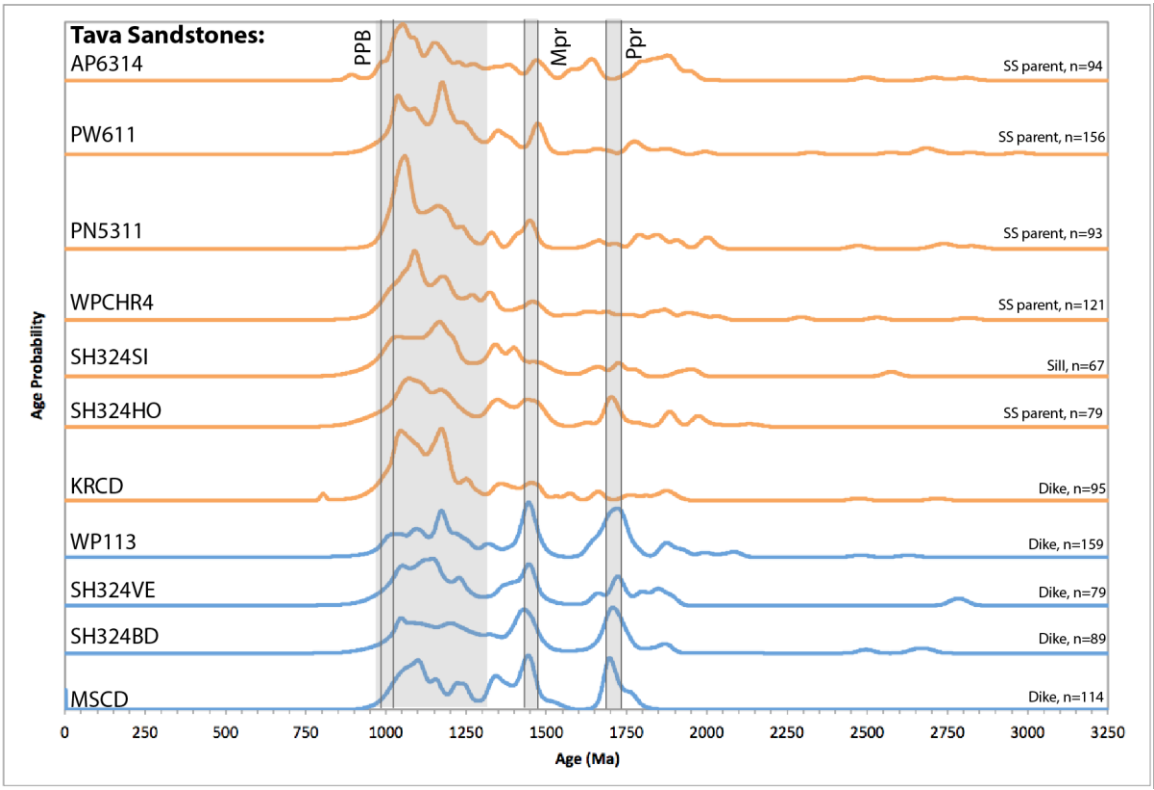

Figure 19: Normalized probability plot comparing all 11 Tava samples based on the abundance of ~1.4 and ~1.7 Ga detrital zircons, reflected by the size of the ~1.4 and ~1.7 Ga age peaks. The orange spectra correspond to large sandstone parent bodies or early dikes while the blue spectra correspond to cross cutting dikes. The ~1.4 and ~1.7 Ga aged peaks are sharp and well defined in the younger dikes. We interpret this to mean that exhumation of crystalline bedrock to the surface, erosion and incorporation of locally derived zircons in quartzose sediments occurred during the time of accumulation and remobilization of Tava.

Alternatively, the Tava sandstone dikes contain sediment that was earlier deposited, more deeply buried and contained a higher abundance of locally derived detrital zircons eroded from already exhumed Colorado bedrock, and then was buried by an influx of sediment with DZs derived predominantly from Grenville sources.

The age span of plutonic sources shown with narrow bars (PPB-Pikes Peak Batholith, Mpr-Mesoproterozoic plutons, Ppr-Paleoproterozoic plutons) and the age of Grenville plutonism is indicated by the broad grey shaded area.

SCANNING ELECTRON MICROSCOPE IMAGES:

The purpose of SEM images was to determine if some of the well-rounded quartz and zircon grains were transported by wind. Grains transported by fluvial systems can be well-rounded but are usually more ellipsoidal in shape, have smooth surfaces, and are transparent. Aeolian transported grains are also well-rounded but are more spherical in shape, have pits on the surface, and are frosted (not transparent). Quartz grains from all seven samples exhibit pitted and frosted surfaces. Most grains are very spherical. Clasts ranged from 20-500 μm (Figure 8B).

Zircon grains are also very well-rounded with a few prismatic grains present. Their surfaces are extremely smooth. Fewer pits existed on the surface of the zircon grains than on the quartz grains because zircon grains are much more resistant to surface processes. Overall, zircons were much smaller and had a higher degree of rounding than the selected quartz grains, ranging in size from 40-250 μm (Figure 8A). In summary, the SEM images provided evidence that some of the hand picked, well-rounded quartz and zircon grains resulted from aeolian transport.

SEDIMENTARY RESULTS:

The notable differences among the three sites were the structures and the presence or absence of lithic granite fragments. Overall, the mineral composition, grain size, and degree of rounding of grains in the parent bodies were very similar. The most prominent outlier of the parent bodies was in Pine. The green shapeless body (Figure 16) that contains large (10 to 20 mm) clasts of lithic fragments of granite was only observed at that outcrop.

The sedimentary characteristics of the dikes had more differences than did the parent bodies. For example, dikes had larger clasts, more variable mineral composition than the parent bodies, and varied in shape, extent and width. The dikes at the Sugarlump varied greatly in sedimentary characteristics. The basement-hosted dike (SH324BD) has very large quartz pebbles and coarse grained sand matrix (0.5-1.0 mm) while the vertical dike (SH324VE) has fine and medium grained sand matrix (0.13-0.5mm) and contains some green clay. The sill (SH324SI), however, had sedimentary characteristics very similar to the parent bodies at the "Sugarlump." The dikes at the "Duplex" were hosted by Tava sandstone parent bodies and were lighter in color but similar in grain size and composition to dikes at the other sites. In summary, dikes exhibit variation in sedimentology while the parent bodies show more consistent features.

VI. Discussion

The goal of this thesis research is to explore the use of DZ spectra of the Tava sandstone in combination with physical characteristics (crosscutting relationships, sedimentology, etc.) to make inferences about the paleoenvironment of Rodinia during the Proterozoic. The DZ samples were quantitatively compared using statistical analysis. The weighted means of each peak in the DZ spectra of Tava were be compared to the U-Pb ages of zircons taken from local plutonic and metamorphic sources in Colorado to determine where the ~1.4 and ~1.7 Ga aged peaks originated from. Weighted means, margin of error, and number of grains corresponding to the weighted mean for all 11 Tava samples is summarized in Table 4. Then, sedimentology of sandstone parent bodies and injectites will be discussed with respect to the DZ spectra of 11 Samples.

COMPARISON OF DZ ABUNDANCES AND AGES WITH K-S TEST

A way to quantify the similarity in provenance between Tava samples is by using the Kolmogorov-Smirnoff (K-S) statistical comparison. The K-S test can determine whether two samples are not from the same parent source but is unable to confirm the two are from the same source using error and the Cumulative Difference Function (CDF) (related to normalized probability plot). The K-S test compares the differences between CDFs for two samples; the larger the difference, the smaller the P-value. P-values produced by the K-S test are sensitive to number of analyses, age peaks and age peak abundances. The K-S test was run at a 95% confidence interval. Table 2 displays P-values from north to south. Although the K-S

Test cannot verify if two samples are from the same population, it gives the probability that they are from the same source population given by the P-values. Samples with a P-value greater than 0.05 have a high degree of similarity suggesting they incorporated material did not come from the same source population. P-values greater than 0.4 are considered to likely have come from the same source population, but due to the limitations of the K-S Test, it cannot be determined if two populations are definitely from the same source population. The greater the P-value, up to 1.0, the more probable the samples have the same source populations. (Guynn and Gehrels, 2006).

Table 2: 11 Tava samples in order of north to south with corresponding K-S values from running the Kolmogorov-Smirnoff statistical comparison between DZs. The bold values are statistically significant (P>0.05) suggesting the two compared samples possibly came from the same population. The red values are statistically significant and correlative. The P-values greater than 0.4 signify that two populations likely came from the same source population. The test was run at a 95% confidence interval using K-S macro (Gehrels, 2009). This test provides a measure of the probability of statistical correlation between samples.

K-S P-values using error in the CDF

	AP6314	PW611	PN5311	WPCHR4	SH324SI	SH324HO	KRCD	WP113	SH324VE	SH324BD	MSCD
AP6314		0.043	**0.228**	0.216	**0.088**	**0.524**	0.004	**0.189**	**0.794**	**0.332**	**0.124**
PW611	0.043		**0.617**	**1.000**	**0.998**	**0.501**	**0.137**	0.000	**0.177**	0.010	**0.200**
PN5311	**0.228**	**0.617**		**0.753**	**0.696**	**0.577**	**0.430**	0.001	**0.316**	0.007	**0.189**
WPCHR4	0.216	**1.000**	**0.753**		**0.996**	**0.728**	**0.134**	0.000	**0.300**	0.035	**0.326**
SH324SI	**0.088**	**0.998**	**0.696**	**0.996**		**0.796**	**0.327**	0.000	**0.358**	**0.061**	**0.572**
SH324HO	**0.524**	**0.501**	**0.577**	**0.728**	**0.796**		0.028	0.029	**1.000**	**0.448**	**0.968**
KRCD	0.004	**0.137**	**0.430**	**0.134**	**0.327**	0.028		0.000	0.010	0.000	0.007
WP113	**0.189**	0.000	0.001	0.000	**0.134**	0.029	0.000		**0.173**	**0.585**	**0.174**
SH324VE	**0.794**	**0.177**	**0.316**	**0.300**	**0.358**	**1.000**	0.010	**0.173**		**0.709**	**0.847**
SH324BD	**0.332**	0.010	0.007	0.035	**0.061**	**0.448**	0.000	**0.585**	**0.709**		**0.954**
MSCD	**0.124**	**0.200**	**0.189**	**0.326**	**0.572**	**0.968**	0.007	**0.174**	**0.847**	**0.954**	

The K-S values for 11 Tava samples (Table 1) can determine if two samples are not from the same population (P<0.05). From the analysis sessions at the LasercChron Center (Appendix A), ages and errors were calculated on ~100 grains

per sample. Bolded values are P-values > 0.05. In general, the 11 Tava samples have a high probability of sharing source populations.

Two units are accepted as correlative units when P is between 0.4 and 1.0. A sample with exceptional correlation with other Tava samples is SH324HO, which has P>0.4 for 8 out of 10 comparisons. Correlative values for SH324HO are very polarized; if the correlative value is not greater than 0.4, then it is less than 0.03. Samples that do not correlate to SH324HO are dikes. Sample PW611, a Tava sandstone parent body, has P > 0.5 when compared to three other 'parent' sandstones (PN5311, WPCHR4, and SH324HO) and P < 0.12 when compared to all other samples. The similarities among the four samples PW611, PN5311, WPCHR4, and SH324HO indicate that they share similarities in their source populations. In six instances, there are sample pairs that yielded P=1.0 (PW611 and WPCHR4; SH324HO and SH324VE). Therefore, there is a high probability that they came from the same source population. The sample SH324BD, a basement hosted dike, correlates best (P>0.5) with other dikes (WP113, SH324BD, and MSCD) and less (P<0.34) with the parent bodies.

From the K-S results, it is apparent that WP113, an isolated injectite dike within PPG, has little to no probability of correlation to other samples. It has P=0.0 to PW611, WPCHR4, SH324SI, and KRCD. This can be interpreted as WP113 sharing very little source material with all except for SH324BD. In other words, the DZs that makeup WP113 differ greatly from the other nine Tava samples. With P=0.585, WP113 and SH324BD likely have moderate correlation. WP113 has more correlation (P>0.05) to dike injectite samples than to Tava sandstone parent body

samples. Similar to WP113, KRCD has low to moderate correlation with other Tava sites. KRCD is correlated best (P=0.430) with PN5311. Interestingly, KRCD and PN5311 are the most southern and northern sample site along the UPF. Although KRCD is a dike injectite, its highest P-values are when it is compared to Tava sandstone parent bodies.

Overall, there seems to be no correlation with respect to location among the 11 Tava samples. There is a relationship when correlating parent bodies to parent bodies and injectites to injectites. The parent body and dike samples have been labeled as orange and blue, respectively (Table 2). The orange samples generally correlate best with orange samples while the blue samples correlate best with blue samples.

DZ PROVENANCE BASED ON AGE:

After quantifying the relationships among the Tava samples, it is logical to examine the peaks of the individual DZ spectra for the 11 Tava samples (Figure 19). Developments in U-Pb geochronology have allowed geologists to date individual zircon grains. The laser ablation method was used in this study to analyze individual grains that had little zoning, cracks or inclusions.

The age spectra for the Tava samples (Figure 19) have three major peaks. The first, is a broad, low-sloping peak at ~1.1 to ~1.35 Ga. The broad, gradual shape corresponds to DZs transported from a distant source. This peak also appears in units in the Western USA and the source for this broad ~1.1 to 1.35 Ga age peak has been identified as the Grenville Orogen (Gehrels et al., 2011; Yonkee et al., 2014).

The second and third major peaks are narrow, sharp peaks at ~1.4 and ~1.7 Ga that indicate local sources (Doe et al., 2012). There are widespread plutonic and metamorphic rocks from the Proterozoic basement rocks in Colorado (Figure 20) and the West that are probable sources for these peaks because they correspond to the ~1.4 and ~1.7 Ga ages of the peaks. In order for Proterozoic source rocks of Colorado to contribute sediment, including DZs, they must have been exposed at the surface, eroded, and transported.

Table 3: Weighted mean ages of Tava samples compared to U-Pb zircon Proterozoic database for Colorado age. Ages taken from (Klein et al., 2009; Jones et al., 2009, 2010 and 2012; Amato et al., 2011). Data were combined in the Appendix E. This table indicates specific plutons that may have been at the surface during the time of emplacement of Tava. Un-bolded ages are peaks that have insufficient (<5) numbers of grains to be significant.

Sample	WM Age (Ma)	+/-	n	Source	Rock Type
PN5311	**1051**	**33**	**35**	**PPG or Grenville**	
	1443	**45**	**9**	**Mount Evans Pluton**	**Monzogranite**
	1794	92	3	Boulder Creek Granodiorite	Granodiorite
	1850	120	4	Boulder Creek Granodiorite	Granodiorite
KRCD	**1043**	**10**	**32**	**PPG or Grenville**	
	1155	**66**	**22**	**PPG or Grenville**	**Monzogranite**
	1455	**120**	**7**	**Elevenmile Canyon batholith**	**Granite**
	1655	150	3	Boulder Creek granodiorite	Granodiorite
WP113	**1066**	**52**	**10**	**PPG or Grenville**	
	1173	**56**	**7**	**PPG or Grenville**	
	1442	**79**	**7**	**Mount Evans Pluton**	**Monzogranite**
	1714	**44**	**10**	**Twin Mountain Pluton**	**Granodiorite**
MSCD	**1067**	**65**	**27**	**PPG or Grenville**	
	1093	**67**	**18**	**PPG or Grenville**	
	1435	**59**	**23**	**Elevenmile Canyon Batholith**	**Granite**
	1715	**52**	**19**	**Phantom Canyon Quartzite**	**Quartzite**

The local Precambrian rocks in Colorado are reasonable candidates for being the source of sediment and zircons in the Tava sandstone (Figure 20). By comparing weighted means of DZ populations in each Tava sample to the age of igneous

sources and detrital zircon populations of Proterozoic igneous rocks in Colorado, potential local igneous sources for zircons can be identified. U-Pb age data for plutonic rocks in Colorado are available from a geochronology database (Klein et al., 2009). Four age groups of interest are: 980 Ma-1.17, 1.38-1.50, 1.60-1.695, and 1.70-1.74. These include the phases of the *ca.* 1.7 Ga Boulder Creek granodiorite (Routt Suite of Tweto and Sims, 1963), the *ca.* 1.4 Ga Silver Plume granite (Berthoud Suite), and the Pikes Peak Granite that is 1.08 Ga (Howard, 2014). An additional potential source of 1.74 Ga-aged DZs is the Mesoproterozoic metaquartzites of Colorado (Jones et al., 2009).

K-S comparison of Tava DZ results with U-Pb ages for individual plutons is not possible due to the disparity in analytical methods. The method for dating DZs requires analyses of hundreds of individual grains using laser ablation (Gehrels, 2009), but while a single age for plutonic rocks determined by isotopic dilution – thermal ionization (Klein et al., 2009).

Tava samples selected for DZ provenance comparison include the most northern and southern site on the UPF: Pine (PN5311, parent body) and Keeton Ranch (KRCD, dike) with two sites in between: Woodland Park (WP113, dike) and Manitou Springs (MSCD, dike). The weighted mean ages were calculated using Isoplot 4.1 (Table 3; Table 4; Appendix F) (Ludwig 2008). The weighted means for PN5311 are 1051 ± 33 (n=35), 1443 ± 45 (n=9), 1794 ± 92 (n=3), and 1850 ± 120 (n=4) Ma. The weighted mean ages for KRCD are 1043 ± 10 (n=32), 1155 ± 66 (n=22), 1455 ± 120 (n=7), and 1655 ± 150 (n=3) Ma. The weighted mean ages for WP113 are 1066 ± 53 (n=10), 1173 ± 56 (n=7), 1442 ± 79 (n=7), and 1714 ± 44

(n=10) Ma. The weighted mean ages for MSCD are 1067 ± 65 (n=27), 1093 ± 67 (n=18), 1435 ± 59 (n=23), and 1715 ± 52 (n=19) Ma.

Table 4: This table shows the weight means of the peaks on the DZ age spectra (Figure 18 A-K) with error and number of grains used to calculate the weighted mean. Weighted means calculated with <5 grains are bolded and considered insufficient to correlate to a plutonic source.

	WMAge (Ma)	+/-	n
AP6314	1051	8.4	26
	1445	27	12
	1649	6.1	6
KRCD	1043	10	32
	1155	66	22
	1455	120	7
	1655	**150**	**3**
MSCD	1067	65	27
	1093	67	18
	1435	59	23
	1715	52	19
PN5311	1051	33	35
	1443	45	9
	1794	**92**	**3**
	1850	**120**	**4**
PW611	1046	32	39
	1156	27	48
	1356	53	14
	1477	45	12
	1683	**110**	**3**
	1776	38	6
SH-dikes	1683	87	12
	1732	51	22
	1874	75	9
SH324HO	1061	79	23
	1154	87	17
	1416	73	17
	1708	90	8
SH324SI	1043	100	21
	1415	120	9
WP113	1066	52	10
	1173	56	7
	1442	79	7
	1714	44	10
WPCHR4	1067	41	37
	1075	37	46
	1178	75	19
	1457	110	8
	1657	90	6
	1845	65	5

Based on the weighted means of each sample it is possible to identify specific plutonic or metamorphic sources from Colorado bedrock (Table 3 and Figure 20) using the USGS geochronological database and Precambrian basement map (Sims et

al., 2001). PN5311's youngest weighted mean occurs at 1051 ± 33 Ma. The local source for this comes from the Pikes Peak Batholith. The second weighted mean is 1443 ± 45, which likely came from the Monzogranite, Mt. Evans Pluton (Table 3; Figure 20). The 1794 ± 92 (n=3) and 1850 ± 120 (n=4) Ma ages contain less than five grains and are insufficient to point to a source. The KRCD sample has two ~1.1 Ga weighted means that occur at 1043 ± 10 and 1155 ± 66 Ma, and their local source is closest in age to the Pikes Peak Batholith. The second mean age occurs at 1455 ± 120 Ma, and its closest local plutonic source is the Elevenmile Canyon Batholith, yet also within the Mount Evans Pluton. The KRCD sample has its oldest weighted mean age at 1655 ± 150 (n=3) Ma, but since there are insufficient grains (n<5), conclusions cannot be made about its plutonic source. WP113's youngest weighted means occur at 1066 ± 53 and 1173 ± 56 Ma, which locally had to come from the Pikes Peak Batholith. The second weighted mean occurs at 1442 ± 79 Ma and its source most likely comes from the Mount Evans Pluton or the Elevenmile Batholith (due to large error). The last weighted mean for WP113 occurs at 1715 ± 52 Ma and its source likely comes from the Twin Mountain Pluton. MSCD's first weighted mean occurs at 1067 ± 65 and 1093 ± 67 Ma. The only local possibility for these DZs comes from the Pikes Peak Batholith. The second weighted mean occurs at 1435 ± 59 Ma, and its source is possibly the Elevenmile Canyon Batholith or surrounding ~1.4 Ga sources (Figure 20). The last weighted mean occurs at 1715 ± 52 Ma and its source comes from the Phantom Canyon Batholith.

The three major age peaks in the Tava sandstone DZ spectra can be separated into two shapes: a broad plateau, the ~1.1 Ga age peak, and two sharp

narrow peaks, the ~1.4 and ~1.7 Ga aged peaks. The DZs in the Tava sandstone that fall within the narrow age ranges are of such high abundance, it is likely that they represent a local zircon source. Tava sandstone thus provides evidence that plutonic and metamorphic rocks that crystallized at depths of 12km or more (Shaw et al., 2013) were exposed at the surface and subject to weathering, erosion, and transport by the time of the deposition of Tava sandstone in the Cryogenian period.

On the basis of age alone, the provenance of Tava sandstone DZs that are ~1.1 Ga in age cannot be determined. The 1.1 Ga grains are a component of a broad peak with gradual margins that suggests distant transport and thorough mixing (Gehrels et al., 2011). The DZ ages overlap in time with the span of Grenville plutonism (Spencer et al., 2015). Clasts of the Keeton-Porphyry, a hypabyssal equivalent of PPG, that were sampled from Pennsylvanian Fountain Formation yielded a weighted mean age of 1108 ± 2 Ma and minimum ages of 1075 and 1078 Ma (Sanders and Hawkins, 1999). Plutonism during the Grenville orogeny in other parts of Rodinia occurred from 1.19-0.85 Ga (Rivers, 1997; Rainbird et al., 1992).

There were no plutonic events in Colorado between 1.35 and 1.15 Ga, so local sources cannot account for the DZs dated from 1.08 to 1.35 Ga. To find a source for the zircons that are older than 1.15 Ga, plutonic sources must be identified elsewhere. Extensive DZ research in the Western USA and sources globally has shown that the broad age peak is a signature of 'Grenville' orogeny-derived detrital zircons (Gehrels and Pecha, 2014).

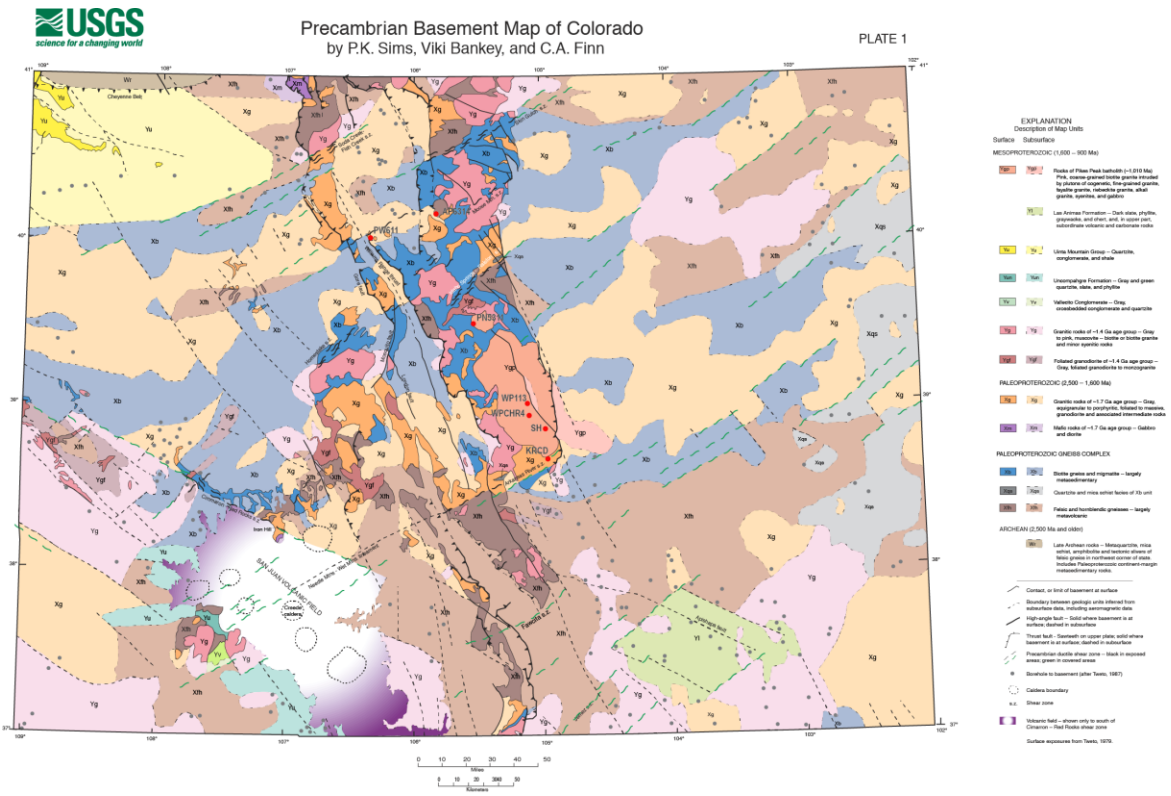

Figure 20: Map of Proterozoic and Archean rock in Colorado with corresponding pluton age locations determined from U-Pb geochronology of zircons. Different symbols are based on the four age groups indicated in the legend. Tava samples compared are shown on the map include AP6314, PN5311, WPCHR4 and KRCD. Note the blue and yellow metamorphic fabric running NE-SW with the interruption of the UPF and younger Proterozoic units. UPF must be younger than the metamorphic fabric in the background. The blue and yellow units are ~1.7 Ga, the purple and pink units are ~1.4 Ga, and the orange unit is ~1.1 Ga exclusively the Pikes Peak Batholith. Taken from Sims et al., 2001.

DZ SPECTRA BASED ON PEAKS:

The statistical analysis provides strong evidence that the UPF-associated Tava sandstones were derived from an integrated sand system, and this system had a greater regional extent than has been previously thought. P-values correlate best between parent bodies and parent bodies (except for KRCD) and between injected dikes and injected dikes (Table 2). The detrital zircon age spectra for all basement-hosted sandstones currently analyzed in Colorado exhibit differences in spectra despite their proximity to one another (Figure 19). All Tava sandstone bodies have a broad peak from 1.3 Ga to 850 Ma, but it is the older, sharp, and narrow peaks that differ among samples. DZ spectra for sediment from basins from the Grenville Orogeny in Labrador (Figure 21; Spencer et al., 2015) show the characteristic broad Grenville age peak that resembles the Tava sandstone broad peaks. The age span and abundances of zircon for the syn-orogenic phase of the Grenville Orogeny most resemble the Tava DZ age vs. abundances, reflected in the size and intensity of its peaks. This further confirms that the distal source responsible for the broad ~1.1 Ga plateau and zircon grains came from Grenville sources.

There is a dramatic difference in abundance of DZs within the three major U-Pb age groupings for Tava sandstone (~1.1 Ga plateau (Grenville, distal) and the ~1.4 and ~1.7 Ga narrow peaks (local) when parent sandstones and large dikes are compared to smaller-scale, crosscutting Tava injectites. The parent sandstones and large dikes have a large abundance of 'Grenville'-derived grains and low abundance of ~1.7 and ~1.4 Ga detrital zircons shown by the orange spectra (Figure 19). The crosscutting dikes have a lower abundance of 'Grenville' aged grains, distributed

across a diffuse, ill-defined peak, and an abundance of ~1.7 and ~1.4 Ga grains that correspond to prominent, narrow age peaks.

The two "types" of Tava sandstone correspond to the orange and blue group (Figure 20). Between the Tava sample sites that correspond to the orange and blue spectra, there was a change in bedrock exposure that allowed the blue group to contain local ~1.4 and ~1.7 Ga aged zircons but not the orange group. Outcrops show crosscutting relationships between parent bodies and dikes. This relationship is evidence for two emplacement events, further supported by two distinct Tava spectra. One event emplaced the large parent bodies while the other injected the dikes.

A notable distinction between the two DZ spectra groups is that the orange group consists primarily of large parent bodies while the blue group is exclusively composed of injected crosscutting dikes. The separation of these two bodies reveals an opportunity for an improved interpretation of the paleography of Rodinia during the time of Tava sandstone deposition.

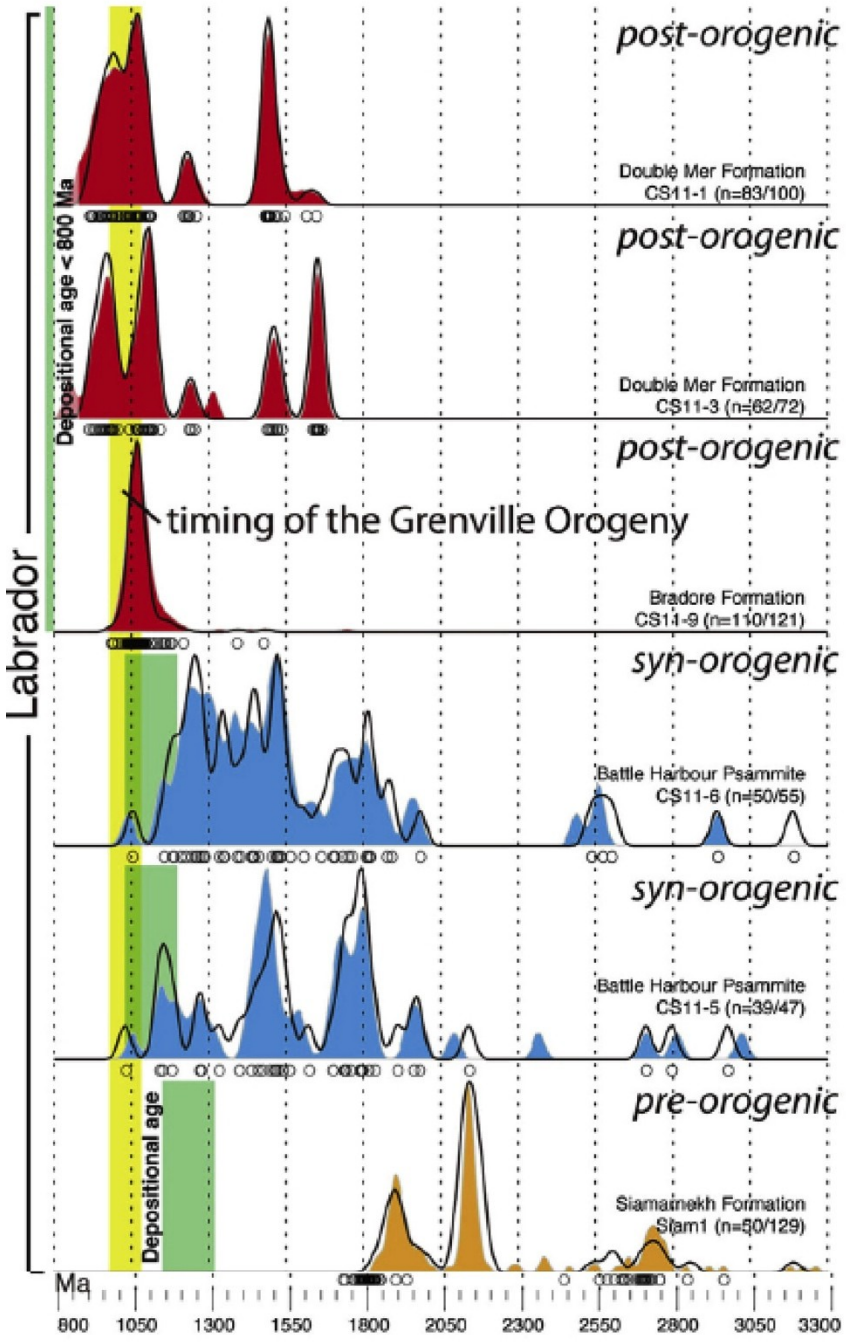

Figure 21: Detrital zircon ages of samples representing the depositional and orogenic ages of the Grenville Orogeny during three phases: pre-orogenic, syn-orogenic and post-orogenic. Sediment sourced from basins from the Labrador Mountains. Figure taken from Spencer et al., 2015.

INTERPRETATION OF TAVA SANDSTONE DEPOSITION

The differences in DZ spectra and sedimentology suggest that during the time of Tava sandstone deposition, changes in bedrock exposure and DZ provenance occurred. The changes could be a result of tectonism with faulting leading to bedrock uplift and unroofing (Flowers and Schoene, 2010) or delivery and deposition of voluminous sediment that covered local bedrock. Unroofing refers to the thickness of rock removed through erosion or tectonism, and uplift refers to the increase in surface elevation. Crosscutting relationships of Tava sandstone dikes indicate two or more emplacement events; the DZ age distributions denoted in blue in Figure 19 were emplaced after sandstones forming the large bodies, with DZ age distributions indicated in orange. However, the exposure and erosion of local bedrock, from which were derived the DZs that form the ~1.4 and ~1.7 Ga aged peaks, could have occurred either before or after the deposition of sediment from Grenville sources that contained abundant DZs that form the broad ~1.0 to 1.35 Ga age peaks. There are two possible sequence of events are outlined in Scenario 1 and Scenario 2

i. Scenario 1: Deposition of Grenville sediment first (Figure 22 A)

This scenario begins with local bedrock at depth, protected from surface processes. The Grenville sediment was transported from its source and deposited in Colorado over the local bedrock before any tectonism occurred. The sediment (containing minimal ~1.4 and ~1.7 Ga grains) mixed with other grains and then solidified, forming the Tava sandstone parent bodies. Then, as tectonism began, rifting

began to occur along what is currently the UPF. This rifting lead to the exhumation of local bedrock. Surface processes eroded the bedrock and mixed it with the previously transported Grenville sediment. This new mixture (continaing ~1.4 and ~1.7 Ga grains) was deposited into the basin. Rifting of continents is associated with seismicity. This seismicity liquified the sediment and injected it into the fractures of the parent body, forming the crosscutting dikes. The injection would have been directed lateraly based on paleomagnetic data (Freedman, 2014).

Sediment deposited before any rifting occurred corresponds to the orange population (Figure 19). Sediment that was injected due to seismicity and tectonism corresponds to the blue population. In summary, this scenario outlines first, the transport of Grenville grains from Grenville sources before the exhumation of bedrock. The bedrock was exhumed as a consequence of rifting and injected into the parent bodies forming the crosscutting relationships. This scenario captures the time of injection of local derived sediment and a time of high seismicity during the Neo-Proterozoic.

ii. Scenario 2: Deposition of Grenville sediment second (Figure 22 B)

This scenario begins with local bedrock exposed at the surface. Rifting had already begun and a basin that is currently the UPF had formed. The local bedrock containing locally derived DZs in Tava,

~1.4 and ~1.7 Ga aged, grains was eroded away and deposited in bottom of the basin. Second, the sediment coming from Grenville sources were transported across Rodinia and deposited on top of the locally derived sediment. The lower level of sediment was injected into the Grenville dominant Tava as a result of liquefaction from seismicity. In this scenario, Tava captured the time of arrival of Grenville derived sediments coming from their source.

These two scenarios do not account for the absence of Pikes Peak Granite aged zircons in the DZ spectra for Tava. The U-Pb ages for DZs have provided a powerful means to determine the age and uncover regional variations in source of 'locally derived' zircons. The age distributions cannot be used to distinguish specific intrusive centers as sources, however, for example to address the question whether the Tava sandstone's abundant circa 1.1 to 1.35 Ga zircons derived from plutons in the eastern/northeastern sector of the Grenville orogeny or the Texas sector. Research of this involving other isotopic methods must be used to tie zircon isotope ages and signatures to the isotopic ages and signatures for igneous sources (Kemp et al., 2006). A hafnium investigation of Tava sandstone detrital zircons is in progress by a MSc student Aaron Hantsche and his advisor G. Lang Farmer (Hantsche and Farmer, in progress), that should soon illuminate the question of which sector of the Grenville orogenic belt eroded and supplied DZs to the Tava sandstone in Colorado.

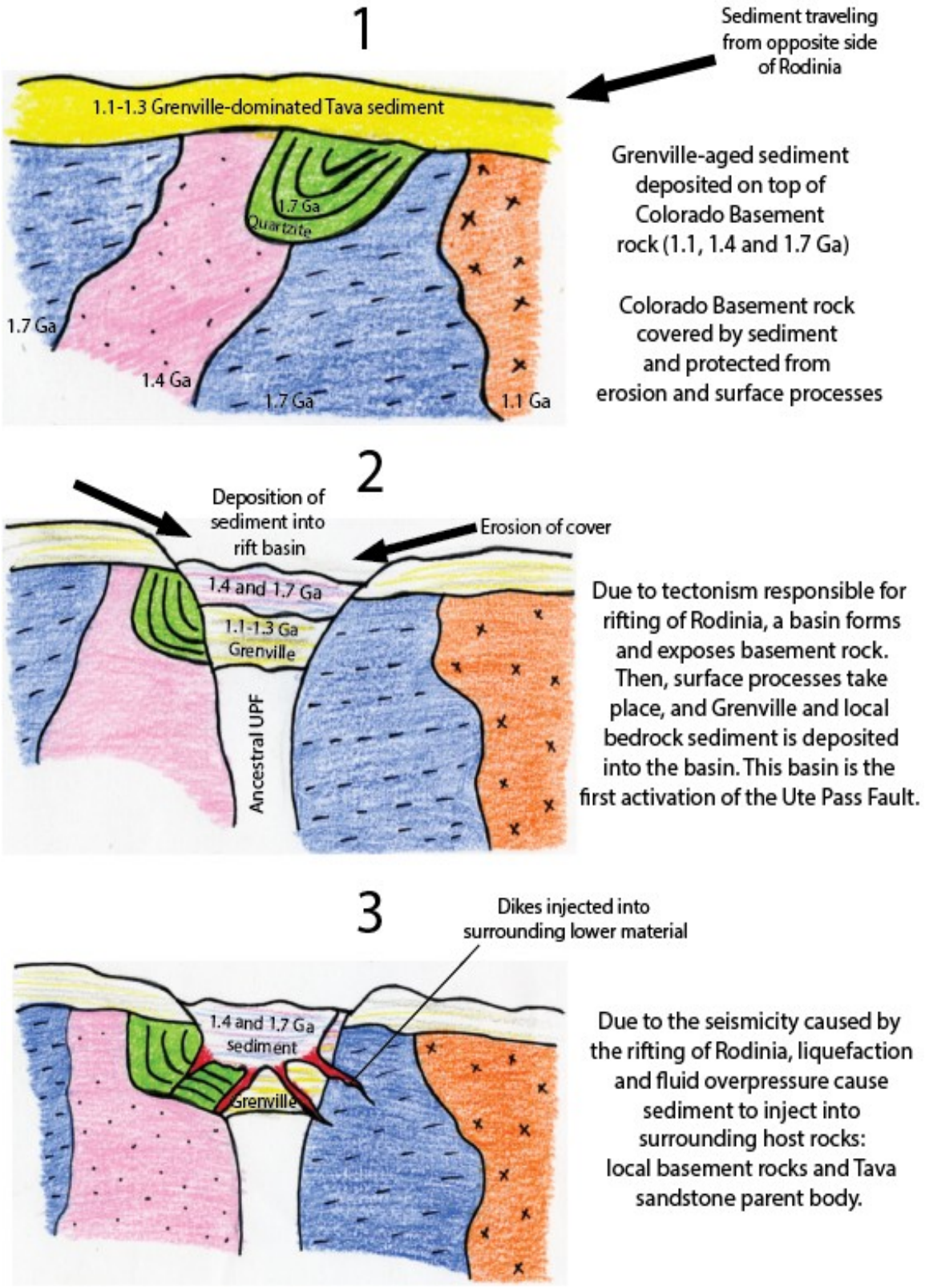

Figure 22 A: This figure outlines Scenario 1 in the deposition of the Tava sandstone.

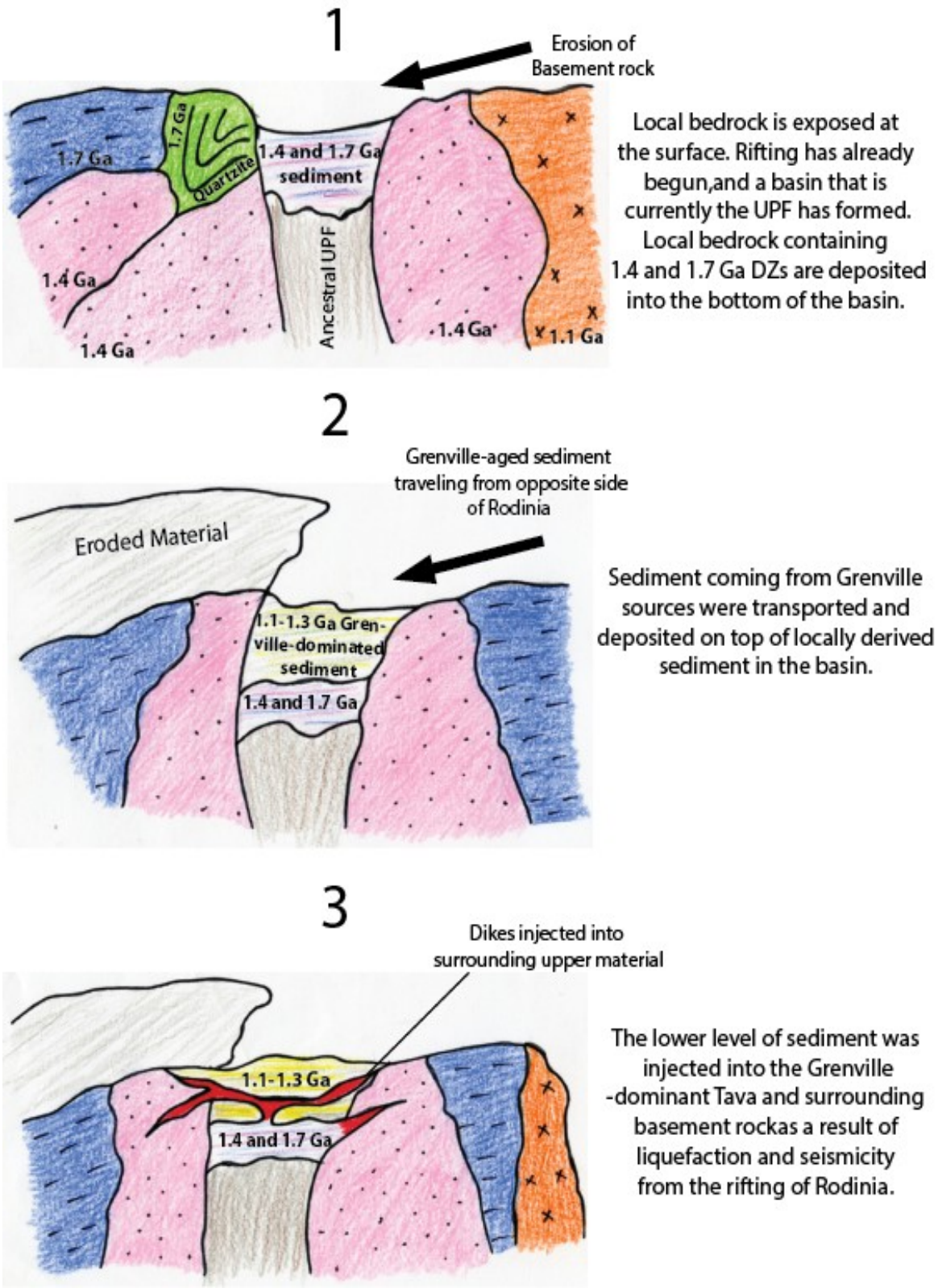

Figure 22B: This figure outlines Scenario 2 in the deposition of the Tava sandstone.

VII. Conclusions

The differences in the DZ spectra of the Tava sandstone (~11 km apart) can be attributed to the presence of topography during the Neoproterozoic. The comparison among Tava samples and isotopic information for local Proterozoic rocks of Colorado imply that the ~1.4 Ga and ~1.7 Ga rocks came from local plutonic sources (Table 3), The variations in DZ spectra create two types of Tava sandstones indicated by the orange and blue DZ spectra (Figure 19). Additionally, the variations in sedimentology between parent bodies and dikes make these two groups apparent through field observation.

The cross-cutting relationships (Figure 12) between the dikes and the Tava sandstone parent bodies imply multiple emplacement events. These two events are apparent in the sedimentology and the DZ spectra. Two create this difference in DZ spectra, bedrock exposure must have changed from the orange group to the blue group. Furthermore, to create the difference in sedimentology, the two emplacement events must have been far enough apart in the age succession and depth to have different sedimentary characteristics.

Moreover, the preservation of these two generations of the Tava sandstone appears along the UPF, a large fault that cuts through the metamorphic fabric of the Precambrian basement rock of Colorado (Figure 20) and preserves the Tava sandstone. This structure could be a remnant of the intracontinental basin formed through the rifting of Rodinia that captured local sediment being eroded from the river system and preserving it in the ancient UPF. The sequence of events that lead to the formation of the Tava sandstone and its differences in DZ spectra are outlined

in Figure 22. Due to the tectonism since, the UPF has been uplifted, exposing the Tava sandstone at the surface. The combination of the sedimentology and the U-Pb geochronology on DZs in the Tava sandstone lead to evidence for an intracontinental basin during the Neoproterozoic.

SEDIMENTARY SYNOPSIS

There is little sedimentary variation among the Tava sandstone parent bodies at the three sample sites: the "Sugarlump" (SH), the "Duplex" (DX), and Pine (PN). The three parent bodies remain consistent in matrix size and makeup, pebble size and degree of rounding, and mineralogy. Of the three sites investigated for sedimentary characteristics, only SH and PN had U-Pb analyses performed. SH and Pn fall into the orange group (Figure 19) that lacks well-defined peaks at ~1.4 and ~1.7 Ga. Although both SH and PN parent bodies were hosted by granite, the PN5311 age spectra has a well-defined peak at ~1.1 Ga in comparison to SH324HO. This difference could be accounted for due to the parent body outlier (Figure 16) observed at Pine and its distance away from the UPF.

There is sedimentary variation among the injectites (dikes and sills) primarily in clast makeup and clast size. All injectites exhibited a fine and medium grained sandstone matrix (like the parent bodies) and were primarily (<95%) made of quartz. There are slight differences in the clast makeup. For example, some injectites exhibited large pebbles of lithic granitic fragments while others exhibited large, rounded quartz pebbles. Additionally, the presence of clay in the vertical dike (SH324VE) and the large pebbles in the basement-hosted dike (SH324BD) are

differences in injectites within a short distance (~150 m). The sill (SH324SI), however, shares similar characteristics with the Tava sandstone parent body and within 200 m of other exposures (VE and BD). As there are no DZ analyses for for dikes from the "Duplex" or from Pine, only the DZ spectra for the injectites at the "Sugarlump" can be compared. The sill falls under the orange category (lacking defined ~1.4 and ~1.7 Ga peaks) while the VE and BD injectites fall under the blue category for DZ spectra (exhibits defined ~1.4 and ~1.7 Ga peaks, Figure 19).

In summary, the injectite that exhibits sedimentary characteristics similar to the Tava sandstone parent bodies also exhibits similar DZ spectra to the Tava sandstone parent bodies. The injectites that differ in sedimentary characteristics from the sandstone parent bodies have different DZ spectra. The differences in sedimentology between dikes and Tava sandstone parent bodies and sills are apparent in differences in the DZ spectra. Additionally, evidence of multiple generations and emplacement events is further supported by this difference in sedimentology. Therefore, the dike filling material must have come from a different stratigraphic level than the host and indicates that the parent sand volume was not homogenized. The two events had a large enough difference in age succession that the injected dike was comprised of different material at the time of emplacement.

IMPLICATIONS FOR PALEOENVIRONMENT OF RODINIA

The Grenville orogeny took had topography along the east of the United States and down into Texas. The extent and intensity of its relief was a consequence of tectonics responsible for forming Rodinia. It has been established that the high

elevations of the Grenville orogeny allowed for extensive river systems to spread Grenville sediment across the United States (Yonkee et al., 2014; Rainbird et al., 1992 and 2012). Grenville-aged DZs were spread across Rodinia and lithified over time. Surface processes eroded Paleozoic-aged sediment from the CFR, causing the Great Unconformity and 500 million years of missing rock record.

Changes in bedrock exposure at the surface during the Proterozoic are indicated by two emplacement events provided by differences in DZ spectra and sedimentology. The presence of correlative sedimentary units in the Western USA (Figure 3; Siddoway and Gehrels, 2014) coupled with the absence of Proterozoic sedimentary units in Colorado calls for an alteration of the paleoenvironment shown by Blakey's Late Paleozoic reconstruction (Figure 23). His reconstruction illustrates a flat plain that allowed for the erosion and transport of Grenville-aged grains that traveled across Rodinia, but there must have been a difference in topography between the Grenville Orogeny, Colorado, and the Western United States to account for the absence of Proterozoic sedimentary units in Colorado and the presence of these units to the west of Colorado.

This suggests that there was rugged topography and at least some development of highlands where crystalline rocks were exposed and undergoing erosion, together with intermontane basins that accumulated sediment from sources having different DZ provenances (Figure 23). The existence of highlands is consistent with the hypothesis that the Tava sandstone sedimentary characteristics (massive, structureless, conglomeratic quartz arenites) are best explained as a consequence of earthquake-induced liquefaction and sediment remobilization.

Seismicity along the ancestral UPF, and other faults in a regional array, probably was accompanied by differential movement of fault blocks that led to tectonic exhumation of basement in upthrown blocks.

The tectonics responsible for the rifting of Rodinia, the formation of the UPF, and the emplacement of the Tava sandstone opened up the continent, creating an intracontinental basin (Figure 23). As the basin formed, it altered the bedrock exposed at the surface, causing the variations seen in the DZ and sedimentary data for Tava.

All but one Tava sample (PW611) is directly associated with a fault. Sample PW611 does not lie directly on a fault but is located near the William's Range Thrust (Figure 20). Due to the relationship between Tava exposures and major faults (UPF, Rampart Range Fault, UPF splays), it is likely that the intracontinental basin (Figure 23) is the first rupture of the present-day UPF. Some Tava samples are not directly on the UPF (PN5311, PW611, and AP6314). This could be a result of ~800 to ~600 Ma faults closing up and rupturing in new places due to subsequent mountain building events (the Ancestral Rockies and the Laramide Orogeny).

Figure 23: Late Paleozoic (~680 Ma) reconstruction of Rodinia, adapted from R. Blakey. This shows an intracontinental rift interpretation for Rodinia. The first rupture of brittle faults across the Meosoproterozoic tectonic trends can be interpreted as the first activation of the UPF. Blakey

REFERENCES CITED:

Amato, J. M., Heizler, M. T., Boullion, A. O., Sanders, A. E., Toro, J., McLemore, V. T. and Andronicos, C. L., 2011, Syntechtonic 1.46 Ga magmatism and rapid cooling of a gneiss dome in the southern Mazatzal Province: Burro Mountains, New Mexico: Geological Society of America Bulletin, v. 123, issue: 9, p. 1720-1744, doi: 10.1130/B30337.1

Austin, S.A. and Morris, J.D., 1986, Tight Fold and Clastic Dikes as Evidence for Deposition and Deformation of Two Very Thick Stratigraphic Sequences, *in* Proceedings, The First International Conference on Creationism, Pittsburgh, Pennsylvania August 4-6, 1986, p. 3-13.

Black, L.P., Kamo, S.L., Williams, I.S., Mundil, R., Davis, D. W., Korsch, R. J. and Foudoulis, C., 2003, The application of SHRIMP to Phanerozoic geochronology; a critical appraisal of four zircon standards: *Chemical Geology*, v. 200, p. 171-188, doi: 10.1016/S0009-2541(03)00166-9

Cecil, M.R., Gehrels, G.E., Ducea, M.N., and Patchett, J., 2011, U-Pb-Hf characterization of the central Coast Mountains batholith: Implications for petrogenesis and crustal architecture: *Lithosphere*, v. 3, p. 247-260, doi: 10.1130/L134.1.

Davidson, A., 1998, An overview of Grenville Province geology, Canadian Shield; Chapter 3 *in* Geology of Precambrian Superior and Grenville Provinces and Precambrian Fossils of North America, (co-ord.) S.B. Lucas and M.R. St-Onge; Geological Survey of Canada, Geology of Canada, no. 7, p. 205-270 (*also* Geological Society of America, The Geology of North America, v. C-1).

Daziel, I. W. D., 2014, Cambrian transgression and radiation linked to an Iapetus-Pacific oceanic connection: *Geology*, v. 42, p 979-982, doi: 10.1130/G35886.1

Dehler, C.M., Fanning, M.C., Link, P.K., Kinsbury, E.M., and Rybczynski, D., 2010, Maximum depositional age and provenance of the Uinta Mountain Group and Big Cottonwood Formation, northern Utah: Paleogeography of rifting western Laurentia: *The Geological Society of America Bulletin*, v. 80, doi: 10.1130/B30094.1

Dockal, J.A., 2005, Sandstone 'dikes' within the Arapaho Pass fault, Indian Peaks Wilderness, Boulder and Grand Counties, CO: *The Mountain Geologist*, v. 42, p. 143-158.

Doe, M.F., Jones, James V. III, Karlstron, K. E., Thrane, K., Frei, D., Gehrels, G., Pecha, M., 2012 Basin formation near the end of the 1.60-1.45 Ga tectonic gap in southern Laurentia: Mesoproterozoic Hess Canyon Group of Arizona and implications for ca. 1.5 Ga Supercontinent configurations: *Lithosphere*, v. 4, no. 1, p. 77-78, doi: 10.1130/L160.1.

Duller, R.A., Moutney, N.P., Russell, A.J., 2010, Particle fabric and sedimentation of structureless sand, southern Iceland: *Journal of Sedimentary Research*, 2010, v. 80, doi: 10.2110/jsr.2010.055

Flowers, R. M. and Schoene, B., 2010, (U-Th)/He thermochronometry constraints on unroofing of the eastern Kaapvaal craton and significance for uplift of the southern African Plateau: *Geology*, v. 38, p. 827-839, doi: 10.1130/G30980.1

Freedman, D.J., 2014, Paleomagnetism and Anisotropy of Magnetic Susceptibility of the Basement-Hosted Tava Sandstone of the Colorado Front Range [B.A. thesis]. Colorado Springs, Colorado, Colorado College, 35 p. and appendices.

Gehrels, G. E, 2000, Introduction to detrital zircon studies of Paleozoic and Triassic strata in western Nevada and northern California: *The Geological Society of America Special Papers*, v.347, p. 1-17, doi: 10.1130/0-8137-2347.7-7.1

Gehrels, G.E., Valencia, V., Pullen, A., 2006, Detrital zircon geochronology by laser-ablation multicollector ICPMS at the Arizona LaserChron Center: *Paleontological Society Papers*, v. 12, doi: 10.1029/2007GC001805

Gehrels, G.E., Valencia, V.A., and Ruiz, J., 2008, Enhanced precision, accuracy, efficiency, and spatial resolution of U-Pb ages by laser ablation–multicollector–inductively coupled plasma–mass spectrometry: *Geochemistry, Geophysics, Geosyststems*, v. 9, Q03017, doi:10.1029/2007GC001805

Gehrels, G.E., 2010, U-Pb-Th analytical methods for Zircon: Arizona LaserChron Center, University of Arizona: https://docs.google.com/file/d/0B9ezu34P5h8eMzkyMGFlNjgtMDU0Zi00MTQyLTliZDMtODU2NGE0MDQ2NGU2/edit?hl=en&pli=1 (June 2014).

Gehrels, G.E., 2011, Detrital zircon U-Pb geochronology: Current methods and new opportunities, *in* Busby C. and Azor A., eds., Tectonics of Sedimentary Basins: Recent Advances: *Chichester*, UK, John Wiley & Sons, doi: 10.1002/9781444347166.ch2.

Gehrels, G.E., Blakey, R., Karlstrom, K.E., Timmons, M.J., Dickinson, B., and Pecha, M., 2011, Lithosphere: Detrital zircon U-Pb geochronology of Paleozoic strata in the Grand Canyon, Arizona: The Geological Society of America, v. 3, doi:10.1130/L121.1

Gehrels, G.E., and Pecha, M., 2014, Detrital zircon U-Pb geochronology and Hf isotope geo- chemistry of Paleozoic and Triassic passive margin strata of western North America: *Geo-sphere*, v. 10, p. 49–65, doi:10.1130/GES00889.1.

Guynn, J. and Gehrels, G.E., 2006: Department of Geosciences, University of Arizona, Tucson: https://docs.google.com/file/d/0B9ezu34P5h8eZWZmOWUzOTItZDgyZi00NDRiLWI4ZTctNTljNTM5OTU1MGUz/edit?hl=en&pli=1 (March 2015).

Gruszka, B. and Zielinski T., 1966, Gravity flow origin of glaciolacustrine sediments in a tectonically active basin: *Annales Societatas Geologorom Poloniae*, v.66, p. 59-81.

Hantsche, A. and Farmer, G. L., in progress, Hafnium isotope investigation of Neoproterozoic-Cambrian strata of the western USA, for evaluation of possible pluton sources in the Grenville orogen.

Harms, J.C., 1965, Sandstone Dikes in Relation to Laramide Faults and Stress Distribution in the Southern Front Range, Colorado: The Geological Society of America, v. 76, p. 981-1002, doi: 10.1130/0016-7606(1965)76

Howard, A.L. 2013, Hafnium isotope evidence on the provenance of ~ 1.1 ga detrital zircons from western north America [Masters thesis]: Boulder, University of Colorado, 108 p.

Hurst, A. and Glennie, K.W., 2008, Mass-wasting of ancient Aeolian dunes and sand fluidization during a period of global warming and inferred brief high precipitation the Hopeman Sandstone (late Permian), Scotland: *Terra Nova*, v. 20, p. 274-279.

Hurst, A., Scott, A., Vigorito, M., 2011, Physical characteristics of sand injectites: *Earth-Science Reviews*, v. 106, p. 214-246, doi: 10.1111/j.1365-3121.2008.00817.x

Johnston, S., Gehrels., G.E., Valcencia, V., and Ruiz, J., 2009, Small-volume U-Pb zircon geochronology by laser ablation-multicollector-ICP-MS: *Chemical Geology*, v.259, p.218-229, doi: 10.1016/j.chemgeo.2008.11.004

Jones J. V. III., Connelly, J. N., Karlstrom, K. E., Williams, M. L. and Doe, M. F., 2009, Age, provenance, and tectonic setting of Paleoproterozoic quartzite successions in the southwestern United States: The Geological Society of America *Bulletin*, v. 121, p. 247-264; doi: 10.1130/B26351.1

Jones, III, J. V., Siddoway, C. S. and Connelly, James N., 2010, Tectonic implications of a Proterozoic mid-crustal section, Wet Mountains, Colorado, U.S.A.: *Lithosphere*, v. 2, p. 119-135, doi:10.1130/L78.1.

Jones, III, J. V. and Thrane, K., Correlating Proterozoic synorogenic metaseidmentary successions in southwestern Laurentia: New insights from detrital zircon U-Pb geochronology of Paleoproterozoic quartzite and metaconglomerate in central

and northern Colorado, USA: *Rocky Mountain Geology*, v. 47, no. 1, p. 1-35, doi: 10.2113/gsrocky.47.1.1

Keller, J.W., Siddoway, C.S., Morgan, M.L., Route, E., Sacerdoti, R. and Stevenson, A., 2005, Geologic Map of the Manitou Springs Quadrangle, El Paso County, Colorado: Colorado Geological Survey, Denver, CO, Open-File report 03-19. Map at 1: 24,000 and text (41 pgs).

Kemp, A. I. S., Hawkesworth, C. J., Paterson, B. A., and Kinny, P. D., 2006, Episodic growth of the Gondwana supercontinent from hafnium and oxygen isotopes in zircon: *Nature*, v. 439, p. 580-583, doi: 10.1038/nature04505

Klein, T. L., Evans, K. V., and DeWidd, E. D., 2009, Geochronology database for central Colorado: U. S. Geological Survey Data Series 489, 13 p.

Kost, L., 1984, Paleomagnetic and Petrographic Study of Sandstone Dikes and the Cambrian Sawatch Sandstone, Eastern Flank of the Southern Front Range, Colorado [M.S. thesis]: Boulder, Colorado, University of Colorado, 173 p.

Ludwig, K., 2013, Isoplot 4.1: Berkeley Geochronology Center Special Publication 4, 77 p.

Morgan, M. L., Siddoway, C. S., Rowley, P. D., Temple, J., Keller, J.W., Archuleta, B. H., and Himmelreich, J. W., Jr., 2002, Geologic Map of the Cascade Quadrangle, El Paso County, Colorado: Denver, Colorado, Colorado Geological Survey Open-File Report 03-18, scale: 1:24,000 and text (http://geosurvey.state.co.us/pubs/gis/mapping.asp)

Mueller, P. A., Foster, D. A., Mogk, D. W., Wooden J. L., Kamenov, G. D., and Vogl, J. J., 2007, Detrital mineral chronology of the Uinta Mountain Group: Implications for the Grenville flood in southwestern Laurentia: *Geology*, v. 35p. 431-434, doi: 10.1130/G23148A.1

Pepper, M., Simpson, G., Pecha, M. and Gehrels, G., 2012, Field processing of geochron samples: Arizona LaserChron Center, University of Arizona, Tucson: https://docs.google.com/file/d/0B9ezu34P5h8eMjliNTg3ZGYtM2M5ZC00YmVkLTg1OWMtN2NiMTUzZjNlNTEz/edit?pli=1 (June 2014).

Pullen, A., Juan, R., Pecha, M. and Gehrels, G., 2011, Rock crushing & water table instruction manual: Arizona LaserChron Center, University of Arizona: https://docs.google.com/a/laserchron.org/file/d/0B9ezu34P5h8eYWU3MWMxOWMtMzgxNS00MDNjLTgzYjUtZDU0MmRkYTkxNGMw/edit?hl=en&pli=1(June 2014).

Pullen, A. and Pepper, M., Preparing & Cleaning Mounts for analysis at the Arizona LaserChron Center, University of Arizona, Tucson: https://drive.google.com/a/laserchron.org/file/d/0B9ezu34P5h8eYzljNWRlYzgtYzM3Ny00OTY0LWI0NDktZWYyNTk0NTIzNjM1/view?pli=1

Rainbird, R.H., Heaman, L. M. and Young, G., 1992, Sampling Laurentia: Detrital zircon geochronology offers evidence for an extensive Neoproterozoix river system originating from the Grenville orogeny: *Geology*, v. 20, p. 351-354, doi: 10.1130/0091-7613(1992)020<0351:SLDZGO>2.3.CO;2

Rainbird, R.H., Cawood, P., Gehrels, G., 2012, The great Grenvillian sedimentation episode: Record of supercontinent Rodinia's assembly *in* Busby, C. and Azor, A., *eds.*, Tectonics of Sedimentary Basins: Recent Advances: *Chichester*, UK, John Wiley & Sons, doi: 10.1002/9781444347166.ch29.

Rivers, T., 1997, Lithotectonic elements of the Grenville Province: review and tectonic implications: *Precambrian Research*, v. 86, p. 117-154, doi: 10.1016/S0301-9268(97)00038-7

Rodriguez, N., Cobbold, P.R., Loseth, H., 2009, Physical modeling of sand injectites: *Tectonophysics*, v.474, p. 610-632, doi: 10.1016/j.tecto.2009.04.032.

Sanders, R., And Hawkins, D., 1999, U-Pb geochronology of porphyritic clasts from the Pennsylvanian Fountain Formation, Colorado Front Range: Volcanic equivalents of the Pikes Peak batholith: Geological Society of America Abstracts with Programs, v. 31, no. 7, p. 178.

Scott, G.R., 1963, Bedrock Geology of the Kassler Quadrangle: USGS Professional Paper 421-B. 123 p.

Shaw, C. A., Heizler, M. T., and Karlstrom, 2013, K. E., $^{40}Ar/^{39}Ar$ Thermochronologic Record of 1.45-1.35 Ga Intracontinental Tectonism in the Southern Rocky Mountains: Interplay of Conductive and Advective Heating with Intracontinental Deformation, *in* The Rocky Mountain Region: An Evolving Lithosphere Tectonics, Geochemistry, and Geophysics, American Geophysical Union, Washington, D. C., doi: 10.1029/154GM12

Siddoway, C., Myrow, P., and Fitz-Díaz, E., 2013, Strata, structures, and enduring enigmas: A 125th Anniversary appraisal of Colorado Springs geology: doi: 10.1130/2013.0033(13).

Siddoway, C.S., and Gehrels, G.E., 2014, Basement-hosted sandstone injectites of Colorado: A vestige of the Neoproterozoic revealed through detrital zircon provenance analysis: *Lithosphere*, doi: 10.1130/L390.1.

Simpson, G., Pecha, M. and Gehrels, G., 2012, Mineral separation instruction manual: Arizona LaserChron Center, University of Arizona: https://docs.google.com/file/d/0B9ezu34P5h8eYzRmZGYwMGItMGI1MC00MGQ3LWE4YzEtNWZiZmFiNDQ5OGRh/edit?pli=1 (June 2014).

Sims, P.K., Bankey V., and Finn, C. A., 2001, Preliminary Precambrian basement map of Colorado – a geologic interpretation of the aeromagnetic anomaly map: U.S. Geological Survey Open File Report 01-364.

Sims, P.K. and Stein, H.J., 2003, Tectonic evolution of the Proterozoic Colorado Province, Southern Rocky Mountains; a summary and appraisal: *Rocky Mountain Geology*, v. 38, p. 183-204.

Sonnenberg, S.A. and Bolyard, D.W., 1997, Tectonic History of the Front Range in Colorado, *in* Geologic History of the Colorado Front Range: Rocky Mountain Geologists, RMS-AAPG Field Trip #7, Guidebook, p. 1-8.

Spencer, C. J., Cawood, P. A., Hawkesworth, C. J., Prave, A. R., Roberts, N. M. W., Horstwood, M. S. A., Whitehouse, M. J. and EIMF, 2015: Generation and preservation of continental crust in the Grenville Orogeny: *Geoscience Frontiers*, p. 1-16, doi: 10.1016/j.gsf.2014.12.001

Strachan, L., 2002, Slump initiated controlled syndepositional sand remobilization: an example from the Namuriam of County Clare, Ireland: *Sedimentology*, v. 49, p. 25-41. doi: 10.1046/j.1365-3091.2002.00430.x

Temple, J., Madole, R., Keller, J., and Martin, D., 2007, Geologic map of the Mount Deception quadrangle, Teller and El Paso Counties, Colorado: Colorado Geological Survey, Open-File Report OF-07-7, scale 1:24 000, 1 sheet.

Tweto, O., and Sims, P.K., 1963, Precambrian ancestry of the Colorado mineral belt: Geological Society of America Bulletin, v. 74, p. 991-1014, doi: 10.1130/0016-7606(1963)74[991:PAOTCM]2.0.CO;2

Vigorito, M. and Hurst, A., 2010, Regional sand injectite architecture as a record of pore-pressure evolution and sand redistribution in the shallow crust; insights from the Panoche giant injection complex, California: Journal of the Geological Society of Longdon, v. 167, p. 889-904, doi: 10.1166/0016-76492010-005.

Vitanage, P.W., 1954, Sandstone Dikes in the South Platte Area, Colorado: *The Journal of Geology*, v. 62, p. 493-500.

Yonkee, A., Dehler, C., Link, P., Balgord E., Keeley, J., Hayes, D., Wells, M., Fanning, C.M. and Johnston, S., 2014, Tectono-stratigraphic framework of Neoproterozoic to Cambrian strata, west-central U.S.: Protracted rifting, glaciation, and

evolution of the North American Cordilleran margin: *Earth-Science Reviews*, v. 136, p. 59-95, doi: 10.1016/j.earscirev.2014.05.004